VARIABLE IMMUNITY AND ITS CONSEQUENCES FOR PARASITE DYNAMICS

BY

TARA E. STEWART MERRILL

DISSERTATION

Submitted in partial fulfillment of the requirements
for the degree of Doctor of Philosophy in Ecology, Evolution, and Conservation Biology
in the Graduate College of the
University of Illinois at Urbana-Champaign, 2019

Urbana, Illinois

Doctoral Committee:

Professor Carla E. Cáceres, Chair and Director of Research
Associate Professor Zoi Rapti
Associate Professor Brian F. Allan
Professor Rebecca C. Fuller
Associate Professor James P. O'Dwyer

ABSTRACT

Infectious disease represents a growing concern for our developing world. Human diseases result in morbidity, mortality, and suffering. Agricultural diseases can decimate food resources, leading to starvation and economic instability. Wildlife diseases affect the abundance and distribution of species, destabilizing the natural ecosystems on which we rely. Despite these varied contexts, infectious diseases can be united by three common factors: susceptible hosts, parasites, and environmental conditions.

Over the past three decades, disease ecology has provided overwhelming evidence that environmental conditions can shape disease risk by altering host-parasite interactions. For example, shifting global temperatures can increase the density of pathogen vectors, thereby increasing pathogen transmission to humans. Such work has long relied on simple mass action principles of transmission, where infections are driven by rates of exposure and hosts are ascribed a single value denoting their susceptibility to infection. However, accumulating evidence suggests that this single value is biologically unrealistic, with most organisms exhibiting considerable variation in their natural levels of susceptibility. Moreover, theoretical models predict that variation in susceptibility can have profound consequences for the spread of disease. Connecting variable susceptibility to its epidemiological outcomes has become an emerging goal in ecology which I have addressed using observation, modeling, and experiments.

At the heart of host susceptibility is the immune response. All living organisms are threatened with parasites and, in turn, utilize a suite of immunological defenses to prevent infection. Because immune defenses are important for defeating infections at the individual level, they may also present a barrier to disease transmission at the population level. I have investigated immune defenses and their consequences for parasites in an aquatic host-parasite system: the zooplanktonic host *Daphnia dentifera* and its fungal pathogen *Metschnikowia bicuspidata*.

In my first chapter, I describe the complete life cycle of *Metschnikowia*, detail its within-host interactions with *Daphnia*, and outline the potential defenses *Daphnia* use to prevent infection. Through Chapter one, I overturned a longstanding assumption that *Daphnia* cannot recover from infection and developed a series of metrics for quantifying components of the host-parasite interaction. These empirical metrics are specific to the *Daphnia-Metschnikowia* system, and in my second chapter, I developed a mechanistic modeling approach for estimating host

immune defenses that can be applied across wildlife systems. Working closely with Dr. Zoi Rapti, I developed a discrete-state continuous-time Markov model to estimate the probabilities with which organisms resist and clear parasitic infections. In Chapter 3, I quantified the relative importance of *Daphnia* susceptibility for the emergence of *Metschnikowia* epidemics. From pre- to peak- epidemic periods, I tracked *Metschnikowia* exposure and *Daphnia* recovery rates in six lake ecosystems and found that epidemic emergence depends critically on the interaction between parasite exposure and host susceptibility. In my fourth and final chapter, I tested several hypotheses regarding the nature of *Daphnia* susceptibility and identified which host traits are the most critical for determining the outcome of infection. Together, my dissertation provides a comprehensive set of empirical studies demonstrating how exposure and susceptibility interact to regulate parasites and the spread of disease in wildlife.

ACKNOWLEDGEMENTS

First and foremost, thank you to my PhD advisor Carla Cáceres for her unwavering intellectual, logistical and emotional support. During our first meeting, I had a hunch that Carla and I would make a good match. Our relationship since has only exceeded expectations. Carla, you are a constant source of inspiration for me. Thank you for teaching me how to be a strong woman in science. Of all the lessons you have taught me, I hope to never forget: how to appropriately test for local adaptation, how to duct tape a rowboat, and how to say "no" to things when I have too many items on my to-do list.

Thank you also to my close collaborator (and unofficial mathematics advisor) Zoi Rapti. Every time we discuss models, I walk away enlightened and eager to further explore the juncture between theory and empirical work. Zoi, you taught me how to love numbers, and in the midst of permutations, hidden Markov chains, and differential equations, you filled the room with light, life, and positivity.

My committee members, Brian Allan, Becky Fuller, James O'Dwyer and Zoi Rapti provided invaluable feedback for this dissertation and for my future work. Brian's suggestion to look into dose-response curves became an important component of both Chapter 3 and 4. James' course in theoretical ecology provided the first version of the Markov model developed in Chapter 2. Finally, Becky's questions on the genetic basis of *Daphnia* immunity have led to new directions and analyses on *Daphnia* population genetics.

This dissertation would not have been possible without the help of multiple students at the University of Illinois Urbana-Champaign and at Indiana University: Alex Axthelm, Jonathan Crawford, Kaileen Dinnon, Abigail Erickson, Samantha Gray, Rachel Hanauer, Christopher Holmes, Samantha Kopec, Veronika Laird, Ping Lee, Lauren McKay, Ilona Menel, Bridget Mueller-Brenna, Cecily Negri, Diana Oleksyn, Anna Osborn, Peter Schmucker, Zoe Schnitzler, Andrew Sickbert, Maja Sjlivar, Alex Strauss, Gargi Sundaram, Krti Tallam and Jason Walsman. Thanks also to Grace Abernathy Pixton whose undergraduate thesis provided valuable insight on the importance of the *Daphnia* gut barrier for infection. The National Science Foundation also played a critical role in funding me throughout my dissertation. The material presented in this dissertation was supported by the National Science Foundation under Grant Numbers DGE

1144245 (awarded to TESM), DGE 1069157 (awarded to Andrew Suarez), NSF 1354407 (awarded to CEC), NSF 1701515 (awarded to TESM and CEC), and the University of Illinois.

Ten years ago, I decided to leave dance and pursue biology and I was lucky to receive support and encouragement from a number of scientists at UC Santa Barbara. I thank them for giving me the opportunity to succeed: Armand Kuris, Ryan Hechinger, Kevin Lafferty, and Stephen Rothstein. Multiple collaborators have also supported my research by allowing me to explore ideas in new systems and disciplines. Thank you to Julia Buck, Spencer Hall, Skylar Hopkins, Vanessa Rivera-Quiñones, Stefan Schnitzer, and Mark Torchin.

Thank you to the many women in science have been my role models and friends: Val Buxton, Natalie Christian, Samantha Davis, Ana Garcia, Alejandra Jaramillo, Lindsay Marks, Erin Mordecai, Dana Morton, Maria Stager, Louise Stevenson, Rachel Stewart, Lynette Strickland, Stella Swanson and Kelly Weinersmith. Thank you also to my incredible family: Michael Stewart, Donna Fromm, Manpreet Kaur, Rachel, Travis, Ian and Leah Stewart, Trish Fleming, and Peter and Margaret Merrill.

Finally, thank you to my husband Loren Merrill, who continues to explore the depths of nature with me and remind me of the beauty of biological interactions. May we see every bird, moose, bear and bear tapeworm together.

This body of work is dedicated to my grandfather, Elbert W. Stewart, a social scientist who gave to me a passion for reading, writing, and thinking deeply about the complexities of our world.

TABLE OF CONTENTS

CHAPTER 1: WITHIN-HOST COMPLEXITY OF A PLANKTON-PARASITE INTERACTION[1]

Parasite life cycles can be complex, involving multiple hosts and life history stages. For instance, the protozoan parasite *Toxoplasma gondii* moves from the environment to a small mammal host, and then via trophic transmission to a feline host, all the while undergoing four developmental transformations. Such among-host complexity has informed research at the community level by linking hosts through their parasites and by indicating the strength of host interactions (Lafferty et al. 2008). Moreover, it has solidified a community-level perspective on parasite regulation, since the completion of parasite life cycles often depends on the availability and interaction of host species.

Parasite life cycles are also complex at the within-host level. Parasites can exhibit morphological diversity across within-host developmental stages and, through the infection process, can move among diverse host tissues. Addressing complexity at the within-host level can enrich our understanding of both hosts and parasites. For example, through observing trematode morphological variation in snails, Hechinger et al. (2011) discovered social organization among flatworms, bringing sociality to a new phylum and raising questions about its evolutionary origins and ecological consequences. Additionally, recent work on trypanosomes has moved beyond the vector bite and into the vector midgut, where the majority of fly-trypanosome interactions play out. This shift to within-host interactions has revealed that the fly's midgut prevents the majority of infections from succeeding (Sloan & Ligoxygakis 2017), elevating the role of host defenses in regulating parasites. By peeling back the host exterior and focusing on interactions within, new questions arise, assumptions can be overturned, and we can attain a deeper understanding of how within-host processes scale to the community level.

The complicating factor of within-host life cycles is that they are concealed in a host, which can limit opportunities for observing complete parasite natural histories. Many plankton species are transparent, providing an opportunity to observe host-parasite interactions *in vivo*, and I used this characteristic to describe the within-host interactions of the fungus,

---

[1] This chapter has been previously published in the journal *Ecology*. © 2018 by the Ecological Society of America. Full citation:
Stewart Merrill, T.E. & C.E. Cáceres. 2018. Within-host complexity of a plankton-parasite interaction. Ecology 99:2864-2867. doi: 10.1002/ecy.2483

Metschnikowia bicuspidata, and its host, *Daphnia dentifera*. *Metschnikowia bicuspidata* (Metschnikov) Kamenski is an ascomycete fungus that parasitizes freshwater zooplankton, including *Daphnia*. Designated an "obligate killer", *Metschnikowia* exhibits a parasitoid life history strategy (*sensu* Lafferty & Kuris 2002) requiring the death of its host for transmission (Ebert 2005). Portions of the infection process (spore, conidia, and ascus stages; see Appendix A for glossary of life cycle terms) were described, as was the host haemocyte response, in the late 19th century (Metschnikoff 1884). But since then, the within-host life cycle has been largely neglected, despite this parasite's prominence in studies of freshwater disease (Cáceres et al. 2014). This oversight has led to a pervasive assumption that *Daphnia* cannot and do not recover from infection (Hall et al. 2007, Duffy et al. 2009), which has directed research away from within-host processes and toward broad-scale ecological factors that mediate exposure. Herein, I describe the complete within-host life cycle of *Metschnikowia*, which I resolved by observing *Daphnia* over a ten-day period following inoculation. My observations produced a sophisticated picture of within-host events (Fig. 1.1) and yielded novel findings and questions regarding host immunity and cryptic infections. First, I detail the progression of parasite development that occurs across five morphological stages. I then discuss how the resolution of this interaction overturns the assumption of no recovery and informs our understanding of the within-host controls of parasites.

Metschnikowia infects the host passively via ingestion when the *Daphnia* is filter feeding (Ebert 2005). Twenty-four hours after exposure to *Metschnikowia*, I observed spores in the lumen of the host gut (mean number of spores: 46.2, range: 10-114; Fig. 1.2A) moving posteriorly with intestinal contents (e.g. ingested algae). Most of the ingested spores were passed with waste. However, some "attacking" spores punctured the gut epithelium (mean number of spores: 8.8, range: 2-26, Fig. 1.2B) and a subset of attacking spores fully crossed the epithelium and entered the host body cavity (mean number of spores: 2.3, range: 0-10, Fig. 1.2C). All exposed hosts had at least two spores attacking their gut membranes, and approximately 75% of exposed hosts had spores that fully crossed the gut barrier to infect the body cavity. Spores that did not cross the gut barrier gradually left the lumen, potentially from digestive action or the shedding of the gut lining during molt. The *Daphnia* gut is C-shaped, and most attacking spores (85%) were located at the anterior and posterior bends, where the gut approximates two right angles. This pattern suggests that spore penetration is a physical process; the spores are needle-

shaped and those that are unable to make the turn at the bends are shunted into the epithelium. Host feeding and digestion may contribute to the number of spores that puncture by providing peristaltic force. Structural host defenses, like a robust gut, may prevent spores from infecting.

Spores that infected the body cavity began producing hyphae 2-4 days after exposure (Fig. 1.2D). The web-like hyphae extended from the spores and adhered to nearby surfaces. During the spore and hyphae stages, host haemocytes (immune cells) proliferated and moved rapidly through the body cavity. Haemocytes attached to spores upon contact, resulting in large congregations of haemocytes on spores and/or hyphae (Fig. 1.2D). As observed by Metschnikoff (1884), congregating haemocytes regularly coalesced to engulf the parasite.

Hyphae that survived the haemocyte response developed sporocysts 4-5 days after exposure. Sporocysts are small, sack-like structures that contain the next stage (conidia). Sporocysts appear to grow through time as conidia develop within them, and sporocysts were often found aggregated near the mother spore. Sporocysts were also observed overtaking large muscular tracts of the host, and in some cases, floated freely through the host body cavity. Because many sporocysts are produced from a single spore and its hyphae, this stage may represent the point at which the infection becomes pathogenic (*sensu* Lafferty & Kuris 2002). Conidia, which are small and oblong-elliptical in shape, emerged from sporocysts 6-8 days after exposure and rapidly increased in abundance via budding. The conidia are another pathogenic phase of infection; a small group of localized conidia can proliferate into thousands, dispersing and filling the host body in as few as 24 hours. Early in this stage, small clusters of conidia can be found almost anywhere within the host. I have observed conidia along the gut, concentrated in the post-abdominal claw, in the antennae, and even hugging the eye's ommatidia.

The conidia developed into the final stage, the ascus, around 9-10 days after exposure. The ascus is an elongated cylindrical structure that houses the needle-shaped ascospore that is infective to susceptible hosts. Asci, which number in the thousands to tens of thousands, are released into the water column when the host dies. Morphological descriptions of the ascus were provided by Miller and Phaff (2000).

Fully infected hosts appear opaque due to the dense clustering of asci throughout the body. Because asci are conspicuous at low magnification, the ascus stage has traditionally designated hosts as infected (e.g. Cáceres et al. 2006). However, with low magnification (40x) an advanced conidia infection can present as an uninfected host, and spores, hyphae, and sporocysts

are not detectable. Only one fifth of this parasite's life history stages are observable using conventional methods, leading to a high false-negative rate and a vast underestimate of infection prevalence and parasite abundance (e.g. Fontes et al. 2017; Stewart et al. 2018). Indeed, in one natural population I observed ascus prevalence at 4% while the prevalence of all five stages combined was 64%. Disease ecology is predicated on understanding the roles of ecological processes in mediating parasite exposure, and my results highlight how traditional measures of prevalence can fail as metrics for exposure. For parasites whose late stages are used to detect infection, prevalence is the final manifestation after both exposure to a host and success within that host have played out. While my field observation of 4% ascus prevalence could suggest low exposure, this value may also be an outcome of high exposure and low host susceptibility. By integrating life cycles into our observations, exposure and susceptibility can be disentangled, allowing for the identification of environmental versus host controls of transmission. Further, the inclusion of early infections provides better estimates of parasite abundance, highlighting their potential importance for regulating host populations.

My observations provided new information regarding *Daphnia* immune defenses, and in particular, overturned the paradigm that *Daphnia* cannot recover from infection (e.g. Hall et al. 2007, Duffy et al. 2009). At exposure, most *Daphnia* experience early infections with spores or hyphae; however, only a subset of early infections ultimately produce late infections (Fig. 1.2F). By tracking cohorts and individuals through time, I have found that *Daphnia* can clear spores, hyphae, and sporocysts. Although rare, I have observed one *Daphnia* recovering from an ascus infection. Clearance of early infections is common under laboratory conditions but may be sensitive to environmental stressors. Future work should explore its incidence in natural populations to determine its epidemiological importance.

The immune defense responsible for clearing infections appears to be haemocytes, which I observed attacking spores, hyphae, and in some cases, sporocysts. *Daphnia* are highly variable in the number of spores they defend (Fig. 1.2E) and in the magnitude of their haemocyte response. Identifying the immunological controls of parasites is an emerging goal in ecology (Hawley & Altizer 2011) that can be realized with simple observation in this system, and I encourage using the haemocyte response to investigate questions at the intersection of eco-immunology and disease ecology. By capitalizing on the ability to observe haemocytes in real time, future work can examine within- and among-population variation in immunity, sensitivity

of immune responses to ecological factors, and associations between immunological activity, parasite fitness, and transmission.

My observations indicate that the path from exposure to infection is anything but simple: there is variation at every step and both host and parasite are involved in a dynamic interaction that ultimately determines their fitness. Within-host complexity is a general black box in disease ecology that, if opened, has broad potential to shift and complement our current understanding. My description of the *Metschnikowia* life cycle allows the quantification of parasite exposure, attack rate, and infection success. The five resolved life history stages allow one to gauge disease progression and disentangle exposure and susceptibility. The host immune response can be estimated by counting haemocytes and quantifying infection clearance. Ultimately, the resolution of this interaction provides a new and powerful system for examining the contribution of within-host interactions to parasite ecology.

Figures

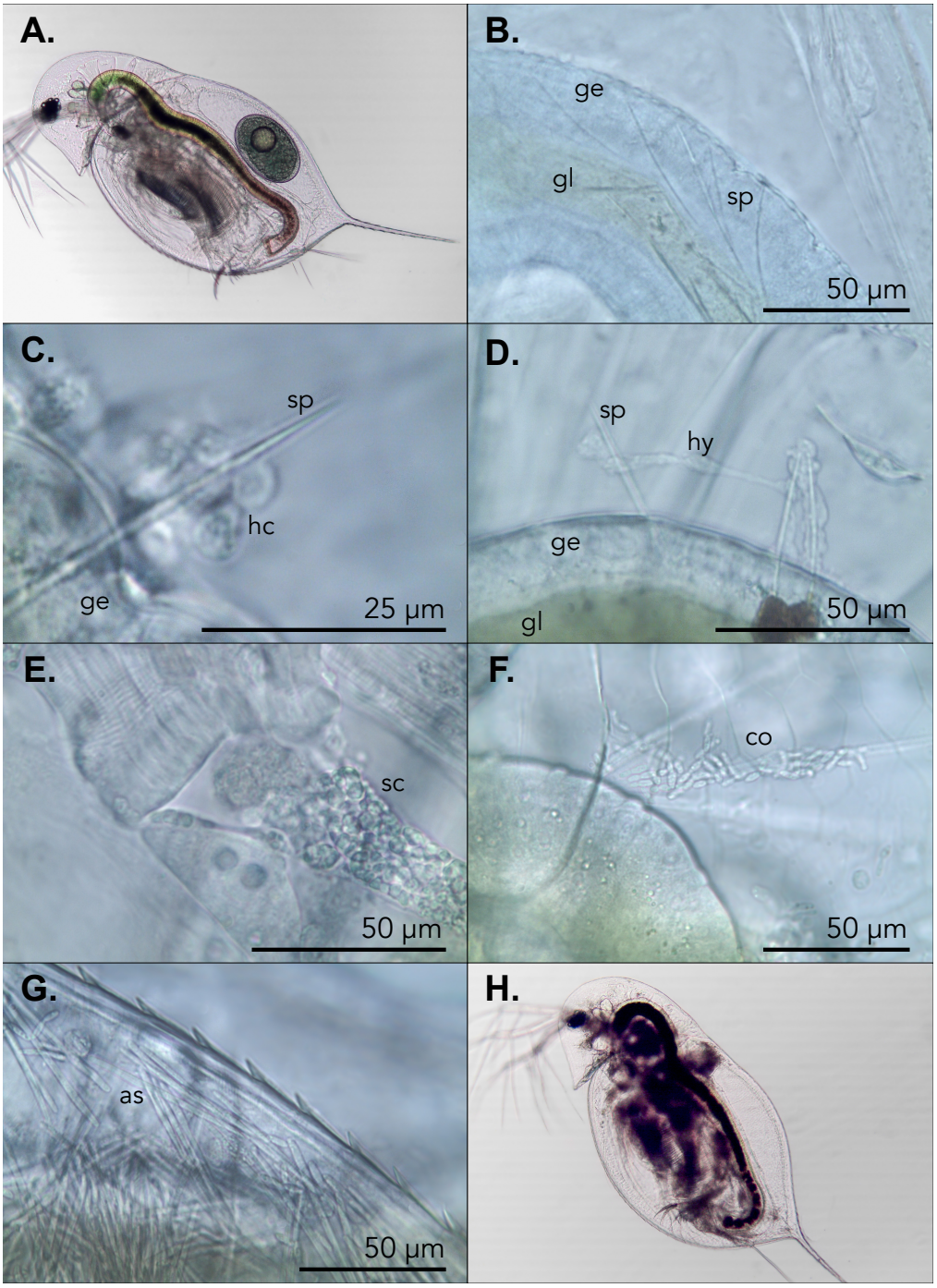

Figure 1.1. The progression of infection of *Metschnikowia bicuspidata* in its host *Daphnia dentifera*. Uninfected hosts (**A**) consume ascospores, some of which attack the gut membrane (**B**). Spores that cross the gut barrier are met by the host haemocyte response (**C**). Surviving spores produce hyphae (**D**) that develop into sporocysts (**E**). Sporocysts rupture and release conidia (**F**) that replicate and spread throughout the body. Fully infected hosts are filled with asci (**G** and **H**). Labels: ge- gut epithelium, gl- gut lumen, sp- spore, hc- haemocyte, hy- hyphae, sc- sporocyst, co- conidia, as- ascus.

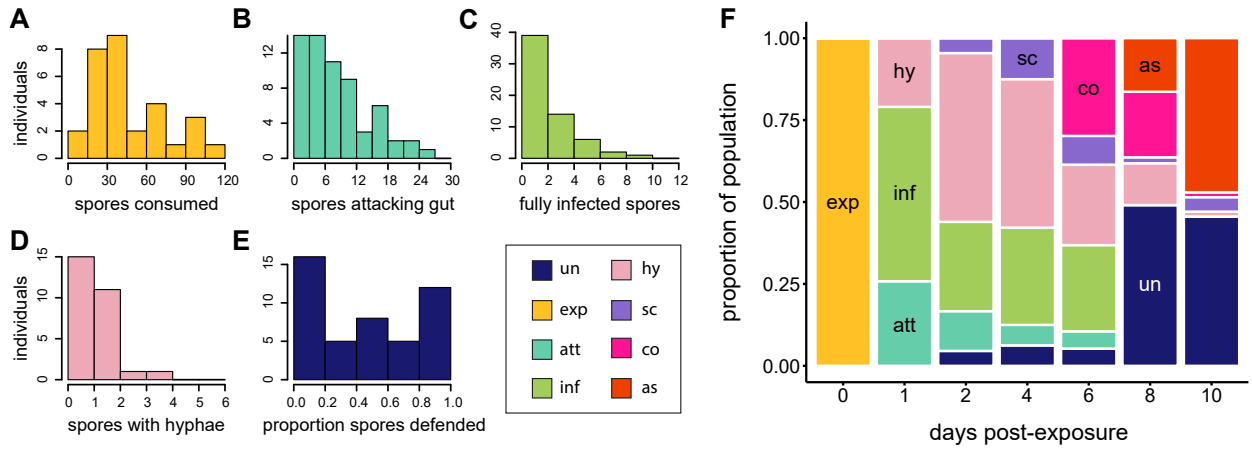

Figure 1.2. *Metschnikowia* spores can be decomposed into multiple steps of infection, each with a declining probability of success. Hosts are exposed to spores while feeding (**A**) and a subset of consumed spores attack the gut (**B**). Some attacking spores enter and infect the body cavity (**C**), but few produce hyphae (**D**). Hosts vary in the proportion of spores they defend with haemocytes (**E**). Hosts transition among infection stages through time (**F**) and infection clearance is evidenced by the increased proportion of uninfected individuals toward the end of the ten-day period. Labels: **un**- uninfected (dark blue), **exp**- exposed (yellow), **att**- attacked (teal), **inf**- infected (green), **hy**- hyphae (pale pink), **sc**- sporocyst (purple), **co**- conidia (dark pink), and **as**- ascus (red).

CHAPTER 2: HOST CONTROLS OF WITHIN-HOST DISEASE DYNAMICS

Abstract

Infectious disease is a global issue, affecting our ecosystems, our economy, and our public health. As we try to understand and predict infectious disease, it is important to know what processes regulate the spread of infection. Historically, disease ecologists have focused on the between-host determinants of transmission, involving both biotic and abiotic factors in the environment. However, because the host itself is an environment, there is a current push for more integrative perspectives that consider how host immunity and within-host processes affect disease. Such integrative work can be challenging to accomplish due to costs and difficulties associated with measuring host immunity, and this is particularly true for invertebrate systems for which a paucity of information on immunological mechanisms and their variation has hindered progress. I propose a general model for measuring host immune defenses and within-host disease dynamics which I developed using an invertebrate host—fungal pathogen system. The Resistance Clearance Markov model breaks the infection process down into its constituent steps of exposure, invasion, and establishment and provides associated probabilities for a host's ability to resist and clear infections. Application of a Gillespie algorithm to the model-estimated probabilities allows for the visualization of within-host dynamics and determination of the rate-limiting step for parasite and pathogen populations. In my model system (*Daphnia dentifera* and the fungal pathogen, *Metschnikowia bicuspidata*) both resistance and clearance constrain the prevalence of infection; that is, identical levels of exposure can result in pronounced differences in infection outcomes based on the strength and interactions of resistance and clearance. The Resistance Clearance Markov model will be a powerful tool for estimating immunological traits and within-host dynamics of understudied host-parasite interactions.

Body

Parasites and pathogens reside primarily within their hosts but attempts to understand the ecology of infectious disease often neglect within-host processes. The hidden nature of within-host disease dynamics can make them difficult to observe and quantify. Moreover, a living host ecosystem introduces unique complexities and feedbacks that are absent from abiotic systems (Rynkiewicz et al. 2015). Despite these challenges, linking within-host dynamics with between-

host transmission has become a central goal for understanding infectious disease (Ellner et al. 2007; Graham et al. 2007; Beldomenico et al. 2009; Beldomenico et al. 2010; Handel & Rohani 2015). One of the primary features that distinguishes within-host from between-host disease dynamics is the immune response, a suite of physiological defenses that hosts use to prevent the invasion and establishment of an infection or suppress its growth. For infectious diseases of both economic and public health concern, we have a limited understanding of how immunological processes regulate parasites and pathogens in non-human hosts (Hawley & Altizer 2011) and this is particularly true for invertebrate hosts.

Six of nine neglected tropical diseases- causing over one billion human infections per year- are transmitted to humans by invertebrates (Hollingsworth et al. 2015), but the immunological mechanisms of these medically important species remain vastly understudied (Fig. 2.1; Loker et al. 2004; Pila et al. 2016; Azambuja et al. 2017; Sloan & Ligoxygackis 2017). For instance, the basic characterization of haemocytes in mosquito vectors is only a recent endeavor (Wang et al. 2011), despite knowledge of these cellular effectors since the late 1800s (Metschnikoff 1884). While for some invertebrates there is increasing understanding of the sophistication of immune mechanisms (e.g. immunological specificity and memory in snails, Adema & Loker 2015; Coustau et al. 2015; Pinaud et al. 2016), few studies have addressed how these mechanisms operate in natural systems, how sensitive they are to environmental change, and how they modulate disease risk and transmission (Fig. 2.1). Determining the relative importance of immune defenses in the natural world is critical as invertebrates face novel environmental stressors that can disrupt or decrease levels of immunity. Moreover, the movement of infectious diseases to new geographic regions presents an urgent need to determine whether and how naïve populations will defend against disease invasion. Ultimately, a rudimentary understanding of invertebrate immunity and its variability will hinder attempts to generalize regarding how immune function contributes to natural disease processes.

Understanding the basis and extent of variation in host susceptibility, and how that variation contributes to disease regulation, is a prerequisite for predicting and controlling disease. From trypanosomes in triatomine insects to schistosomes in snails, many parasites and pathogens of invertebrates possess distinct within-host stages from which immune defenses can be estimated. Simple models that distill and quantify these immune defenses, and particularly those that are grounded in data, have immense value for our understanding of infectious disease

(Graham et al. 2007; Handel & Rohani 2015; Bradley & Jackson 2008). Here, I propose a general model for quantifying invertebrate immune defenses which I developed using a *Daphnia* host – fungal pathogen system with environmental transmission. The Resistance Clearance Markov model (hereafter, "RCM model") is a discrete-state continuous-time Markov model used to measure two broad classes of immune defense and to characterize within-host dynamics. Infection is a multistage process, beginning with exposure and culminating in the production of infective stages, and I used this process to guide my classification of immune defenses. First, when hosts are exposed to parasites or pathogens, infection can be prevented by *resistance*. Resistance bars parasites from entry and encapsulates physical and chemical barriers, such as those present in the midguts of Dipteran vectors (Michalski et al. 2010). Second, if an infection successfully establishes, the infection can be eliminated by host *clearance*. Clearance removes parasites and comprises the immunological processes occurring within the host body, such as the killing of trematode sporocysts by snail cellular and humoral responses (Pinaud et al. 2016). Both resistance and clearance are accounted for as general immune defenses in the RCM model.

In the RCM model, I collapsed a pathogen's complex within-host life cycle (Stewart Merrill & Cáceres 2018) into a finite set of translatable epidemiological states (Fig. 2.2A). I then used the RCM model (Fig. 2.2B) to estimate probabilities of resistance (the transition from exposed to uninfected) and clearance (the transition from infected to uninfected) from empirical data and applied a Gillespie algorithm to model the movement of hosts through the Markov process (Fig. 2.3). Through the RCM approach, I isolated resistance from clearance and found that successful infections in the *Daphnia*—fungus system were largely driven by genetic variation in clearance (Fig. 2.4). Experimental tests confirmed each defense as important for regulating infection (Appendix B.10). Within-host dynamics estimated with the Gillespie algorithm well approximated longitudinal results (Fig. 2.2A) and demonstrated that infections peak early after exposure, decline as hosts clear infections, and stabilize when infected hosts achieve late infection stages that cannot be cleared (Fig. 2.3). This finding was confirmed by empirical results in which clearance declined with the progression of infection (Appendix B.10). Visualizing these within-host dynamics provided key information on host defenses: maximal pathogen prevalence was constrained by host resistance, with greater probabilities of resistance resulting in lower prevalence peaks (Fig. 2.3A and Appendix B.4), and clearance determined the

growth in the size of the uninfected class from maximal prevalence to the end of the pathogen's within-host development (Fig. 2.3B and Appendix B.4).

By accounting for the multiple steps of infection- from parasite exposure, to invasion, to establishment- this study refines the connection of between-host and within-host disease dynamics and provides a simple quantification for the host controls of disease. Since the pioneering work of Anderson & May (1981), host susceptibility and immune defense have been described by two parameters: susceptibility is embedded in the transmission coefficient, β, and movement from infected to susceptible or immune classes is described by the recovery coefficient, γ. Both of these coefficients can be estimated phenomenologically, although β remains particularly challenging to parameterize because it encompasses many different processes and is often back-calculated from prevalence data (McCallum et al. 2017). My model-estimated transmission rates (Appendix B.7) consider these linear steps to infection, and by tracking individuals and their states, provide direct estimates of the recipient portion of β. Likewise, my model-estimated clearance rates (Appendix B.7) provide empirically derived estimates of γ by tracking transitions from the infected state back to the uninfected state. These rates likely exceed traditional estimates of γ because they incorporate the immediate recovery from nascent infections that often go undetected (Stewart Merrill & Cáceres 2018).

When integrating within-host dynamics into infectious disease models, the increase in understanding is not always worth the cost of model complexity. For instance, models that nest within-host processes into between-host transmission (e.g. Feng et al. 2013) often incorporate immunological responses that can be challenging to measure, may not always be informative (Bradley & Jackson 2008; Graham et al. 2011) and may be inessential for understanding between-host dynamics (Mideo et al. 2008). But simple instantaneous transitions from uninfected to infected states, such as those encapsulated by the transmission coefficient β, neglect important biological information (McCallum et al. 2017). The RCM framework is a functional alternative to nested models because it accounts for immune defenses but does not rely on their direct measurement; in other words, the model focuses on immunological outcomes without measuring the mechanisms that produce those outcomes. By isolating the steps of host exposure, barriers to infection, and infection clearance, my model allows the identification of the rate-limiting step for parasite populations, which may have broad relevance across disciplines.

The results of this study demonstrate that the infection of susceptible hosts, even in purportedly simple invertebrates, is regulated by factors beyond pathogen exposure. Resistance and clearance probabilities varied considerably among host genotypes, with resistance values ranging from 5% to 40% and clearance values ranging from 0% to 60% (Appendix B.9). The ability to quantify these probabilities may be a powerful tool for understanding infection patterns in vectors. With the observation that disease prevalence is typically low in invertebrate vector populations, scientists have begun to suspect that immune processes may be filtering out natural infections (Sloan & Ligoxygakis 2017; Coustau et al. 2015). However, these studies have not quantified exposure so have been unable to measure the extent to which host immunological traits constrain prevalence. The genetic and environmental factors that shape immune function in invertebrates are being described at an increasing rate (Fig. 2.1b), but these findings typically emerge from laboratory-controlled studies that do not replicate natural environmental conditions. While uniting field patterns with the underpinnings of immunity may be currently unrealistic, estimating natural variation in their emergent properties, resistance and clearance, is a feasible objective. Quantitative methods like the RCM answer the call to find integrated avenues for disease management that include vectors and their flexible immunity (Adema et al. 2012).

Infection is considered theoretically as an instantaneous process, moving an individual from a susceptible to an infected class. By estimating resistance and clearance probabilities, I apportioned this process to two separate ecological steps: parasite invasion and establishment. Resolving these and additional steps of infection can drive progress in biodiversity-disease research. For instance, heterogeneous susceptibility in populations and communities has been attributed to the presence of susceptible disease “amplifiers” and resistant disease “diluters”. This framework - the dilution effect - predicts an increase in disease risk with the loss of diluter hosts (Ostfeld & Keesing 2000). However, fundamental questions remain as to whether putative diluters consistently function as such, and what mechanisms enable diluters to filter out infections. Accounting for within-host processes is an important step for identifying diluter species and for disentangling the relative roles of exposure, resistance, and clearance in shaping diluter capacity.

Accounting for immune defense also broadens the conceptual framework of disease ecology to include the energetics of within-host processes, which may allow us to better estimate the effects of parasites on host populations. I found that clearance was the strongest predictor of

prevalence in *Daphnia* hosts (Fig. 2.4), which reinforces two important ideas. First, that early infections can be pervasive and exceed the prevalence of late and conspicuous infections (Fig. 2.3; Stewart Merrill & Cáceres 2018; Stewart et al. 2018), and second, that uninfected hosts can have hidden histories of exposure to and clearing of parasitic infections. The immune defenses that promote clearance are often energetically costly, potentially resulting in decreased growth and productivity of the host. When clearance is the dominant defense within a population, that population may face high energetic costs in response to chronic pathogen exposure. Hence, quantifying clearance opens the door for exploring hidden and non-consumptive regulatory effects of parasites (Kuris et al. 2008).

Contrary to clearance, hosts exhibited low probabilities of resistance (Fig. 2.4a). These low values are likely an outcome of the high density of pathogen spores provided in the experimental inoculum. Indeed, the confirmatory experiment used a lower pathogen dose and yielded higher probabilities of resistance (Appendix B.10). With greater exposure to infectious agents, the probability that a single agent will successfully infect a host increases (Nguyen et al. 2013); that is, the probability of complete resistance declines with dose. Clearance should also become less effective as the density of established infections achieves a threshold value above which immune defenses become overwhelmed. Identifying how resistance and clearance co-vary with exposure may help decompose and explain non-linearity of dose-response curves.

The results generated from the RCM model demonstrate that infectious disease can be regulated by both host traits and within-host processes. Use of this model on invertebrates in natural systems will reveal the extent to which invertebrate immunity contributes to the distribution and transmission of disease.

Methods

Background and experimental design

I selected a host-pathogen system with environmental transmission, where infection results from the consumption of infective stages. The host, *Daphnia dentifera*, is a cyclically parthenogenetic zooplankton that is widely distributed across the Midwestern United States and the pathogen, *Metschnikowia bicuspidata*, is a common ascomycete fungus. *Metschnikowia* produces environmentally transmitted spores that are consumed by filter-feeding *Daphnia*. Ingested spores attack the host's gut membrane, and spores that successfully cross the gut barrier

develop into a series of infection stages that ultimately produce thousands of infective ascospores that are released upon host death (Ebert 1995; Stewart Merrill & Cáceres 2018).

I standardized the maternal effects of eight *Daphnia* genotypes by rearing *Daphnia* for at least three generations under controlled conditions (Lynch & Walsh 1998). Experimental individuals were then collected from standardized mothers as <24-hour-old neonates. Neonates were isolated individually into 45 ml of filtered lake water and fed daily with $4x10^4$ cells of the high quality algae, *Ankistrodesmus falcatus*. Eight days after isolation, experimental *Daphnia* were transferred to inoculation chambers (15 *ml* falcon tubes) containing 10 *ml* of filtered lake water, and were inoculated with 500 spores per *ml* of *Metschnikowia*. *Daphnia* remained in inoculation chambers for a 24 *h* inoculation period during which tubes were inverted hourly for the first 12 *h* to ensure suspension of the infectious spores. After this inoculation period, *Daphnia* were transferred to individual tubes containing 45 *ml* fresh and spore-free filtered lake water. Exposed *Daphnia* were then culled at 1, 2, 4, 6, 8, and 10 *d* post-exposure and assessed under high magnification (400x) to determine the individuals' stages of infection (Stewart Merrill & Cáceres 2018). Infection staging was destructive, and each day's examination was performed on a new cohort of individuals. Sample sizes varied due to differential reproduction and mortality among genotypes (Appendix B.5).

Following Stewart Merrill & Cáceres (2018), individuals were classified into the following seven infection stages: **Exposed**, where *Metschnikowia* spores had entered the host gut and had punctured the gut epithelium without fully crossing into the *Daphnia* haemocoel, **Stage I**, where at least one *Metschnikowia* spore had fully crossed into the host haemocoel, **Stage II**, where at least one spore had emitted hyphae, **Stage III**, where fungal sporocysts were detectable, **Stage IV**, where conidia had been released from sporocysts and were free-floating within the haemocoel, **Stage V**, the traditional diagnostic form of this infection, where spore-containing asci completely filled the host haemocoel, and **Uninfected**.

Discrete-state continuous time Markov model

The infection stages were collapsed into a simplified discrete state space (Fig. 2.2a and Appendix B.1). This state space consists of four states: exposed (*E*), infected (*I*), uninfected (*U*), and dead (*D*), with the four states allowing for the estimation of the probabilities of infection, resistance, clearance, and mortality (Fig. 2.2b). Transition probabilities among states were

modeled with a continuous Markov process (Appendix B). This approach is well suited for longitudinal aggregate data, where state distributions are assessed over evenly distributed time points using separate cohorts of individuals. In brief, maximum likelihood was used to estimate the state-to-state instantaneous transition rates, which produced transition rate matrices, or *Q*-matrices. Resulting *Q* matrices were then exponentiated to calculate the probability matrices, or *P*-matrices, which described the probabilities of state-to-state transitions. I paired all Markov models with Ordinary Differential Equations to ensure parameter identifiability.

Model assumptions

For my model assumptions, I allow hosts to transition forward in the infection process and assume no reverse transitions. In particular, reversals to the exposed state are not possible because the exposure period was restricted to 24 *h*, after which individuals were transferred to parasite-free water. Further, hosts were maintained in isolation, thereby precluding exposure after the 24 *h* inoculation period. I allow hosts to transition from exposed to uninfected, which reflects parasite resistance, and I allow hosts to transition from infected states to uninfected, reflecting parasite clearance (Fig. 1.2b). While limiting exposure may reduce susceptibility in *Daphnia* hosts, I confirmed that the spore dose was sufficiently high to result in exposure for all individuals; all of the *Daphnia* that were examined at 24 *h* post-inoculation (N=71) had pathogen spores either partially or fully penetrating their gut epithelia. I assumed constant mortality for all states based on preliminary analyses and prior knowledge of this system. While *Metschnikowia* must kill its host in order to be transmitted, pathogen-induced mortality occurs in time periods later than those studied in the current experiment. *Daphnia* that clear infections still possess spores in their gut membranes that serve as signatures of their past encounters with the parasite. Spores lodged in the gut were witnessed throughout the ten-day experiment and I assumed that spores present after eight days post-exposure were inactive, due to the almost complete absence of hyphae growing from spores after day eight.

Model output

Markov models were run for each genotype individually and for all genotypes combined as a common population. Due to low sample sizes in some of the genotypes, four genotypes were combined into low (genotype N = 2) and medium (genotype N= 2) susceptibility populations

(S1). I ran 500 iterations of each model to assess convergence, to quantify error, and to determine each model's sensitivity to initial conditions (Appendix B). For each transition probability, I calculated the mean and standard error of the distributions resulting from the 500 iterations. Finally, I used a Gillespie algorithm to model each population's transition through the Markov process. Markov models were constructed and run in MatLab version 9 and statistical analyses were run in R version 3.3.2. Figures were generated in MatLab and in R using ggplot2.

Experimental confirmation

For most internal parasites and pathogens, detecting infection is destructive to the host, and the Markov models are structured to allow for host destruction. However, *Daphnia* have the useful attribute of being transparent, and as a proof of concept, I used their transparency to evaluate whether resistance and clearance were definitively occurring. I exposed 33 total *Daphnia* from the same eight genotypes to *Metschnikowia* following the previously described inoculation methods, but at a lower spore dose (200 spores/ml). Following exposure (examination 0), *Daphnia* individuals were examined twice throughout the infection process: once at variable time points between days two and eight post-inoculation (examination 1), and once at day 10 when patent infections are observable (examination 2). The tracking of individual *Daphnia* across three time points allowed for the direct empirical confirmation of infection, resistance, and clearance (Appendix B.10).

Systematic literature survey

I conducted a systematic literature survey focused on studies of invertebrate immunity and susceptibility for six neglected tropical diseases transmitted by invertebrate hosts (Hollingsworth et al. 2015). Results were restricted to those studies returned from Web of Science using three keyword categories: 1) invertebrate host descriptors, 2) disease descriptors, and 3) immunity/susceptibility. For example, a search for studies on immunity/susceptibility of snails hosting *Schistosoma* spp. took the form: "snail*" AND "Schistosom*" AND "susceptibil* OR immun*". Of the resulting studies, only those measuring or reviewing susceptibility and immunity in invertebrate hosts were retained (studies of humans or mouse models were discarded). Studies were then characterized by the type of study. "Functional" denotes studies in which the basis and mechanisms of susceptibility, including underlying immune responses, were

characterized either in control hosts or in hosts exposed to the target pathogen. “Variable” denotes studies in which variation in susceptibility or immune responses was measured in the laboratory. These studies included extrinsic treatments like temperature, diet, additional parasite species or strains, and microbiome manipulations, as well as the measurement of intrinsic factors that may influence susceptibility and immunity, like host age, sex or genetic background. “Ecological” denotes studies in which susceptibility and/or immune responses were characterized from natural populations in order to examine their variation across environments and possible responses to environmental factors (e.g. heat, altitude, precipitation). In total, 448 invertebrate studies were retained from an initial 1,910 search results and were grouped by disease and type of study (Appendix B.11).

Figures

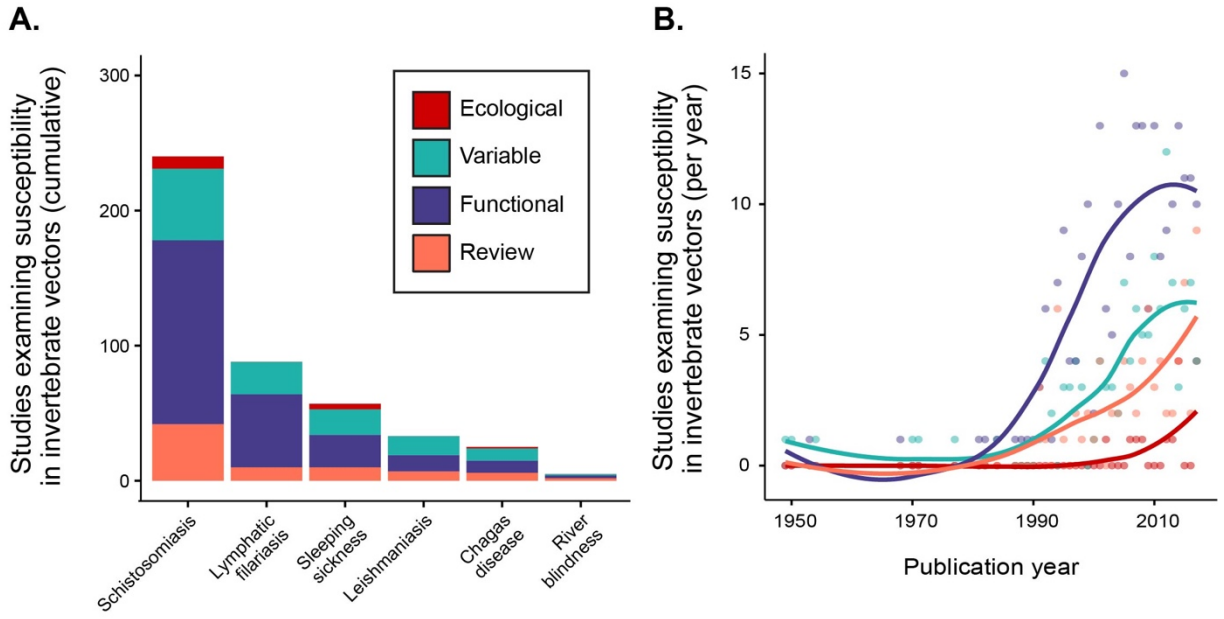

Figure 2.1. Susceptibility and immunity in invertebrate vectors of neglected tropical diseases is understudied and studies documenting natural variation in vector immunity (red) are particularly rare. **A**: A comparison of the number of publications on invertebrate host susceptibility/immunity for six neglected tropical diseases (NTDs) categorized by type of study: review papers (orange), studies characterizing functional aspects of immunity/susceptibility (purple), laboratory studies measuring immunological variability (green), and ecological studies measuring natural variation in immunity/susceptibility (red). **B**: Cumulative number of studies (all six NTDs combined) per year, by study type. Research on vector susceptibility accelerated in 1980s, with the functional characterization of susceptibility/immunity representing the dominant form of study.

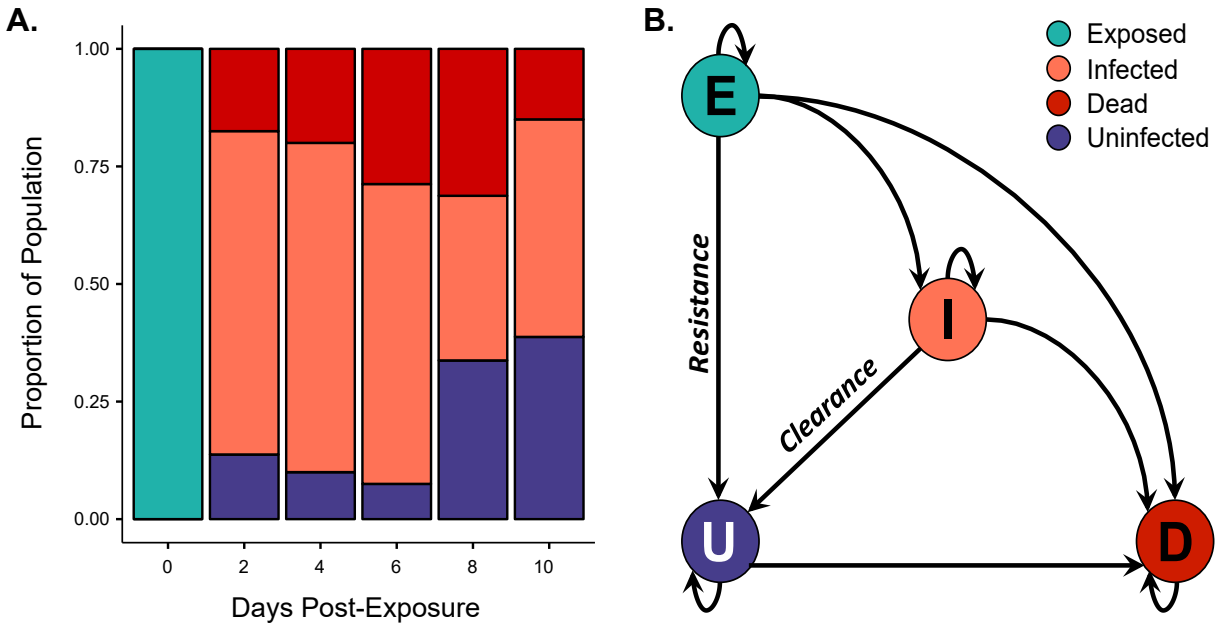

Figure 2.2. A. The progression of hosts across Markov states through time. Hosts were exposed to the pathogen inoculum on day 0 and were observed microscopically to stage their infections on days 2, 4, 6, 8 and 10 (N day^{-1}=80). Infections were collapsed into four discrete Markov states: exposed (green), infected (orange), uninfected (purple), and dead (red). **B**. The Resistance Clearance Markov model is a discrete-state continuous-time Markov model to estimate broad classes of immune defense from epidemiological classes. Host resistance is quantified as the probability of transitioning from exposed to uninfected. Host clearance is quantified as the probability of transitioning from infected to uninfected. Death is an absorbing state from which hosts cannot transition.

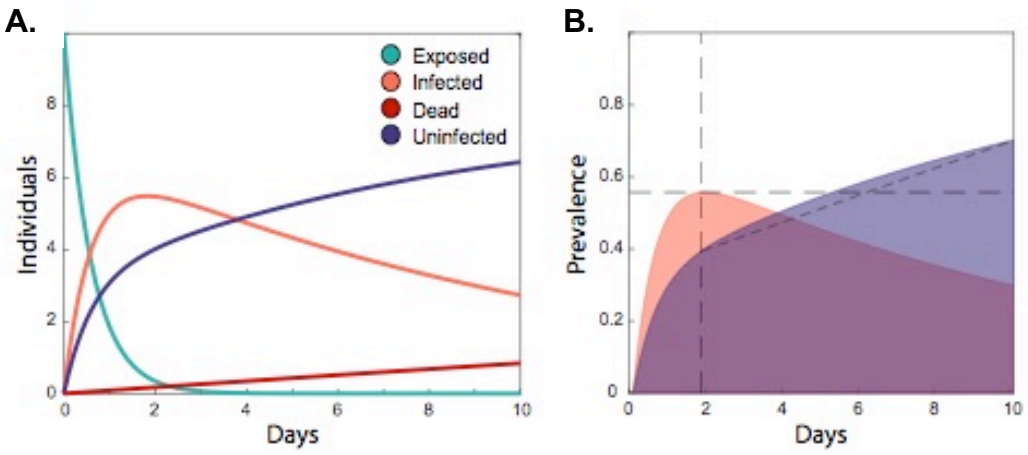

Figure 2.3. A. Application of a Gillespie algorithm to the model-estimated rates for one host genotype (W2) shows the transition of ten hosts among the four states through time. Hosts quickly transition out of the exposed state (green) as they become infected (orange) or as infections are resisted. The uninfected class (purple) grows with initial resistance and with the clearance of infections through time. Mortality is constant, so dead individuals (red) accumulate through time. **B.** These within-dynamics show signatures of both resistance and clearance. Here, I show the proportion of the live population that is infected (orange) and uninfected (purple). The early peak in prevalence (intersecting dashed lines) is strongly associated with the model-estimated probabilities of resistance ($p<0.001$, $R^2=0.99$), while the average growth of the uninfected class from this early peak to the end of the pathogen's development (dashed slope) is strongly associated with the model-estimated probabilities of clearance ($p=0.012$, $R^2=0.83$). I provide an analytical solution demonstrating the relationship between defense probabilities and the properties of the within-host dynamics (Appendix B.3).

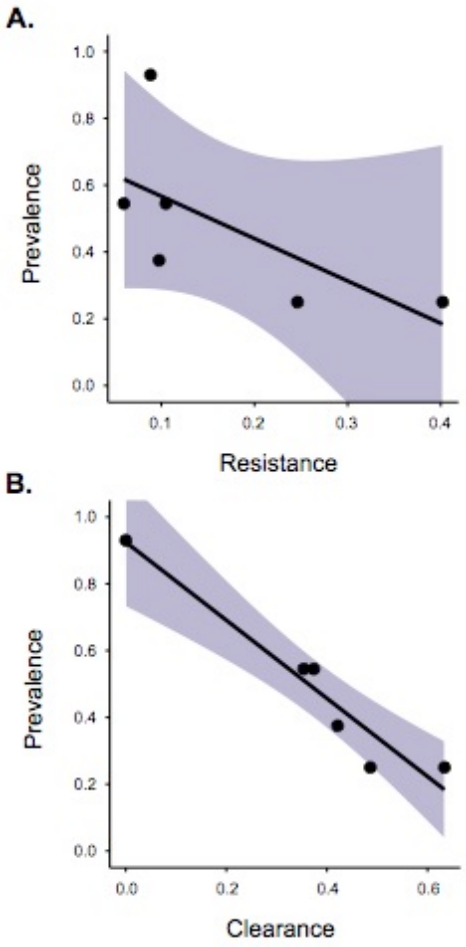

Figure 2.4. Final infection prevalence is predicted by the probability of clearance (**B**; $p = 0.002$; $R^2 = 0.93$), but not resistance (**A**; $p = 0.157$; $R^2 = 0.43$) for six host populations. Prevalence data were collected empirically by calculating the proportion of live hosts that were infected ten days after pathogen exposure. Resistance and clearance probabilities were estimated from approximately 500 iterations per population of the Resistance Clearance Markov model. Shading represents standard error of the fit regression.

CHAPTER 3: PARASITE EXPOSURE, HOST SUSCEPTIBILITY, AND THE EMERGENCE OF EPIDEMICS

Abstract

Disease emergence is thought to depend on a population's level of parasite exposure and its individuals' susceptibility to infection. However, the relative contribution of these two factors to disease remains unclear. The interaction between the aquatic host, *Daphnia dentifera*, and its fungal parasite, *Metschnikowia bicuspidata*, provides powerful solutions for measuring parasite exposure, host susceptibility, and disease spread in natural systems. I used this host-parasite interaction to evaluate the relative importance of exposure and susceptibility for driving epidemic emergence. In six lake ecosystems, I tracked the following metrics from the pre- to peak- epidemic periods: parasite exposure (the number of parasite spores found attacking wild-caught hosts), host susceptibility (the number of parasitic spores a host can recover from), host immunological traits, and the prevalence of infection for all stages of parasitic development. Early infection stages were common in the months prior to epidemics, suggesting that parasite exposure alone is insufficient to trigger epidemic emergence. Bringing together parasite exposure and host susceptibility data revealed that epidemics depended critically on their interaction; epidemics only emerged when a population's level of exposure exceeded its hosts' capacity for recovery. Additionally, I found that the host immune response (haemocytes) played a strong role in regulating parasites at the population level. My empirical work provides a comprehensive demonstration of how parasite exposure and host susceptibility interact to drive infectious disease and highlights how individual immune responses can scale up to affect broad epidemiological patterns.

Introduction

Theory predicts that disease can spread when two criteria are met: *i*) infectious propagules must be present in the environment and *ii*) hosts must be able to acquire and support infection to the point of transmission (Gilbert & Parker 2006). More generally stated, disease depends on both parasite exposure and host susceptibility (Fig. 3.1A; Combes 2001; Hall et al. 2010). Accordingly, disease should fail to emerge when either or both of these criteria are not met, but we lack strong empirical evidence linking both exposure and susceptibility with the

failure or success of disease. One challenge contributing to this data deficiency is that disease in wildlife is typically studied only after it becomes detectable. Without baseline data, we cannot observe failures of disease emergence, and it becomes difficult to isolate and determine the set of conditions required for successful emergence (Harvell et al. 2002; Plowright et al. 2008). An additional challenge is that reliable metrics for exposure and susceptibility have been largely absent from wildlife disease research (McCallum et al. 2017). Levels of parasite exposure are often approximated from the prevalence of infection, which can dramatically underestimate the true level of exposure within a population (Stewart et al. 2018). Conversely, susceptibility and its immunological basis is typically neglected in wildlife disease research, because the tools to measure immunity can be costly, complicated, and at times, uninformative (Boughton et al. 2011; Graham et al. 2011; Pedersen & Babayan 2011; Downs et al. 2014).

Exposure and susceptibility are interconnected processes; neither can be interpreted without its counterpart. This connection is best illustrated through the dose-response curve, which describes how an individual's probability of infection increases as a function of parasite exposure (Fig. 3.1B). The dose-response curve demonstrates that the risk posed by a particular level of exposure is ambiguous without knowing the host's susceptibility. For instance, the relative risks posed by one flu virion, one malaria-infected mosquito, and one hookworm egg cannot be adequately compared without a general idea of their respective dose-response curves. Likewise, host susceptibility is conditional on parasite exposure and cannot be defined without reference to the level of exposure a host faces. Because exposure and susceptibility are intrinsically linked, understanding and predicting epidemic emergence may require the dual consideration of these processes, as well as their interaction.

How do we measure exposure and susceptibility in wildlife systems? This question has long plagued disease ecologists, and I propose that the developmental trajectory of parasites inside of their hosts may be a powerful way to measure these two factors. Many parasites have a series of within-host morphologies or complex within-host migrations over which they transition through time. For instance, parasitic trematodes enter their snail hosts as miracidia, develop into sporocysts and rediae, and ultimately produce infectious cercariae (Esch & Fernandez 1994). Similarly, the fungal pathogen *Ophiocordyceps unilateralis* attaches to an ant as an ascospore, breaches the ant's exoskeleton as a hypha, then reproduces within the ant before later emerging as a fruiting body (Evans et al. 2011). The temporal dynamics of host-parasite interactions carry

key information: the earliest developmental stages are the manifestation of exposure, while the latest developmental stages are the outcome of the host's susceptibility to infection.

Susceptibility is an intrinsic property of the host, resulting from host traits and within-host processes that can inhibit parasites during the infection process. In a broad sense, the infection process can be decomposed into the steps of parasite exposure, parasite invasion, and parasite establishment, which together yield two critical transitions at which hosts can halt infection (Chapter 2). First, as parasites attempt to enter the host, hosts can fight back with resistance, using constitutive physical and chemical barriers to prevent invasion. Parasites that breach host barriers will attempt to grow and reproduce within the host, but can be impeded by host clearance, in which immunological responses are used to kill establishing parasites. In determining how susceptibility contributes to disease dynamics, measuring host traits associated with resistance and clearance may help describe how within-host processes regulate the parasites that cause disease.

In this study, I examine the relative contributions of parasite exposure and host susceptibility to the emergence of disease epidemics and ask how host traits contribute to the regulation of parasites. The study system, *Daphnia dentifera* and its fungal parasite, *Metschnikowia bicuspidata*, is particularly tractable for my questions for two reasons. First, *Metschnikowia* produces annual epidemics in lakes that serve as units of replication for disease emergence (Cáceres et al. 2014), such that I can track host populations before epidemics emerge and tabulate disease failures and successes. Second, recent descriptions of the complete *Metschnikowia* life cycle, as well as host responses to infection, enable the precise estimation of parasite exposure and host susceptibility in natural systems (Chapter 1; Chapter 4; Stewart Merrill & Cáceres 2018; Stewart Merrill et al. 2019). Together, these elements provide a powerful system for empirically testing how exposure and susceptibility interact to influence the emergence of epidemics.

I measured parasite exposure by tracking *Metschnikowia* developmental stages and *Metschnikowia* spore levels in natural *Daphnia* populations for six months spanning the pre-epidemic and epidemic periods. Using experimental infections on wild-caught *Daphnia*, I also measured a series of host traits and quantified each population's susceptibility through time. I followed multiple lines of inquiry to assess the importance of exposure and susceptibility for the emergence of epidemics. By uniting the requirements for disease (Fig. 3.1A) with their

interconnectedness (Fig. 3.1B), I found that *Metschnikowia* epidemics depended on a critical interaction between parasite exposure and host susceptibility.

Materials and Methods

Study System

Metschnikowia bicuspidata is an ascomycete fungal parasitoid of the freshwater zooplankter, *Daphnia dentifera*. *Daphnia* hosts are exposed to *Metschnikowia* spores while filter-feeding, and consumed spores must penetrate the *Daphnia* gut and enter the body cavity to initiate infection. Once *Metschnikowia* spores breach the gut barrier, they progress through a series of developmental stages, including the hypha, sporocyst, conidium, and ascus stage (Chapter 1; Stewart Merrill & Cáceres 2018). *Daphnia* respond to infection with an up-regulated cellular response that can kill *Metschnikowia* during its early development (Chapter 4; Stewart Merrill et al. 2019). If the infection is not cleared, *Metschnikowia* is lethal, as death of the host is required to release spores back into the environment (Ebert 2005).

In temperate *Daphnia* populations, annual *Metschnikowia* epidemics tend to emerge in late August and early September, but there can be variation in the timing of emergence (Cáceres et al. 2006; Hall et al. 2011; Shocket et al. 2018). To understand the processes that result in epidemic emergence, I sampled *Daphnia* populations over six months spanning the pre-epidemic and epidemic periods. I sampled six lakes in Central Indiana every two weeks between 5-Jun and 4-Dec 2017 (see Appendix C.1 for a complete description of the sampling regime, locations, and resulting sample sizes). Plankton were collected using three vertical tows of a 12-cm diameter Wisconsin-net (70 μm mesh). Tows were pooled in 2L Nalgene containers and held on ice during transport back to Indiana University. Upon returning to the lab, adult female *Daphnia dentifera* were isolated individually for use in one of two datasets. The "exposure dataset" stemmed from immediate observations of wild-caught *Daphnia* and identified natural infection patterns of *Metschnikowia*, including the prevalence of each developmental stage and levels of spore exposure in *Daphnia* populations (Table 3.1). The "susceptibility dataset" stemmed from experimental infections performed on wild-caught *Daphnia* to quantify a series of host traits and each population's spore threshold (Table 3.1). In both datasets, individual-level measurements were taken to quantify population-level averages at each sampling event.

Exposure Dataset

Field collected *Daphnia* were observed to measure each population's exposure to *Metschnikowia*. Within 24 h of collection, approximately 50 adult females per lake were haphazardly selected from plankton samples and examined under high magnification using a Leica DMLB compound microscope paired with a 40x objective (yielding total magnification of 400x).

Metschnikowia exposure via developmental stages: Each *Daphnia* individual was examined for the presence of *Metschnikowia*. If the parasite was absent, the individual was recorded as unexposed. If the parasite was present, I recorded the *Metschnikowia* developmental stage it possessed. These stages, in order of development, include: attacked, spore, hyphae, sporocyst, conidia, and ascus (Chapter 1; Stewart Merrill & Cáceres 2018). From these developmental stages, *Daphnia* were classified into four groups (Table 3.1). "Exposed" consisted of individuals harboring any *Metschnikowia* developmental stage. "Early interaction" consisted of individuals either in the attacked stage (spores were attacking their gut barriers and *Daphnia* could recover through resisting spore attack) or individuals with early infections inside the body cavity (*Daphnia* possessed spore, hyphae or sporocyst infections and could recover through clearing infection). "Within-host infection" comprised individuals with any *Metschnikowia* developmental stage within the body cavity (recovery, if possible, could only occur through clearing infection). "Late infection" consisted of the two latest *Metschnikowia* developmental stages (conidia and ascus) from which *Daphnia* could not recover. Further rationale for these groupings is provided in the statistical portion of the methods.

Metschnikowia exposure via spore counts: I scanned the full length of each *Daphnia* individual's gut and counted the number of *Metschnikowia* spores embedded in the gut barrier as well as those that successfully crossed into the body cavity (Chapter 4; Stewart Merrill et al. 2019). The sum of spores in these two locations (gut barrier and body cavity), or attacking spores, represents a measure of exposure at the level of the individual. Analagous to a predator attacking its prey in its attempt to consume the prey, attacking spores are those directly attacking their host in their attempt to infect the host. Using counts of attacking spores, I calculated three summary metrics for *Metschnikowia* exposure within a population (Table 3.1). Spore abundance is the average number of spores among all sampled *Daphnia*, both exposed and unexposed (analogous to parasite abundance, as defined in Bush et al. 1997). Spore intensity is the average

number of spores among exposed *Daphnia* (analogous to parasite intensity, as defined in Bush et al. 1997). Spore max is the highest spore count observed within an individual. While water samples have been used to estimate *Metschnikowia* spores in the environment (Civitello et al. 2013), my metrics provide direct estimates of what individuals are actually ingesting.

Susceptibility Dataset

An additional sample of field-collected *Daphnia* were isolated for use in experimental infections. At each sampling event, approximately 50 adult female *Daphnia* per lake were haphazardly selected from plankton samples. Individuals with conspicuous late infections (i.e. those with *Metschnikowia* infections detectable to the naked eye) were excluded in order to limit my assessment to susceptible individuals. Within 24 h of collection, *Daphnia* were placed individually into 10 ml filtered lake water and were inoculated with 200 spores/ml *Metschnikowia* along with 1 mg C/L of the high-quality algae, *Ankistrodesmus falcatus*. Tubes were inverted every 2 hours for the first twelve hours following inoculation to ensure suspension of the infectious spores.

Quantifying Daphnia traits: Parasitic infections result from a host's level of parasite exposure, the strength of its barriers to infection, and the efficacy of the its internal defenses. *Daphnia* traits associated with these three factors (parasite exposure, barriers, and internal defenses) were previously described and quantified for the current susceptibility dataset (Chapter 4; Stewart Merrill et al. 2019). In brief, after the 24 h inoculation period, *Daphnia* were examined microscopically (400x magnification) to track the spores they had been inoculated with. I scanned the length of each individual's gut and counted spores based on their locations. I counted spores free-floating in the gut lumen, spores embedded in the gut epithelium, and spores infecting the body cavity. The sum of spores in all three locations represents the host's spore consumption. The sum of spores embedded in the gut epithelium and infecting the body cavity represents the host's level of spore attack. The number of spores that successfully entered the body cavity represents the host's level of spore infection. Finally, I counted the number of spores infecting the body cavity that had host haemocytes (immune cells) aggregating on them and termed these "defended spores". Spore consumption (Table 3.1) is my proxy for a parasite exposure trait because it tallies the total number of spores observed in the host following inoculation. By regressing infecting spores on attacking spores, I evaluated my proxy for

barriers: gut penetrability (Table 3.1). Gut penetrability is the likelihood that spores attacking the host gut will successfully move into the body cavity. By regressing defended spores on infecting spores, I evaluated a proxy for internal defense: spore defense (Table 3.1). Here, spore defense is the likelihood that a spore infecting the body cavity will be defended against by host haemocytes.

Daphnia susceptibility via spore thresholds: On a monthly basis (every second sampling event) I held a target sample size of 25 inoculated *Daphnia* per lake until nine days post-inoculation to determine their infection fate. The average level of susceptibility for each population was then estimated using dose-response curves (e.g. Fig. 3.1B). To generate dose-response curves, I constructed generalized linear models (binomial distribution, logit link) testing for the effect of attacking spores on late infection status at day nine. These models allowed me to calculate spore thresholds for each population, or the number of spores required to produce a 50% probability of late infection (Table 3.1; Fig. 3.1; also known as "Infection Dose 50"). Spore thresholds serve as a standard measure of susceptibility in units of spores. Higher spore thresholds indicate lower susceptibility, as more spores are required to produce a late infection (purple line, Fig. 3.1B). Lower spore thresholds indicate higher susceptibility, as fewer spores are required to produce a late infection (red line, Fig. 3.1B).

My monthly assessment of infection fates meant that *Daphnia* susceptibility (via spore thresholds) was assessed over a coarser timescale than *Metschnikowia* exposure (assessed bimonthly, or every two weeks). Additionally, dose-response curves were only constructed using a subset of inoculated *Daphnia* (25 were held out of 50 inoculated). I developed an additional estimate of spore thresholds that used all inoculated *Daphnia* collected over all of the bimonthly samples. The growth of fungal hyphae (the stage of infection following spores infecting the body cavity) is a good early indicator of future infection: among lakes and timepoints, one hypha consistently resulted in a >50% probability of late infection. So, I could estimate spore thresholds for the full set of inoculated hosts by determining the number of attacking spores necessary to produce one hypha. There are tradeoffs involved in both of my approaches to spore thresholds. The monthly spore thresholds measured with classic dose-response curves (infection status regressed on attacking spores) are more precise, as they rely on actual infection outcomes. But these monthly data have lower sample sizes and a coarser timescale. The bimonthly spore thresholds measured using hyphae as an indicator (number of hyphae regressed on attacking spores) are less precise but have greater sample sizes and a finer timescale. In my analyses, I

evaluated both forms of spore thresholds to embrace their exclusive benefits. Further detail and examples of spore thresholds are available in Appendix C.3.

Epidemic Emergence

Epidemics are the pattern of increasing infection prevalence, owing to the spread of infection among individuals. For an infected *Daphnia* to transmit infection, it must die during the final stage of infection and release ascospores to the environment (Ebert 2005). Hence, I characterized epidemics based on the presence of late infections that cannot be immunologically cleared (the conidia and ascus stages). I determined the point of epidemic emergence by evaluating growth in the prevalence of late infections up to its maximal value (or peak prevalence). Epidemic emergence is the point at which late infection prevalence begins to continually increase toward its maximum, while exceeding background rates (Fig. 3.3).

Statistical Analyses

Investigating the drivers of epidemics: I qualitatively examined the roles of *Metschnikowia* exposure and *Daphnia* susceptibility in driving epidemic emergence by decomposing their interactions into early and late stages. During the early phase of this host-parasite interaction, hosts are either attacked by spores or harbor newly developing infections, and *Daphnia* can recover by resisting attack or clearing infection (Early interaction; Table 3.1). In the late phase of infection, *Daphnia* contain the pathogenic conidia and ascus stages (Late infection; Table 3.1). Because *Daphnia* cannot recover from late infections, their presence represents a measure of susceptibility. If epidemic emergence is driven by *Metschnikowia* exposure alone, epidemics should emerge whenever early interactions are present within a population. However, the occurrence of early interactions paired with the absence of late infections suggests that low *Daphnia* susceptibility may be inhibiting epidemics. I evaluated the prevalence of early interactions and late infections through time to qualitatively test these predictions.

To explicitly test the relative contributions of *Metschnikowia* exposure and *Daphnia* susceptibility in driving epidemic emergence, I developed competing models using an information theoretic approach (Burnham & Anderson 2002). For each lake and time point, I coded epidemic emergence as 0 or 1 and used generalized linear models (binomial distribution,

logit-link) to test the effects of different predictors on epidemic emergence. I developed four model types: 1) Null; 2) Exposure; 3) Susceptibility; and 4) Exposure and Susceptibility. The null model contained only an intercept. The exposure models contained any of the three spore metrics as predictors (spore abundance, spore intensity, spore max; Table 3.1). The susceptibility model contained the spore threshold as a predictor (Table 3.1). Having set exposure and susceptibility in the same currency (spores in the environment and spores required to produce infection) I used their difference, "delta", as a predictor in the exposure and susceptibility models. Delta could be the difference between each population's spore threshold and either its spore abundance, spore intensity or spore max. When delta is positive, the average spore threshold of a population exceeds its level of spore exposure. In this case, I predict an epidemic will not emerge because hosts are not susceptible to their current level of exposure (Fig. 3.1). Likewise, a negative delta value indicates that the level of spore exposure in a population exceeds the population's spore threshold. In this case, I predict an epidemic will emerge because the hosts are susceptible to the current level of exposure (Fig. 3.1). I performed model comparisons for both the monthly susceptibility data, which used late infections to quantify spore thresholds, and the bimonthly susceptibility data, which used hyphae to quantify spore thresholds.

For each model, I calculated AIC values and ranked models from lowest to highest AIC. The lowest AIC value represents the most likely model given the data. I compared model fits based on their performance relative the best-ranked model (ΔAIC), where a ΔAIC of two or greater represents substantially better fit. Finally, I compared models based on their model weights (w_i), which represent the probability that a model fits best, given the suite of models considered (Burnham & Anderson 2002). I initially included lake as a random effect in these models, but lake neither improved model fit (evaluated via AIC values) nor altered the qualitative results, so was removed to simplify model structure.

Evaluating whether and how Daphnia traits regulate Metschnikowia populations: Parasite exposure and host susceptibility represent two filters that, when simultaneously open, allow parasites to persist in an environment. But if parasites are present and the susceptibility filter is closed, parasites will be removed or "filtered" from the system (Fig. 3.1A; Combes 2001). Shifting focus from epidemic emergence to the underlying parasite population, I asked which *Daphnia* traits acted as the strongest filters for *Metschnikowia*. Late infections arise

through a linear series of events, and by breaking these events into their constituent steps, I could first determine whether a particular step filtered *Metschnikowia* out of the system. To make this determination, I regressed the prevalences of exposure, within-host infection, and late infection (each defined in Table 3.1) against each population's spore abundance. Then, I fit saturating Michaelis-menten curves to each of the three regressions (Real 1977). If host traits do not act as filters for the parasite population, all three curves should converge on the same shape: positively saturating as spore abundance increases up to a maximum prevalence. If host barriers impose filters, the within-host infection and late infection curves should deviate from the exposure curve: growing more slowly to their maximum prevalence. If host internal defenses impose filters, the late infection curve should deviate from the exposure and within-host infection curves: growing even more slowly to its maximum prevalence. While visual comparison of these curves was sufficient to evaluate model fit, I also compared each model's half-saturation constant (K_m) and standard errors.

Comparison of Michaelis-menten curves provided an indication of where in the infection process parasites were filtered from the system. But I also wanted to more directly investigate which host traits contributed to parasite removal to understand how changes in host traits might allow *Metschnikowia* to spread or epidemics to emerge. I evaluated three host traits- spore consumption (parasite exposure), gut penetrability (a barrier), and spore defense (an internal defense)- during periods of host filtering and epidemic emergence. Periods of host filtering represent times when parasite exposure was high, but late infections were low at the subsequent sampling event (e.g. the bottom right quadrant of Fig. 3.1A). I determined each lake's strongest host filtering period by evaluating the prevalence of early interactions at $t = i$ and the prevalence of late infections at $t = i + 1$ and then selecting that period which exhibited the largest decrease. Using general linear models, I then compared host traits across the two time periods.

In total, I processed 6,781 *Daphnia* hosts (3,289 in the exposure dataset and 3,492 in the susceptibility dataset), which allowed me to qualitatively and quantitatively estimate the relative roles of exposure and susceptibility in driving the emergence of disease epidemics. Additionally, my measurement of three host traits allowed me to examine how *Daphnia* hosts themselves contribute to the regulation of *Metschnikowia* populations. Summary tables containing exposure, susceptibility, and developmental stage data are available in Appendix C.2.

Results

Tracking the full set of *Metschnikowia* developmental stages revealed that the latest and most conspicuous infections underestimate the presence of *Metschnikowia* in natural populations. Prevalence of the latest stage of infection (the ascus stage), which typically serves as an indicator for disease in this system, was 4.5 times lower on average than the prevalence of exposure (Fig.3.2). The prevalence of *Metschnikowia* exposure also exhibited considerable variability among lakes and time points, for instance being as low as 0% in early June and achieving 100% during the epidemic period (Fig. 3.2). The patterns of exposure and late infections through time provided qualitative evidence that exposure alone could not explain epidemic emergence. Exposure consistently preceded epidemics across the study populations and never resulted in an epidemic in one lake (Beaverdam; Fig. 3.2).

I tested for the relative importance of parasite exposure and host susceptibility in driving epidemic emergence by competing models in an information theoretic approach (Table 3.2). From the monthly susceptibility data (where spore thresholds were determined using infection outcomes), the best-ranked model included both *Metschnikowia* exposure and *Daphnia* susceptibility. This best-ranked model (Exposure and Susceptibility) had a model weight of 0.58 and outperformed the closest Exposure model and the closest Susceptibility model by more than 4 AIC points. The winning model predicted that epidemic emergence depends on the difference (delta) between each population's spore threshold and its spore maximum, and that epidemics become more likely as this difference approaches zero. All three of the Exposure and Susceptibility models were the most highly ranked of the model set and shared a cumulative weight of 0.86 (Table 3.2).

The monthly susceptibility results were mirrored in the bimonthly susceptibility data (where spore thresholds were approximated using hyphae). Again, the three Exposure and Susceptibility models outperformed all other models with a cumulative weight of 0.64. However, models in the bimonthly set were generally more competitive with one another. The winning model (which included the difference between the spore threshold and spore max) had a model weight of 0.29 and outperformed the next best model by less than one AIC point. This winning model outperformed the closest Exposure model by 2.44 AIC points and the closest Susceptibility model by 1.55 AIC points. Figure 3.4 provides plots of the raw data and associated

model predictions for the winning Exposure and Susceptibility models, the best-ranked Exposure model, and the best-ranked Susceptibility model from both the monthly and bimonthly sets.

Michaelis Menten curves relating spore abundance to the prevalence of exposure, within-host infection, and late infection indicated that *Metschnikowia* is filtered from populations at the within-host to late infection transition (Fig. 3.5). The prevalence of exposure was well-predicted by spore abundance ($p < 0.001$, $K_m = 1.04$, stderr = 0.08; Fig. 3.5 blue line), as was the prevalence of within-host infections ($p < 0.001$, $K_m = 1.76$, stderr = 0.18; Fig. 3.5 purple line). Each of these curves (exposure and within-host infection) shared similar shapes and half-saturation constants (K_m), suggesting that *Metschnikowia* is not filtered from populations by host barriers. The prevalence of late infections exhibited a curve that deviated from the exposure and within-host infection curves. Additionally, the late infection curve had a higher half-saturation constant and higher standard error when related to spore abundance ($p = 0.002$, $K_m = 6.12$, stderr = 1.86; Fig. 3.5 red line). The decoupling of late infections from spore exposure suggests that *Metschnikowia* is filtered from the system during its within-host development, potentially via host internal defenses.

In my final analysis, I compared host traits among time periods of epidemic emergence and host filtering. Spore consumption (a parasite exposure trait; Table 3.1) varied by lake ($F = 8.57$, $p < 0.001$) and by the interaction between lake and time period ($F = 6.39$, $p < 0.001$). However, spore consumption did not change in a general direction from host filtering to epidemic emergence ($F = 2.79$, $p = 0.10$; Fig. 3.6), suggesting that parasite exposure traits are not strong contributors to *Metschnikowia* regulation. Gut penetrability (a host barrier trait) was evaluated through the slope of the relationship between attacking spores and infecting spores (Table 3.1; Fig. 3.6). Gut penetrability varied by lake ($F = 11.02$, $p < 0.001$), and by the interaction between lake and time period ($F = 3.00$, $p = 0.019$), but did not change in a general direction from host filtering to epidemic emergence ($F = 1.27$, $p = 0.261$; Fig. 3.6). Spore defense (an internal defense trait) was evaluated through the slope of the relationship between infecting spores and defended spores (Table 3.1; Fig. 3.6). Spore defense varied by lake ($F = 12.21$, $p < 0.001$) and by the interaction between lake and time period ($F = 2.57$, $p = 0.038$). Unlike spore consumption and gut penetrability, spore defense varied strongly by time period ($F = 28.10$, $p < 0.001$). For four out of the five lakes that experienced epidemics, spore defense was highest during the period of host filtering and lowest at the period of epidemic emergence (Fig.

3.6). The decoupling of late infections from spore abundances (Fig. 3.5) paired with the decline in spore defense from strong host filtering to epidemic emergence together provide strong evidence that *Daphnia* internal defenses regulate *Metschnikowia* populations.

Discussion

The results of this study indicate that parasite exposure and host susceptibility together play critical roles in the emergence of epidemics. I found that *Metschnikowia* exposure was both common and relatively constant within *Daphnia* populations, but that some populations exhibited long-term resilience to epidemics. In support of my predictions, epidemics depended on the appropriate alignment of exposure and susceptibility, emerging when a population's spore exposure matched or exceeded its spore threshold. By decomposing *Daphnia*-*Metschnikowia* interactions into three stages, I determined that *Metschnikowia* is filtered (removed) by hosts during its within-host stage and that host internal defenses contribute to the strength of this filter. The results herein provide strong empirical evidence that host traits can enact considerable constraints on parasite populations and on the emergence of epidemics.

Cryptic infections were common among the host populations and I documented substantially higher prevalences and earlier appearances of *Metschnikowia* than past estimates (Penczykowski et al. 2014; Cáceres et al. 2006; Hall et al. 2009; Hall et al. 2011; Civitello et al. 2015; Strauss et al. 2016; Shocket et al. 2018). These gains resulted from detection of the complete parasite life cycle and confirm that parasite abundance can be vastly underestimated in systems that target only patent or conspicuous stages of infection (Stewart et al. 2018). That hosts hitherto referred to as uninfected were teeming with cryptic infections raises an important question: What is the fate of early host-parasite interactions and how does considering them enhance our perspectives on disease?

Before epidemics emerged, I observed a pattern of abundant early host-parasite interactions and rare or absent late infections. To understand this pattern, it can be helpful to consider the stage distributions of free-living species. In many free-living taxa, populations are dominated by juveniles (right-skewed stage distributions). Such distributions have long provided evidence of low juvenile survival to the adult stage (Koch et al. 2006; Low & Part 2009; Goatley et al. 2016). For parasitic organisms, early host-parasite interactions are analogous to the juvenile stage. Hence, parasite stage distributions dominated by early interactions may indicate their low

survival to late infection stages. One key determinant of parasite survival is host immunity, which can kill parasites and enable recovery of the host. *Daphnia* can recover from infection under controlled laboratory conditions (Chapter 4; Stewart Merrill et al. 2019), and the experimental infections on wild-caught *Daphnia* allowed me to ask whether their natural recovery was removing *Metschnikowia* from lake ecosystems.

Tying in the results from the experimental infections, I observed several instances where spore exposure was high within a lake, but *Daphnia* were resilient to that particular level of exposure. Likewise, I observed instances where *Daphnia* were highly susceptible to infection, but spores were virtually absent from the lake. When considered in isolation, these two factors were each associated with epidemic emergence in the predicted direction. Susceptibility (measured using spore thresholds from experiments) increased the likelihood of an epidemic, and exposure (measured as maximum spore values in the field) also increased the likelihood of an epidemic. But these one-factor models suffered from high error, poor AIC rankings and low model weights. By uniting the two factors, I aimed to account for their mismatches. As predicted, the combination of *Metschnikowia* exposure and *Daphnia* susceptibility (indicated using their delta value) consistently led to the best fitting models. The exposure and susceptibility models were always the highest ranked regardless of timescale, spore metric, or method used to estimate spore thresholds. These winning models proposed that parasite exposure and host susceptibility are both changing through time in a non-synchronous manner, and that when they are synchronous, epidemics emerge.

The mutual dependence of epidemics on exposure and susceptibility mirrors Combes' (2001) paradigm, in which parasite encounter and host compatibility filters must be simultaneously opened for a parasite to infect its host. This finding also support the assumptions of parasite transmission models developed by Hall et al. (2010), in which transmission (β) is formulated as a function of an exposure parameter (f) and per spore susceptibility parameter (μ). But while conceptual and theoretical models make clear the importance of exposure and susceptibility for disease, these two processes are rarely investigated jointly in wildlife. Recent and notable exceptions include Gibson et al. (2016), which used the exposure and susceptibility of *Potamopyrgus* snails to *Microphallus* trematodes to explain spatial variation in trematode prevalence. Using mesocosms with tightly controlled levels of exposure, Strauss et al. (2018) demonstrated that *Daphnia* susceptibility directly fuels large *Metschnikowia* epidemics. By

closely tracking chytrid zoospores and amphibian susceptibility to chytrid infection, Voyles et al. (2018) demonstrated how increased host resistance has enabled the rebound of Central American frog populations, despite sustained levels of chytrid exposure. The current study adds to this growing body of empirical research and reaffirms that parasites and the infectious diseases they cause are regulated by both environmental and within-host processes.

Susceptibility of individual hosts to parasites is determined by host traits that either inhibit or promote infection. At higher levels of organization, these host traits may contribute to the regulation of parasite populations. For instance, Halliday et al. (2018) provided strong evidence that plant defenses (immune signaling hormones) regulate the transmission of an aggressive fungal pathogen. Prior work on *Daphnia* found that parasite exposure, host barriers, and host immune responses acted in concert to explain individual infection outcomes (Chapter 4; Stewart Merrill et al. 2019), and I sought to determine whether and how these same traits affected *Metschnikowia* populations. *Metschnikowia* prevalence was decoupled from its spore abundance at the late infection stage, suggesting that *Daphnia* immune responses were regulating *Metschnikowia*. In accordance with this idea, *Daphnia* spore defenses were high during periods of host filtering (when *Metschnikowia* was not spreading), but low at the time of epidemic emergence (when *Metschnikowia* was spreading rapidly). Alternatively, spore consumption and gut penetrability did not exhibit a general pattern among lakes. The within- and among-lake variation in spore defense I observed is likely driven by resources, as the haemocytes involved in defense are energetically costly to produce (Diamond & Kingsolver 2011; Triggs & Knell 2012). Moreover, declines in spore defense may explain prior results in which epidemics emerged when resource quality was poor (Hall et al. 2009). That resources might indirectly regulate parasites through their effects on host immunity has become an important area of research (Cressler et al. 2014; Becker et al. 2015). Future tests of how algal resources affect *Daphnia* defenses may allow us to embed their within-host processes into a broader community context.

A continuing goal in ecology is to achieve a balance between generality and complexity (Marquet et al. 2014). On the side of generality, I was able to predict epidemics using only two pieces of information: parasite exposure and host susceptibility. However, there were limitations in my ability to predict epidemics. In the bimonthly set in particular, there were multiple times in which a lake's delta value was negative (the spore metric exceeded the spore threshold) but epidemics did not emerge. Such prediction failures are bound to occur when an average value is

attributed to a diverse population. Indeed, the maximum spore value was generally the most highly-ranked exposure metric, suggesting that *Metschnikowia* epidemics depend more on one highly exposed individual than on the population's average exposure. Host populations often possess uneven distributions of epidemiologically relevant traits (Martin et al. 2019). This host variation can have considerable effects on parasite transmission (Lloyd-Smith et al. 2005; Dwyer et al. 1997; Hawley & Altizer 2011). By distilling susceptibility into population averages (via the spore threshold) my approach embraced spatial and temporal variation at the population-level but did not include individual-level variation. Measuring traits at the individual level might provide an indication of how important outliers, such as super-spreaders, are to epidemic dynamics. Another reason epidemics might have failed to emerge, even when exposure and susceptibility were aligned, is if host density was too low. Future incorporation of host density effects, including density-dependent transmission and safety in numbers effects (Civitello et al. 2013; Buck et al. 2017), may enhance our ability to predict epidemics.

The past two decades of disease ecology have seen the repeated prediction that environmental change will compromise host immunity, increase host susceptibility, and facilitate the spread of disease (Mydlarz et al. 2006; Acevedo-Whitehouse & Duffus 2009; Martin et al. 2010; Harvell et al. 2009; Hing et al. 2016). This cascade of events has been inferred for multiple species, from corals (Mydlarz et al. 2010) to amphibians (Kiesecker 2011). While these narratives have sparked interest on the role host susceptibility plays in disease (Bradley & Jackson 2008; Hawley & Altizer 2011; Tompkins et al. 2011), rigorous empirical studies linking susceptibility with epidemiological outcomes remain somewhat elusive. My results provide strong empirical evidence that observable disease represents only a subset of parasite invasion attempts, and that increases in host susceptibility are an important condition for epidemic emergence. Additional study of whether parasite exposure and host susceptibility abide by predictable ecological patterns, or are idiosyncratic in their dynamics, may allow us to identify the environmental conditions under which these key processes align.

Tables and Figures

Term	Definition	Att	Sp	H	SC	C	A
Exposure dataset: observations of field-collected animals							
Unexposed	Absence of any *Metschnikowia* developmental stage within a *Daphnia* host						
Exposed	Presence of any *Metschnikowia* developmental stage within a *Daphnia* host	•	•	•	•	•	•
Early interaction	Early phase of the host-parasite interaction. *Daphnia* can recover by resisting attack at the gut barrier and by clearing a within-host infection	•	•	•	•		
Within-host infection	Parasite has successfully crossed host barriers. *Daphnia* can only recover by clearing a within-host infection		•	•	•	•	•
Late infection	Late phase of the host-parasite interaction. *Daphnia* are full of conidia or asci and have reached the point of no recovery					•	•
Spore abundance	Mean number of spores in the bodies of all examined *Daphnia* (denominator includes exposed and unexposed hosts).						
Spore intensity	Mean number of spores in the bodies of exposed *Daphnia* (denominator includes only exposed hosts)						
Spore max	Maximum number of spores in the bodies of all examined *Daphnia*						
Susceptibility dataset: results from experimental infections							
Spore consumption	The number of spores in the host body. Includes spores in the gut lumen, gut barrier, and body cavity						
Gut penetrability	The likelihood that spores attacking the gut barrier will move into and infect the body cavity						
Spore defense	The likelihood that spores infecting the body cavity will be defended against with host haemocytes						
Spore threshold	The average number of spores attacking the gut required to produce a 50% probability of late infection						

Table 3.1. Two datasets were united to examine how parasite exposure and host susceptibility interact to drive the emergence of epidemics. For each dataset, I provide key terms and definitions. The **exposure dataset** (blue; top rows) contains observational data of field-collected *Daphnia*. I classified *Daphnia* by their *Metschnikowia* developmental stage, where stages in progressing order are: Att = attacked, Sp = spore, H = hyphae, SC = sporocyst, C = conidia, A = ascus (shown as columns). Presence of any of the six stages (filled black points) allowed determination of whether hosts were unexposed or exposed, and whether hosts had early interactions, within-host infections and/or late infections. The key distinction between early interactions, within-host infections, and late infections is whether and how *Daphnia* can recover (see definitions). I also counted *Metschnikowia* spores in field-collected *Daphnia* (abundance, intensity, and maximum values). The **susceptibility dataset** (red; bottom rows) contains experimental data resulting from infection assays performed on a separate set of field-collected *Daphnia*. The susceptibility dataset includes three host traits (spore consumption, gut penetrability, spore defense) and spore threshold values estimated from dose-response curves.

Table 3.2: Model competition results examining predictors of epidemic emergence in six temperate lakes in Central Indiana, 2017. Models conformed to four model types based on their predictors. Null models contained only an intercept as a predictor. Exposure models contained one of three metrics for *Metschnikowia* spore levels (spore abundance, spore intensity, spore max; Table 3.1). Susceptibility models contained spore thresholds (Table 3.1). Finally, Exposure and Susceptibility models directly tested my prediction that epidemics become more likely as parasite exposure meets or exceeds a population's exposure threshold (outlined in Fig. 3.1). These models contained delta values as predictors, where delta is equal to the spore threshold minus a given spore metric. The response variable is epidemic emergence (coded as 0 or 1), and the unit of replication is a lake sampled at a particular point in time up to the point of epidemic emergence. Provided for each model are: K (the number of estimated parameters), ΔAIC (indicating model performance relative the best-ranked model), relative likelihood (w_i, the probability that the model fits best, given the suite of models considered), and cumulative relative likelihood (Σw_i, sum of relative likelihoods moving down from the top-ranked model). I constructed the models using two types of susceptibility data. The monthly susceptibility data (top rows; $N = 20$) contains spore thresholds estimated using late infections nine days following inoculation. The bimonthly data (bottom rows; $N = 44$) contains spore thresholds estimated using hyphae as an indicator of future late infections. In both model sets, my prediction was supported: the best-ranked models included both exposure and susceptibility. Exposure and Susceptibility models cumulatively explained 86% of the evidence in the monthly data and 64% of the evidence in the bimonthly data. Maximum spore values (spore max) were generally competitive with or higher ranked as predictors than the other two spore metrics. Raw data and associated model predictions are plotted in Figure 3.4.

	Model type	Predictors	K	ΔAIC	w_i	*cum*
Monthly data	Exposure and Susceptibility	Spore threshold – Spore max	2	0.00	0.58	0.58
	Exposure and Susceptibility	Spore threshold – Spore intensity	2	1.94	0.22	0.79
	Exposure and Susceptibility	Spore threshold – Spore abundance	2	4.34	0.07	0.86
	Susceptibility	Spore threshold	2	4.91	0.05	0.91
	Exposure	Spore intensity	2	5.44	0.04	0.95
	Exposure	Spore max	2	6.08	0.03	0.97
	Exposure	Spore abundance	2	6.75	0.02	0.99
	Null	Intercept	1	9.25	0.01	1.00
Bimonthly data	Exposure and Susceptibility	Spore threshold – Spore max	2	0.00	0.29	0.29
	Exposure and Susceptibility	Spore threshold – Spore intensity	2	0.92	0.19	0.48
	Exposure and Susceptibility	Spore threshold – Spore abundance	2	1.26	0.16	0.64
	Susceptibility	Spore threshold	2	1.55	0.14	0.77
	Exposure	Spore max	2	2.44	0.09	0.86
	Null	Intercept	1	3.06	0.06	0.92
	Exposure	Spore intensity	2	3.86	0.04	0.97
	Exposure	Spore abundance	2	4.41	0.03	1.00

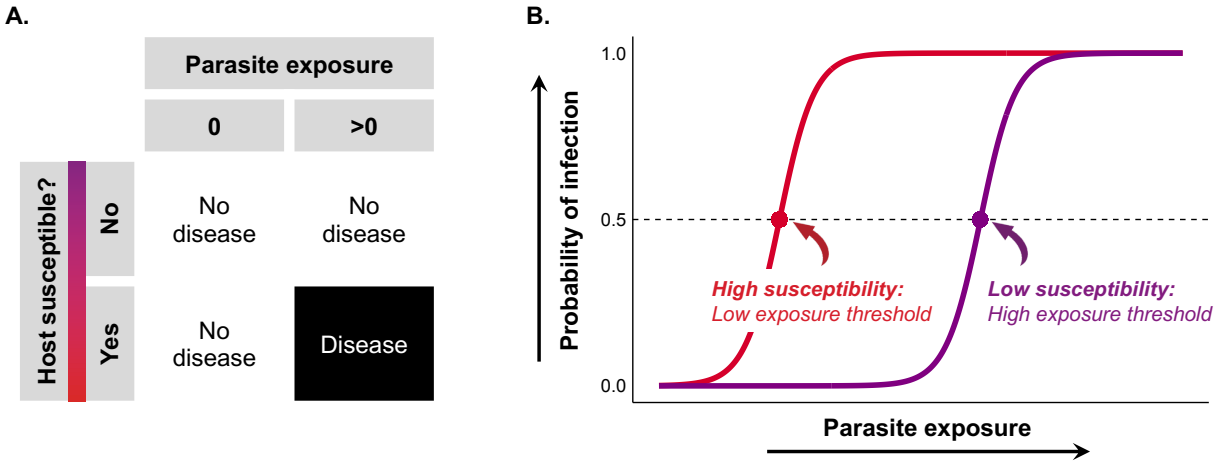

Figure 3.1. Linking parasite exposure, host susceptibility, and disease. **A.** For a single host to acquire a parasitic infection, the host must both be exposed and susceptible to that parasite (adapted from Combes 2001 encounter and compatibility filters). These requirements may scale to the population, where disease can only occur when a population of hosts is both exposed and susceptible to parasites. Because these two factors must be aligned for disease to occur, there are multiple misalignments that will result in the absence of disease. Disease cannot occur in the absence of parasites (parasite exposure = 0), regardless of a population's level of susceptibility. And disease cannot occur if parasites are present (parasite exposure > 0) and the population is not susceptible. But how is host susceptibility quantified and categorized? **B.** By evaluating probability of infection as a function of parasite exposure, the dose-response curve defines host susceptibility. Hosts that are highly susceptible to parasites (red dose-response curve) succumb to infection at low levels of parasite exposure (low exposure threshold). Hosts with low susceptibility (purple dose-response curve) can withstand high levels of parasite exposure before succumbing to infection (high exposure threshold). Uniting the requirements for disease (**A**) with their interconnectedness (**B**), I arrive at the following prediction for disease epidemics in my study system: *Metschnikowia* epidemics will become more likely as a *Daphnia* population's level of parasite exposure meets or exceeds its exposure threshold.

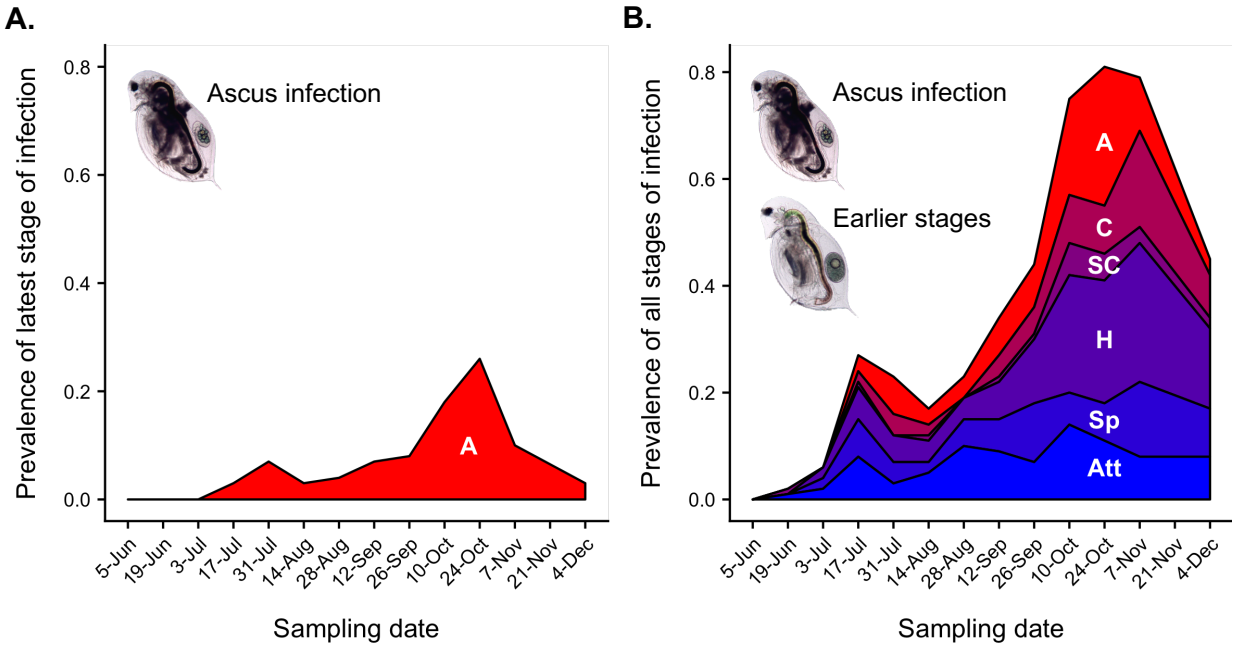

Figure 3.2. Detection of the latest stage of infection dramatically underestimates true prevalence of *Metschnikowia bicuspidata* in its host *Daphnia dentifera*. **A.** Average prevalence of ascus infections (white A) across six lakes in Central Indiana from June to December 2017. Ascus infections are easy to detect because infected hosts are filled with fungal spores that make them opaque (see image for ascus infection). **B.** Average prevalence of *Metschnikowia* in the same six lakes, while including the complete set of developmental stages. Earlier developmental stages can only be detected at high magnification, making infected hosts appear uninfected (see image for earlier stages). Each shaded region represents a different *Metschnikowia* developmental stage, which progress from the earliest stage at the bottom to the latest stage at the top. Overlaid on the shaded areas (in white letters) are the designations of developmental stages: Att = attacked, Sp = spore, H = hyphae, SC = sporocyst, C = conidia, A = ascus.

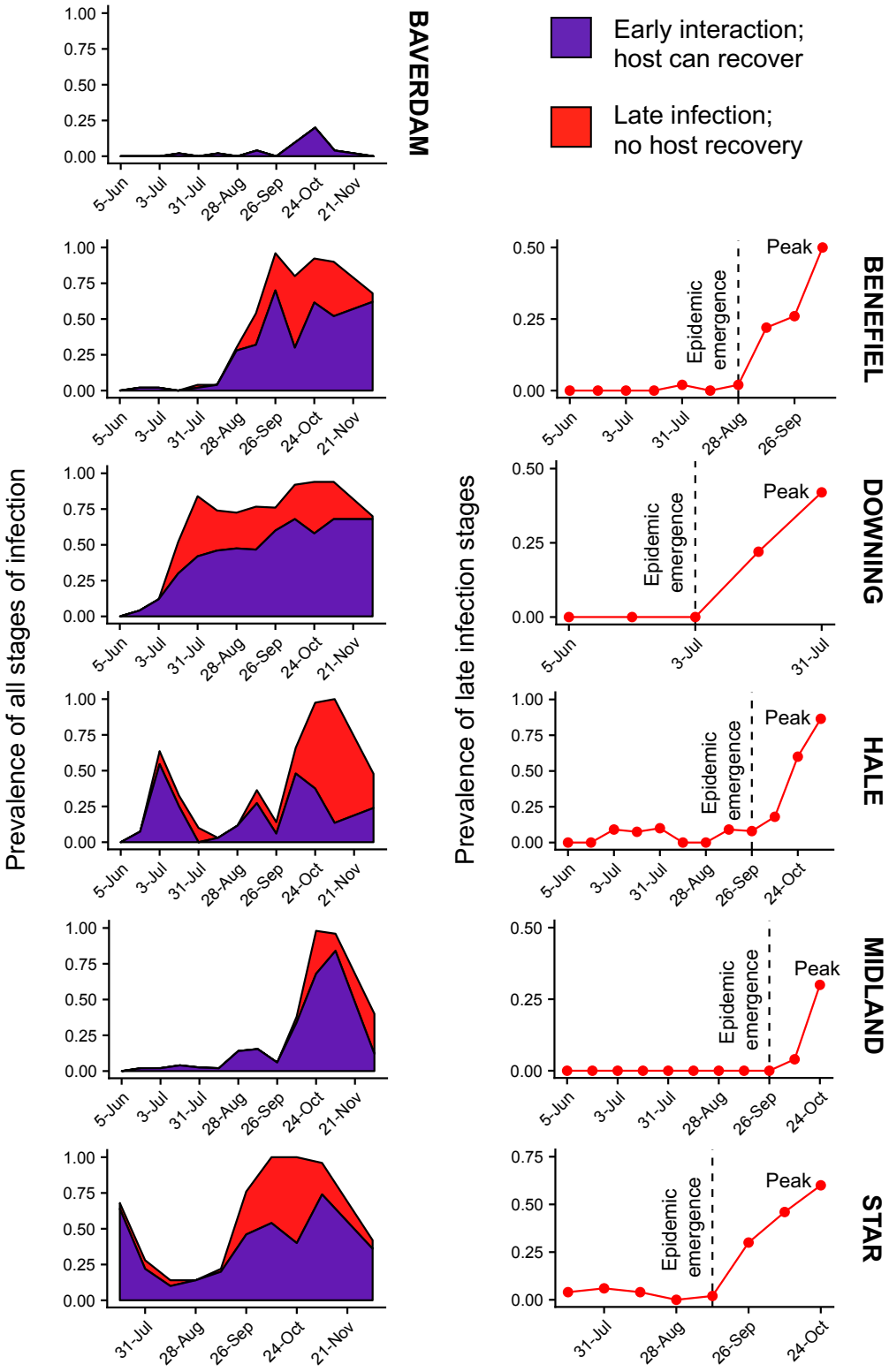
Early interaction;
host can recover
Late infection;
no host recovery
Prevalence of all stages of infection
Prevalence of late infection stages
BAVERDAM
BENEFIEL
DOWNING
HALE
MIDLAND
STAR
Peak
Epidemic
emergence
5-Jun
3-Jul
31-Jul
28-Aug
26-Sep
24-Oct
21-Nov

Figure 3.3.

Figure 3.3. – continued. Qualitative evidence that parasite exposure alone cannot explain epidemic emergence in the *Daphnia-Metschnikowia* system. In the left column, I examine early interactions and late infections through time, where each row represents a lake population. I plot the prevalence of early interactions from which hosts can recover (purple; defined in Table 3.1), and the prevalence of late infections from which hosts cannot recover (red; defined in Table 3.1). In many instances, early interactions are present but late infections are not, suggesting that hosts are not susceptible to infection during those instances. In the right column, I determine the point of epidemic emergence by evaluating growth in the prevalence of late infections (red line) up to the point of maximum (peak) prevalence. Epidemic emergence (dashed line) is the point at which late infection prevalence begins to increase to its maximal value, while exceeding background rates. Evaluating these plots together demonstrates that *Metschnikowia* exposure preceded epidemics in each of the six *Daphnia* populations (note: Beaverdam experienced exposure at low levels, but never experienced an epidemic).

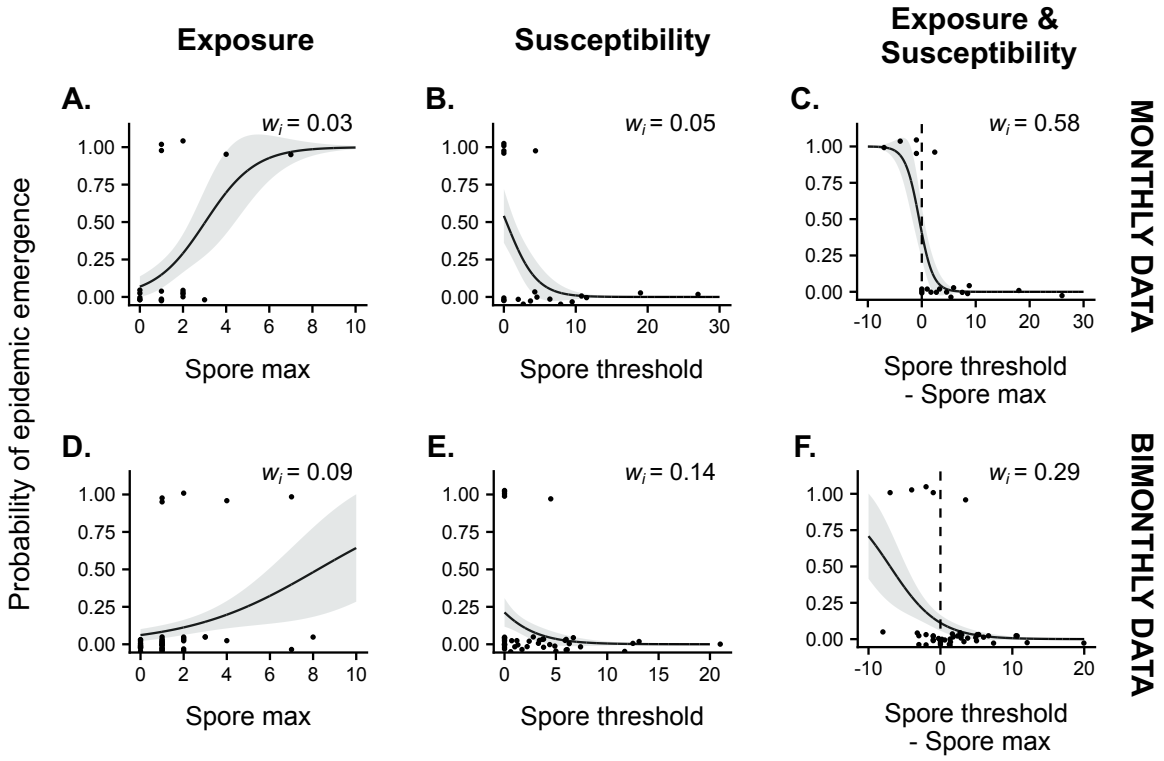

Figure 3.4. Parasite exposure and host susceptibility jointly predict epidemic emergence. All plots contain raw data (points) and model predictions (curves) from models in Table 3.2. The top row (**A** to **C**) contains data and model predictions for the monthly susceptibility data, where spore thresholds were determined using late infections nine days following inoculation. The bottom row (**D** to **F**) contains data and model predictions from the bimonthly susceptibility data, where spore thresholds were determined using hyphae as an indicator of future late infections. In both datasets, *Metschnikowia* exposure, measured as the maximum spore value observed in a population, increased the likelihood of epidemics but was a relatively weak predictor of epidemic emergence (**A** and **D**). *Daphnia* susceptibility, measured as the spore threshold for a given population, decreased the likelihood of epidemics but was also a relatively weak predictor of epidemic emergence (**B** and **E**). The combination of *Metschnikowia* exposure and *Daphnia* susceptibility (spore threshold – spore max) was the winning model in both cases, suggesting that *Metschnikowia* epidemics depend critically on the interaction of exposure and susceptibility (**C** and **F**). All lakes and timepoints are combined in this plot, such that each point represents a value observed on a particular date at a particular lake from the pre-epidemic period to the point of epidemic emergence. Slight vertical jitter is added to visualize overlapping points. Gray shading represents the standard error of the model predictions. Also provided are the model weights (w_i) from Table 3.2.

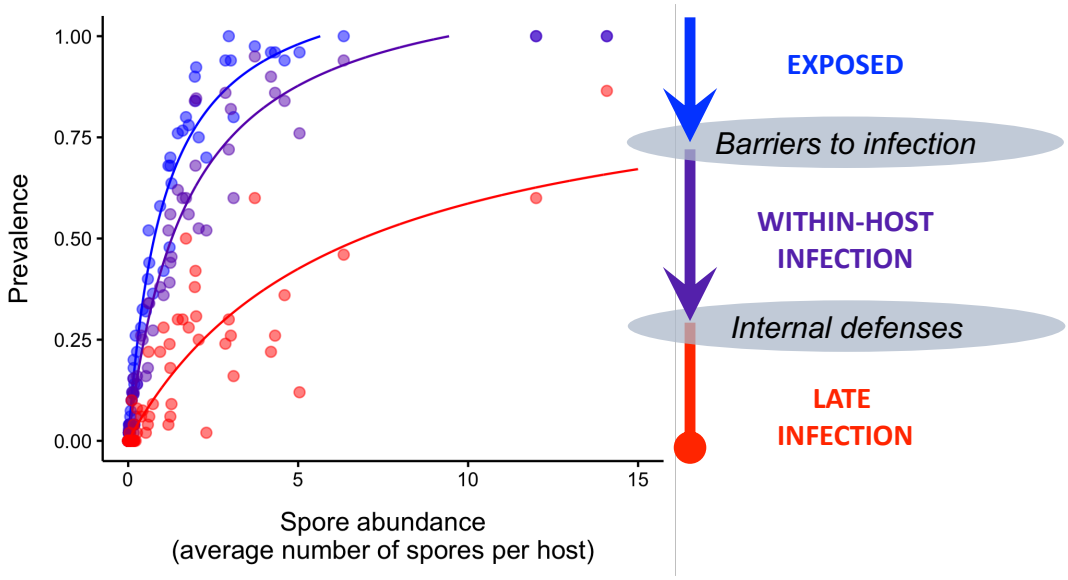

Figure 3.5. Which host filters are removing *Metschnikowia* from the system? Evaluating how spore abundance relates to the prevalence of progressing infection stages can reveal the step of infection at which hosts most strongly regulate parasites. All lakes and time points are combined in this plot; each point represents a value observed on a particular date at a particular lake over the full sampling period. **Blue/Purple:** Spore abundance results in similar prevalences of exposure (blue; Table 3.1) and within-host infection (purple; Table 3.1). The similarity of the blue and purple curves suggests that host barriers are not acting as strong filters for *Metschnikowia*. **Purple/Red:** A breakdown in infection progression is evident as individuals move from within-host infections (purple) to late infections (red; Table 3.1). The disparity between the purple and red curves indicates that the same levels of spore abundance result in far fewer late infections than within-host infections. Hence, host internal defenses may be acting as filters for the within-host infection to late infection transition.

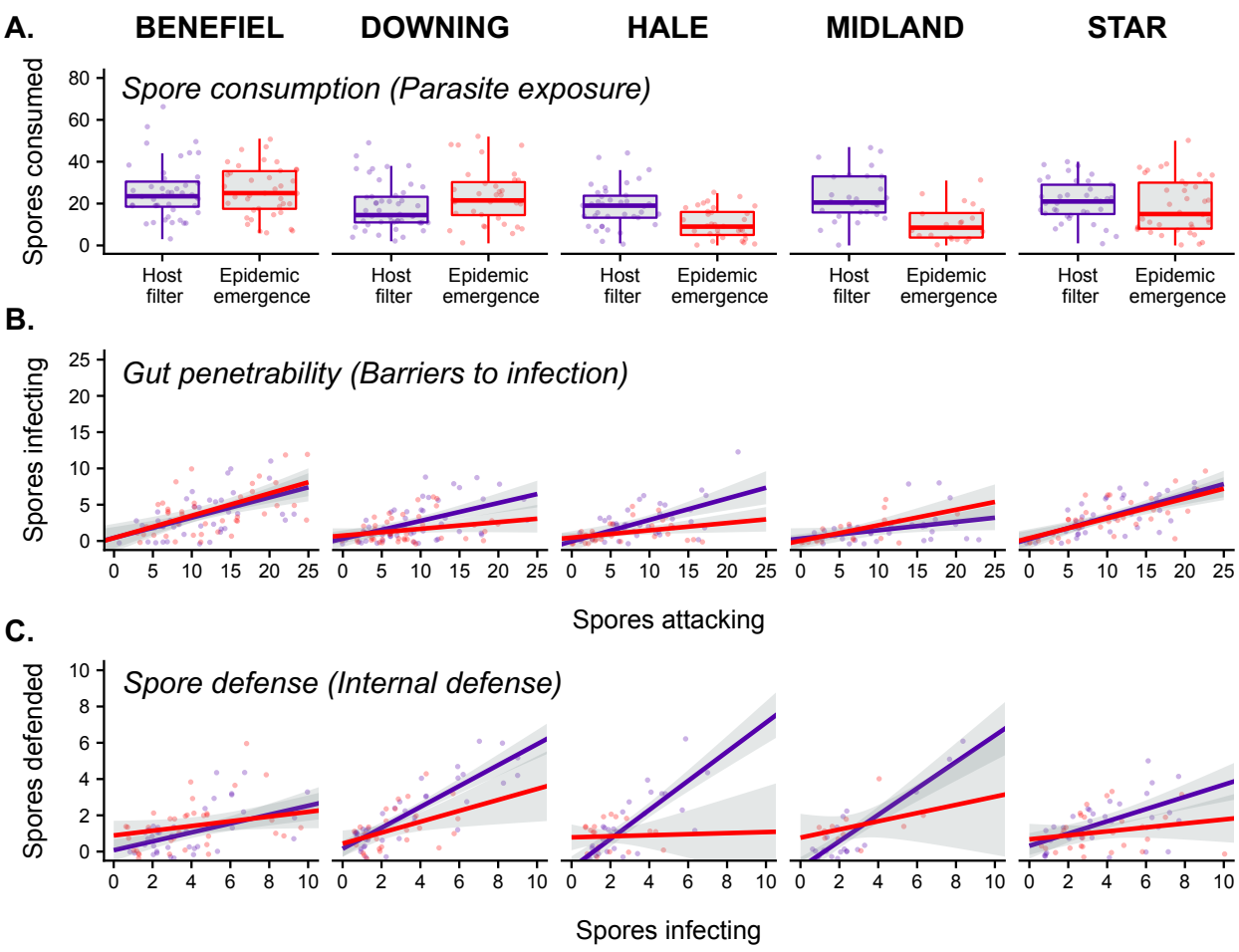

Figure 3.6. Experimental investigation of host traits during periods of host filtering and epidemic emergence. For each lake (indicated by columns), I compared host traits measured when epidemics emerged (red; representing the bottom right quadrant of Fig. 3.1A) with those same traits measured when host filters prevented epidemics (purple; representing the top right quadrant of Fig. 3.1A). **A.** Spore consumption (a parasite exposure trait) was quantified as the number of spores each *Daphnia* host consumed (Table 3.1). Spore consumption exhibited no general change from host filtering to epidemic emergence. **B.** Gut penetrability (a barrier to infection) was quantified by regressing infecting spores on attacking spores (Table 3.1). Gut penetrability also did not exhibit a general change from host filtering to epidemic emergence. **C.** Spore defense (an internal defense), was quantified by regressing defended spores on infecting spores (Table 3.1). In four out of the five lakes that experienced epidemics, spore defense was higher during the period of host filtering and lower at the point of epidemic emergence, although this pattern was not detected in Benefiel. Each point represents a unique *Daphnia* individual and shading around the lines represents the standard error of the fit regression. Note: Beaverdam was excluded from these analyses because it did not experience an epidemic.

CHAPTER 4: VARIATION IN IMMUNE DEFENSE SHAPES DISEASE OUTCOMES IN LABORATORY AND WILD *DAPHNIA*[2]

Abstract

Host susceptibility may be critical for the spread of infectious disease, and understanding its basis is a goal of ecological immunology. Here, I employed a series of mechanistic tests to evaluate four factors commonly assumed to influence host susceptibility: parasite exposure, barriers to infection, immune responses, and body size. I tested these factors in an aquatic host-parasite system (*Daphnia dentifera* and the fungal parasite, *Metschnikowia bicuspidata*) using both laboratory-reared and field-collected hosts. I found support for each factor as a driver of infection. Elevated parasite exposure, which occurs through consumption of infectious fungal spores, increased a host's probability of infection. The host's gut epithelium functioned as a barrier to infection, but in the opposite manner from which I predicted: thinner anterior gut epithelia were more resistant to infectious spores than thick epithelia. This relationship may be mediated by structural attributes associated with epithelial cell height. Fungal spores that breached the host's gut barrier elicited an intensity-dependent haemocyte response that decreased the probability of infection for some *Daphnia*. Although larger body sizes were associated with increased levels of spore ingestion, larger hosts also had lower frequencies of parasite attack, less penetrable gut barriers, and stronger haemocyte responses. After investigating which mechanisms underlie host susceptibility, I asked: do these four factors contribute equally or asymmetrically to the outcome of infection? An information-theoretic approach revealed that host immune defenses (barriers and immune responses) played the strongest roles in mediating infection outcomes. These two immunological traits may be valuable metrics for linking host susceptibility to the spread of infectious disease.

[2] This is a pre-copyedited, author-produced version of an article accepted for publication in *Integrative and Comparative Biology* following peer review. The version of record is available online at: https://academic.oup.com/icb/advance-article-abstract/doi/10.1093/icb/icz079/5505427?redirectedFrom=fulltext
Full citation:
Stewart Merrill, T.E., S.R. Hall, L. Merrill & C.E. Cáceres. 2019. Variation in immune defense shapes disease outcomes in laboratory and wild *Daphnia*. Integrative and Comparative Biology. doi: 10.1093/icb/icz079

Introduction

Susceptibility of hosts to parasites may hold the key to how disease spreads, but it remains one of the most beguiling aspects of disease ecology. At the heart of host susceptibility is the immune system. All living organisms are threatened by parasites, and many have evolved a suite of immunological defenses to prevent infection. As such, ecological immunology provides a framework to link host susceptibility to parasite dynamics and disease spread (Hawley & Altizer 2011; Martin et al. 2016). However, several challenges confront empirical work at the interface of eco-immunology and disease ecology. Immunological defenses can be challenging to measure and interpret (Sheldon & Verhulst 1996; Graham et al. 2011; Moreno-Garcia et al. 2013). Further, it is often unknown which immune defenses regulate particular host-parasite interactions (Boughton et al. 2011). Finally, immunity is complex, highly integrated, and exceedingly variable (Schulenberg et al. 2009; Pedersen & Babayan 2011). Amidst all of the immunological noise, how can we find the signal for susceptibility?

Susceptibility and its immunological basis may be captured by decomposing host-parasite interactions into functional steps (e.g. Johnson & Hartson 2009; Auld et al. 2010; 2012; Hall et al. 2012; Lafferty et al. 2015). These steps include: parasite exposure, parasite entry into the host, and parasite survival within the host until the point of transmission. At each step, host strategies attempt to prevent passage of the parasite to the subsequent step (*sensu* Combes 2001). For instance, avoidance behaviors limit exposure (Buck et al. 2018), barriers impede entry (Soderhall 2010; Davis & Engstrom 2012), and immune responses inhibit parasite survival. By isolating each step, we can first identify key host traits that govern success or cessation of infection. Then, by examining all steps together, we can determine which host traits most strongly determine susceptibility.

A plankton system shows great promise for determining the extent to which host susceptibility explains patterns of infectious disease. In this system, a virulent fungus, *Metschnikowia bicuspidata*, infects a crustacean host, *Daphnia dentifera*. *Daphnia* possess broad variation in susceptibility, which can contribute to the failure or emergence of natural epidemics (Chapter 3) as well as epidemic size (Strauss et al. 2018). Furthermore, descriptions of the parasite's within-host life cycle provide direct links from host traits (including immune defenses) to infection outcomes (Chapter 1; Stewart Merrill & Cáceres 2018). With these new developments, I decompose the infection process into its functional steps and compare four

factors that may govern infection: exposure to parasites, barriers to parasite entry, internal immune responses against parasites, and body size. These commonly-invoked drivers distill complex host-parasite interactions into a linear set of tractable mechanisms (Fig. 4.1). I test them using laboratory-reared and field-collected *Daphnia* to forge a balance between tight experimental control and broad ecological reality.

In the first part of this study ("Identifying mechanisms of infection"), I mechanistically test the four drivers of infection in isolation to understand their biology and to explore the range of host variation present at each infection step. I present each driver of infection as a unique module, such that each driver has its own background, methods, and results. In the second part of this study ("Integrating infection steps to understand susceptibility"), I unite the four drivers of infection to determine which play the strongest roles in shaping *Daphnia* susceptibility. Finally, I discuss how the biology of each infection driver informs our broader understanding of host susceptibility.

General Methods

The study host, *Daphnia dentifera*, is a cladoceran zooplankton found in freshwater lakes across North America. The study parasite, *Metschnikowia bicuspidata* (formerly, *Monospora bicuspidata*; Metschnikoff 1884), is an ascomycete fungus that commonly causes epidemics in *Daphnia* populations (Cáceres et al. 2006; Cáceres et al. 2014). *Metschnikowia* is transmitted when *Daphnia* ingest fungal spores (hence, exposure is through feeding). The needle-shaped spores must then pierce through the *Daphnia* gut epithelium, which represents a barrier. If penetration succeeds, the fungus enters the body cavity of its host and must survive defense by host haemocytes (immune cells). The fungus then undergoes 8-10 days of morphological development and reproduction before reaching its terminal stages (the conidia and ascus stages, outlined in Appendix D.1; Metschnikoff 1884; Chapter 1; Stewart Merrill & Cáceres 2018). Terminal infections are those from which the host does not recover; the body cavity fills with new spores that kill the host. Host death is required to release spores back to the environment (i.e., to enable transmission). Because *Daphnia* are transparent, the full sequence of events from spore ingestion to terminal infection can be visualized *in vivo*. In this study, I experimentally inoculated *Daphnia* with fungal spores and observed the early steps of this interaction, during which spores are consumed and invade the body cavity. During these observations, I quantified a

series of host and parasite metrics (Table 4.1) to mechanistically test the four drivers of infection. I then tracked hosts until nine days post-inoculation (when they had either recovered from infection or entered the terminal infection stage) to evaluate which of the four drivers played the strongest role in determining terminal infection outcomes.

In the lab, I reared ten unique multi-locus *Daphnia* genotypes originally collected from lakes in Central Indiana and Michigan. In this rearing protocol, I sought to eliminate maternal effects using standardized laboratory conditions for three generations (Lynch & Walsh 1998). Experimental individuals were collected from standardized mothers as neonates and were inoculated when they were eight-days-old. Field-collected *Daphnia* were sampled from six lakes in Central Indiana between 4-Jun and 4-Dec 2017. Experimental inoculations occurred 24 hours after collection. Further description of laboratory conditions (containment, temperature, and resources) is provided in Appendix D.2.

The dose used for experimental inoculation differed for laboratory-reared vs. field-collected *Daphnia*. In the laboratory study (2015), I used 500 spores/ml of *Metschnikowia*. This dose produced a high prevalence of terminal infections, with low host recovery rates. In the field study (2017), I used a more field-relevant dose (200 spores/ml) to enable greater host recovery. In both studies, after a 24-hour inoculation period in tubes containing spores and 10 ml filtered lake water, live *Daphnia* were examined visually using a Leica DMLB compound microscope paired with a 40x objective (yielding total magnification of 400x). The full length of each host's gut and body cavity was scanned to quantify host and parasite metrics (defined in Table 4.1 and illustrated in Fig. 4.1). Field-collected *Daphnia* that had prior terminal infections with *Metschnikowia* were excluded from all analyses.

I tested predictions using general linear models and ANOVA, with the individual host as the unit of replication. Statistical models were constructed for both laboratory-reared and field-collected *Daphnia* whenever the two datasets contained the required variables. Sample sizes are available (Table 4.1) and consolidated statistical output is provided (Appendix D.3). All models were fit in R version 3.3.3 (R core team 2013). Residuals were evaluated for normality, homoscedasticity, and over-dispersion to ensure compliance with model assumptions.

Identifying mechanisms of infection

H1: Exposure drives infection

Background: Parasite exposure may strongly predict infection. For instance, low prevalence of parasites in natural systems often reflects low exposure, caused by limited infectious propagules or upstream hosts (Skirnisson & Galaktionov 2002; Hechinger & Lafferty 2005, Fredensborg et al 2006; Byers et al. 2008). Of course, exposure represents only a first step in the infection process, and subsequent steps may decouple exposure-infection relationships. For instance, while foraging behaviors amplify exposure in *Daphnia* (Hall et al. 2010; Shocket et al. 2018), broad unexplained variation in exposure-infection relationships exists in this and other systems (Thieltges & Reise 2007; Bertram et al. 2013; Sánchez et al. 2013; Izhar & Ben-Ami 2015; Izhar et al. 2015). I tested whether exposure drives infection by measuring infection success of *Metschnikowia* spores after they are ingested by *Daphnia* hosts.

Methods: To develop and reproduce, *Metschnikowia* spores must first undergo a three-part journey. Spores must be ingested by hosts, cross the gut's epithelial barrier, and enter the body cavity (haemocoel). Therefore, I characterized *Metschnikowia* spores based on their location (Fig. 4.1, Table 4.1). "Lumen spores" represent spores that were free-floating in the gut lumen (hollow) following ingestion. Because the gut is a high flow-through system, lumen spores represent a snapshot of spore ingestion and approximate how many spores a host generally eats. "Barrier spores" represent spores that became partially embedded in the gut epithelium but failed to penetrate into the body cavity, i.e. spores that were blocked by the gut barrier. "Haemocoel spores" represent spores that successfully crossed the gut epithelium and entered the host body cavity. The cumulative tally of spores within the host's body (lumen + barrier + haemocoel) represents total "exposure"; similarly, the number of "attacking" spores (*sensu* Lafferty et al. 2015) was the sum of those which attempted to cross the gut epithelium (barrier + haemocoel). Each host's level of "infection" refers directly to the number of spores infecting the body cavity. Extended definitions of spore types are provided in Appendix D.1.

If exposure (eating spores) drives infection, then ingested spores should predict successful penetrations into the body cavity. Tracing this path, I tested relationships between *i*) lumen spores and spores embedded in gut epithelia (barrier spores), *ii*) barrier spores and infecting spores (haemocoel spores) and, ultimately, I tested whether *iii*) lumen spores predicted haemocoel spores.

Results: In laboratory-reared *Daphnia*, the number of lumen spores predicted barrier spores (Fig. 4.2A; df = 56, estimate[est] = 0.195, $p < 0.001$, $R^2 = 0.399$), but barrier spores did not predict haemocoel spores (Fig. 4.2B; df = 134, est = -0.028, p = 0.455, $R^2 = 0.004$). The lumen to body cavity path was decoupled at the gut barrier; hence, lumen spores did not ultimately predict haemocoel spores (Fig. 4.2C; df = 56, est = 0.013, p = 0.510, $R^2 = 0.008$). In the highly replicated experiment with field-collected *Daphnia*, each relationship was statistically significant. More lumen spores led to more barrier spores (Fig. 4.2D; df = 2037, est = 0.071, $p < 0.001$, $R^2 = 0.032$), then more barrier spores led to more haemocoel spores (Fig. 4.2E; df = 2260, est = 0.086, $p < 0.001$, $R^2 = 0.024$); hence, more lumen spores increased haemocoel spores (Fig. 4.2F; df = 2036, 0.036, $p < 0.001$, $R^2 = 0.026$). However, each relationship was generally weak in field-collected *Daphnia* (i.e. R^2 between 2.4 and 3.2%; Fig. 4.2) and laboratory-reared *Daphnia* also had weak associations (R^2 below 0.01) once spores began moving into the body cavity. These results indicate that the *Metschnikowia* path to infection is riddled with host variation. The weight of evidence for exposure driving infection is low.

H2: Gut thickness creates a barrier to infection

Background: To contend with parasite exposure, organisms possess diverse physical and chemical barriers that resist infection (Soderhall 2010; Davis & Engrstrom 2012). For ingested parasites, such barriers occur within the host's intestinal tract (Garcia-Garcia et al. 2013). For instance, *Wuchereria bancrofti* are killed and melanized during passage across the fly gut epithelium (Michalski et al. 2010), and mosquito-vectored arboviruses may be physically inhibited by the thickness of the mosquito's midgut basal lamina (Grimstad & Walker 1991; Franz et al. 2015). *Daphnia* exhibit strong genetic variation in parasite resistance (Chapter 2), and the midgut epithelium likely mediates susceptibility (Auld et al. 2010; 2011). Because the *Daphnia* midgut epithelium is one cell layer thick, tall epithelial cells (thicker epithelia) may inhibit spores from crossing into the body cavity. To evaluate whether gut thickness creates a barrier to infection, I measured thickness of gut epithelia and how penetrable they were by *Metschnikowia* spores.

Methods: Gut epithelia of live hosts were imaged at high resolution (400x) with Leica Imaging Software. Using ImageJ (Schneider et al. 2012) I measured the height of midgut epithelial cells (basal to apical surface) at both 90-degree bends in the C-shaped gut, where the

majority of fungal spores penetrate (Fig. 4.1; Chapter 1; Stewart Merrill & Cáceres 2018). Three epithelial cells were measured at each bend and, from these values, I calculated the average anterior (top bend) and posterior (bottom bend) epithelium thickness. Cell heights at the three points were strongly correlated, indicating high measurement consistency (average anterior r = 0.91; average posterior r = 0.87). To measure the penetrability of the gut barrier, I used the spore locations from H1 to relate each host's level of infection to its level of attack. Gut penetrability is the proportion of attacking spores that successfully infected the body cavity (Table 4.1). Larger values indicate higher gut penetrability, while zero represents impenetrability.

Results: Daphnia gut penetrability varied from entirely penetrable (100%) to entirely impenetrable (0%), indicating that the gut epithelium can act as a barrier to infection, but that *Daphnia* possess substantial variation in the strength of this barrier. Counter to my prediction, anterior gut thickness increased gut penetrability by spores (Fig. 4.3A; df = 61, est. = 0.035, p = 0.035, R^2 = 0.071). Alternatively, posterior gut thickness was not associated with gut penetrability (Fig. 4.3B; df = 66, est. = -0.009, p = 0.672, R^2 = 0.003). *Metschnikowia* spores, which average 45 μm in length (Ebert 2005), are at least two times longer than the thickest epithelium I observed (22.8 μm), highlighting that epithelium thickness alone does not create a realistic barrier for the spores. The weight of the evidence for gut thickness explaining the gut barrier is intermediate; in the anterior region of the midgut, gut thickness explained 7% of the variation in gut penetrability (but in the opposite manner from which I predicted).

H3: Haemocytes mediate recovery

Background: Parasites that bypass their invertebrate host's barriers face cellular defenses. Host haemocytes are recruited to the site of infection and can kill invading parasites via phagocytosis, melanization, and secretion of humoral effectors (Bayne et al. 2001; Lemaitre & Hoffmann, 2007; Bartholomay et al. 2007; Moreno-Garcia et al. 2013). But linking haemocytes to host recovery presents an interpretation problem (Dittmer et al. 2011; Auld et al. 2011). Haemocytes kill parasites but are also up-regulated during infection. Hence, interpreting haemocytes as mediators of recovery or symptoms of susceptibility is difficult without knowing the host's intensity of infection. By measuring each host's intensity of infection and tracking their infection fate (whether they recovered from infection or succumbed to terminal infection), I

examined if haemocytes merely increase following infection or more directly mediate host recovery.

Methods: To measure haemocytes, I counted the number of haemocytes aggregating on haemocoel spores (Fig. 4.1). This provided two values: total haemocyte recruitment (the total count of haemocytes on spores), and the number of haemocytes per spore. I first tested whether haemocytes were up-regulated in response to infection by evaluating the relationship between total haemocyte recruitment and spores infecting the body cavity. Then, I tested whether haemocytes were associated with recovery. Having tracked field-collected *Daphnia* until nine days post-inoculation, I was able to separate previously infected hosts (those that had spores infecting the body cavity following inoculation) into two categories: hosts that recovered and hosts that succumbed to terminal infection. I compared the number of haemocytes per spore among these two classes.

Results: Total recruited haemocytes increased with the number of infecting spores in both laboratory-reared *Daphnia* (Fig. 4.4A; df = 106, est = 1.609, $p < 0.001$, $R^2 = 0.157$) and field-collected *Daphnia* (Fig. 4.4B; df = 1931, est = 1.508, $p < 0.001$, $R^2 = 0.209$). Of 510 inoculated and tracked *Daphnia*, 13% never became infected (their gut barriers resisted infection), 19% recovered from infection, and 68% succumbed to terminal infection. However, recovery from infection was not associated with the number of haemocytes per spore (Fig. 4.4C; $F_{1,410} = 1.237$, $p = 0.267$). Although haemocytes were upregulated in an apparent attempt at recovery, they had no detectable impact on recovery. Thus, the weight of the evidence for haemocytes mediating recovery is low in this study.

H4: Body size influences infection

Background: Body size itself may determine infection outcomes (Hall et al. 2007; Poulin 2013). For instance, as organisms grow, they can accumulate more parasites over time. Greater host size may also increase encounter rates with parasites that are consumed. Additionally, large organisms may provide a higher quality resource for feeding and developing parasites. However, size can exert opposing effects on other infection mechanisms. For example, large organisms may have more resources to invest in energy-dependent immune responses (Rantala & Roff 2005; Sparkman & Palacios 2009). Therefore, the role of size in host susceptibility depends on the size-dependence and relative importance of each step of the infection process (Downs et al.

2019). In *Daphnia*, body size increases exposure (foraging rate; Ebert 1995; Hall et al. 2007) as well as the size of the resource base (Hall et al. 2009; Civitello et al. 2015). Here, I evaluate the effects of body size on the full set of steps comprising the *Daphnia-Metschnikowia* interaction.

Methods and Results: Body length was measured from the center of the eye to the base of the tail spine. I first tested if body size increased spore ingestion (as lumen spores). Body size increased lumen spores in both laboratory-reared (Fig. 4.5A; df = 54, est = 27.73, p = 0.041, R^2 = 0.075) and field-collected *Daphnia* (Fig. 4.5B; df = 1622, est = 9.434, p < 0.001, R^2 = 0.008). Second, I tested whether body size increased the frequency of parasite attack. Attack frequency is the proportion of spores a host is exposed to that attempt to cross the gut barrier (attack / exposure; Table 4.1). Attack frequency trended negatively with body size in laboratory-reared *Daphnia* (Fig. 4.5C; df = 55, est = -0.112, p = 0.080, R^2 = 0.055) and decreased with body size in field-collected *Daphnia* (Fig. 4.5D; df = 1609, est = -0.201, p < 0.001, R^2 = 0.012). Larger *Daphnia* may have larger gut epithelial cells, so may also have higher gut penetrability. I tested for correlations among gut thickness and body size, and tested whether body size increased gut penetrability. Body size was only weakly correlated with gut epithelium thickness in laboratory-reared *Daphnia* (anterior gut epithelium: r = 0.21, p = 0.060; posterior gut epithelium: r = 0.22, p = 0.069) and did not predict gut penetrability of laboratory-reared *Daphnia* (Fig. 4.5E; df = 110, est = 0.026, p = 0.886, R^2 = 0.001). However, I found a strong negative relationship between body size and gut penetrability in field-collected *Daphnia* (Fig. 4.5F; df = 1728, est = -0.518, p < 0.001, R^2 = 0.073). Finally, I tested whether body size increased immune responses by evaluating body size, haemocoel spores and their interaction on total recruited haemocytes. Here, the interaction effect between body size and haemocoel spores tells us how size influences the response of haemocytes to a given level of infection. In laboratory-reared *Daphnia*, I did not detect an interaction between body size and haemocoel spores (Fig. 4.5G; df =86, est = 2.475, p = 0.251, R^2 = 0.189). In field-collected *Daphnia*, the interaction between body size and haemocoel spores was strong: larger *Daphnia* had greater haemocyte responses for a given level of infection (Fig. 4.5H; df = 1437, est = 5.975, p < 0.001, R^2 = 0.240). The weight of the evidence for body size influencing infection was intermediate and mixed. The amount of variation that body size explained ranged from R^2 = 0.00 to R^2 = 0.24 for multiple infection steps. Knowledge of which steps of infection (exposure, barriers, or immune responses) are the

most important for determining terminal infection outcomes will clarify the role of body size in influencing this host-parasite interaction.

Lab to Field Comparisons with Standardized Regression Coefficients

Laboratory environments can introduce artificial biases into experiments and a common concern is whether interactions observed in a lab approximate those that occur in the natural world. I wanted to know: were the infection drivers I uncovered consistent across laboratory and natural *Daphnia* populations? I tested for consistency in relationships among laboratory-reared and field-collected *Daphnia* by comparing standardized model coefficients with a paired t-test. Fit to z-transformed data, these standardized coefficients scaled all relationships to the same currency. With them, I compared the following *y* by *x* relationships: *i*) haemocoel spores by lumen spores, *ii*) haemocytes by spores, *iii*) lumen spores by body size, *iv*) attack frequency by body size, *v*) gut penetrability by body size, and *vi*) haemocytes by body size (Fig. 4.6). Standardized regression coefficients did not differ among field-collected and laboratory-reared *Daphnia* but fell on or near the 1:1 line ($df = 5$, $t = -0.033$, $p = 0.975$). The processes and traits that drive the steps of infection were highly consistent from lab to field.

Integrating infection steps to understand susceptibility

Isolating the steps of infection provided multiple sound alternative hypotheses. *Daphnia* may face greater risk of infection as their spore ingestion increases and may be particularly susceptible to infection if they have penetrable gut barriers. Susceptibility may be further tuned by the haemocytes produced for a given level of infection, and by the host's body size. Here, I bring these drivers together to determine what factors underlie susceptibility. More specifically, I competed models with AIC (Burnham & Anderson 2002) and determined which hypothetical drivers of infection (1-4) best fit empirical data on terminal infection outcomes.

Having tracked field-collected *Daphnia* until nine days post-inoculation, I had binary data for their terminal infection status (terminal infection: 1; recovery from infection: 0). I constructed generalized linear models (binomial distribution, logit link) assessing how terminal infection status at day 9 was affected by predictors measured post-inoculation. I generated seven model sets within which I manipulated the number and type of interaction effects (Table 4.2). Because terminal infections require exposure, all models (except the null) included exposure as a

covariate (defined in Table 4.1), which allowed me to determine which factors best explained variation in the exposure-terminal infection relationship.

In the first model set (1), "exposure", exposure is the sole predictor of terminal infection. This model assumes that *Daphnia* do not vary in their susceptibility; terminal infection only depends on the cumulative number of spores that enter their bodies. The second model set (2), "body size", included exposure and body size, and consisted of two models containing their additive or interactive effects. In the third model set (3), "barriers", spores that enter the host are inhibited by the gut barrier, and the model set consisted of two models containing the additive or interactive effects of exposure and gut penetrability. In the fourth model set (4), "immune responses", the fungus is killed by host haemocytes, and the two models included the additive or interactive effects of exposure and haemocytes per spore. Exposure, body size, and gut penetrability were combined in the fifth model set (5), "pre-body cavity interactions", which consisted of five models containing their additive and interactive effects (i.e., all possible interactions, then subsets of interactions). Here, terminal infection is primarily determined by processes occurring *before* spores enter the body cavity, including the effects of body size. Then, exposure, body size, and haemocytes per spore were paired in the sixth model set (6), "within-host battle", consisting of five models containing their additive and interactive effects. Here, terminal infection is primarily determined by interactions occurring *within* the host's body cavity, including the effects of body size. Finally, in (7), "total defenses", barriers and immune responses act together to defeat parasites (absent body size), and five models were constructed that included the additive and interactive effects of exposure, gut penetrability, and haemocytes per spore. All models contained an intercept and, within the model competition, I also included an intercept-only null model, and a global model containing all predictors and their interactions. Models were ranked by their AIC values, with the lowest AIC value representing the most likely model given the data. I then compared models based on their performance relative the best-ranked model (ΔAIC) and by their model weights (w_i). Model weights represent the probability that a model fits best, given the suite of models considered (Burnham & Anderson 2002).

The two host immune defenses (barriers and haemocytes) acted in concert to best explain variation in the exposure-terminal infection relationship. The top-ranked model emerged from model set (7), "total defenses", and contained all interactions between exposure, gut penetrability and haemocytes per spore. In this winning model, terminal infection is dictated by how spores

are blocked by the gut barrier and met by the haemocyte response. The best-ranked model had an Akaike weight of 0.84, indicating its high explanatory power relative the other models. Because the second most competitive model was another variant of the "total defenses" set, model set (7) contained over 93% of the weight of the evidence (Table 4.2).

In the model competition, the interaction between gut penetrability and haemocytes per spore (gut pen*haemocytes; Table 4.2) came out as a consistently important predictor: this interaction was only included in three models, and all three models containing the interaction were also the best ranked. I examined the probabilities predicted from the winning model to explore what this interaction means for *Daphnia* (Fig. 4.7). While haemocytes decreased terminal infection probability for *Daphnia* with high gut penetrability, they were associated with increased terminal infection probability for *Daphnia* with low gut penetrability (Fig. 4.7). This interaction effect helps resolve why haemocytes were not associated with recovery in H3 and suggests that haemocytes may mediate recovery for only some *Daphnia*, while signaling susceptibility in others.

Discussion

I found statistical support for four drivers of *Daphnia* infection: ***i***) exposure, where spore ingestion increased the number of spores that infected the host; ***ii***) barriers, where attacking spores were blocked by the gut barrier and thinner anterior epithelia conferred greater resistance; ***iii***) immune responses, where spores that infected the host elicited an intensity-dependent increase in recruited haemocytes; and ***iv***) host body size, which influenced multiple steps of infection, increasing spore ingestion, decreasing attack frequency and gut penetrability, and increasing the magnitude of the haemocyte response. However, when considered alone, each driver exhibited substantial host variation and generally low effect sizes. The weight of the evidence in support of exposure (H1) and immune responses (H3) was low, whereas I found intermediate support for barriers (H2) and body size (H4). By integrating these four drivers, I sought to absorb variation in the complete infection process. I found that each driver of infection differed in its contribution to terminal infection outcomes. Model comparison revealed that host immune defenses, i.e., the combination of gut barriers and haemocytes, explained the most variation in the exposure-terminal infection relationship. Host body size was present in the third best-ranked model but could not compete with barriers and haemocytes. My results illustrate the

hierarchical nature of host immune defenses and raise questions about potential tradeoffs occurring at each step of infection.

Parasite exposure increases disease risk, and avoidance behaviors are a first line of defense for limiting exposure (Buck et al. 2018; Weinstein et al. 2018a). For example, spiny lobsters detect viral infection in conspecifics and reduce their risk of transmission by limiting physical contact (Behringer et al. 2006). But avoidance behaviors may be costly when parasite encounter is tightly coupled with feeding. In this case, hosts must balance the risk of disease against the need for food (Lozano 1991; Hall et al. 2009; Hall et al. 2010). Whether avoiding parasite consumption is costly or beneficial for a host should depend on the parasite's pathogenicity and density in the environment. For low pathogenicity parasites, heightened risk of infection can be worth the benefit of a meal (Lafferty & Morris 1996; Weinstein et al. 2018b), and when parasites are dense across the environment, avoidance may be futile. *Metschnikowia* is both highly pathogenic and highly abundant during epidemics (Chapter 3) and wild *Daphnia* may be forced to feed amidst unavoidable levels of risk. I found only weak relationships between spore ingestion and infection, suggesting that downstream defenses decouple exposure from infection and relax foraging-infection tradeoffs.

For parasites that must be ingested to infect, the gut epithelium presents a physical barrier to infection (Soderhall 2010; Garcia-Garcia et al. 2013). In the test of whether thicker guts were less penetrable by *Metschnikowia*, I was surprised by the result: thicker anterior epithelia were more, rather than less, penetrable by the needle-shaped spores. Given this finding, as well as the large difference between average spore length (45 μm) and average gut thickness (15 μm), it may not be cell height per se that is driving penetrability, but rather, structural attributes that are correlated with cell height. I suspect that the penetrability of the gut barrier is related to its cells' ability to absorb nutrients. In addition to being a site of infection, the anterior midgut is important for resource assimilation and requires its permeability. Anterior midgut epithelia are actively involved in resource absorption (Quaglia et al. 1976; Schultz & Kennedy 1976) and have been observed to shrink during periods of starvation (Theilacker & Watanabe 1989; Elendt & Storch 1990). The potential reliance of parasite resistance and resource assimilation on contrasting aspects of gut morphology could generate a foraging-infection tradeoff at the gut barrier. Similar tradeoffs have been detected in *Drosophila*, where strong pathogen resistance by the peritrophic membrane decreases its permeability and nutrient absorption (Kuraishi et al.

2011; Shibata et al. 2015). Given the broad diversity of parasites that infect via the host gut, future work on host resistance may benefit from the dual consideration of the gut's defensive and digestive properties (Miguel-Aliaga et al. 2018).

Internal immunological responses are a final defense against parasites that cross host barriers. Haemocytes are among the most well-studied immune responses of invertebrates (Bayne et al. 2001; Lemaitre & Hoffmann, 2007; Bartholomay et al. 2007; Moreno-Garcia et al. 2013), but their role in combatting parasites has been called into question in *Daphnia*. In his classic study of invertebrate immunity, Metschnikoff (1884) described *Daphnia* haemocytes attacking *Metschnikowia* spores, highlighting their role in host defense. More recently, Auld et al (2010; 2011) observed the strongest haemocyte responses in the most susceptible *Daphnia*, suggesting that haemocytes were merely a symptom of upstream susceptibility (Graham et al. 2011). My findings revealed a complicated relationship between haemocyte responses and parasite infection. In particular, the model comparison revealed a strong interaction between gut penetrability and the haemocyte response: among *Daphnia* that had more penetrable guts, higher haemocyte levels were associated with decreased terminal infection risk, whereas haemocytes did not dampen terminal infection risk in *Daphnia* with low gut penetrability. The source of the disparate relationship between haemocytes, terminal infection risk, and gut penetrability is unclear, but may stem from tradeoffs between immune defense types. Vertebrates are thought to differentially invest in innate or acquired defenses (Lochmiller & Deerenberg 2000), and invertebrates may likewise invest either in resistant barriers or effective immune responses. If barriers are weak and parasites can easily enter the body cavity, a *Daphnia* host should rely on a well-operating immune response. Alternatively, *Daphnia* with robust barriers may have high internal susceptibility and haemocytes may be a symptom of internal susceptibility. Greater resolution on this potential tradeoff may be achieved by assessing haemocyte quality (in addition to quantity), as well as other immune responses that act against *Metschnikowia*.

Body size often increases exposure to parasite propagules (Ebert 1995; Hall et al. 2007; Civitello et al. 2015) but may have variable effects on a host's susceptibility (Downs et al. 2019). While my results confirmed that body size increases spore ingestion, I found negative size-susceptibility relationships for all subsequent infection steps. In support of Izhar et al. (2015) and Izhar & Ben-Ami (2015), the cumulative effects of body size generally resulted in decreasing terminal infection risk with increasing body size (Appendix D.4). The "total defenses" model,

which included exposure, barriers, and the haemocyte response, substantially outperformed all other models in explaining terminal infection outcomes. But body size was a strong contender. Body size was included in the third most competitive model (the global model), suggesting its important role in infection. That the effects of body size were statistically overwhelmed by those of gut penetrability and haemocytes raises the question of how body size affects those two key traits. Haemocyte responses increased with body size, which is in line with both theory (Sheldon & Verhulst 1996; Sadd & Schmid-Hempel 2008) and empirical work on energy-dependence of immune defense (Siva-Jothy & Thompson 2002; Valtonen et al. 2010; Triggs & Knell 2012).

Gut penetrability decreased with body size, which warrants consideration of the physical processes by which spores enter their hosts. I measured gut penetrability functionally, asking: what proportion of spores does the gut epithelium block? Because this measure results from the interaction of two players (gut and spore), it should depend on both the epithelial cell's permissiveness to puncture as well as the force and direction of the spores. Guts are like pipes, and while increasing host body size will increase the length and surface area of the gut (Hall et al. 2007), it will increase its volume at a faster rate. Hence, as body size increases, there are more opportunities for spores to occupy the gut lumen than contact its edges. In large hosts (big pipes), spores may just barely contact the gut epithelium, with the majority of the spore's length residing in the gut lumen. In small hosts (small pipes), the intraluminal space may be tight enough that spores get stuck and pierce through the gut barrier. For ingested parasites more generally, such scaling relationships between body size, feeding rate, and gut morphology may be important determinants of the body size-infection relationship.

Natural ecological conditions can be varied and unpredictable, such that measurements taken under laboratory settings might paint an artificial picture of an organism's capacity to fight infection (Boughton et al. 2011; Pedersen & Babayan 2011). The laboratory-reared *Daphnia* in this study were standardized to remove maternal effects and were raised in a high-food, low competition and parasite-free environment (until inoculation, at least). Alternatively, the field-collected *Daphnia* were of unknown genetic/epigenetic background and possessed diverse histories with resources, competitors, and exposure to parasites. In spite of these differences, my results were remarkably consistent among laboratory-reared and field-collected hosts. For instance, the relationship between body size and attack frequency had almost identical standardized coefficients in both populations, lending credence to the idea that spore attack is a

purely physical process. Through robust sample sizes, the field-collected *Daphnia* allowed me to detect noisy relationships, and also provided greater insight into one driver of infection: the gut barrier. The strongest deviation in standardized coefficients was in the body size and gut penetrability relationship, which was strong and negative for field-collected *Daphnia* but weak and near zero for laboratory-reared *Daphnia*. Interestingly, individuals from the field also had much lower gut penetrability on average (field mean: 0.30; lab mean: 0.44). Given the importance of gut penetrability for both parasite resistance and resource assimilation, I suspect that resources, which are often poorer quality in the field, and parasites, which are abundant and diverse in the field, may be driving these differences.

Host susceptibility is a simple concept in theory but difficult to measure in practice. By decomposing the infection process, I gained new biological insight into four drivers of infection in *Daphnia*. When considered in isolation, these drivers weakly explained infection outcomes, but when united, they became powerful predictors of *Daphnia* susceptibility. In both laboratory-reared and field-collected *Daphnia*, I found dramatic variation in the four host traits that drive infection. Spore ingestion ranged over two orders of magnitude, gut penetrability varied from completely penetrable (100%) to completely impenetrable (0%), and haemocytes varied both in number and ability to prevent infection. It is no stretch to link this variation to resources. Host feeding brings spores into the body, the epithelial cells comprising the gut barrier process resources, and haemocytes are likely resource-dependent. A resource perspective (e.g. Hall et al. 2009, 2010, 2012; Cressler et al. 2014) on the genetic and plastic components of susceptibility will propel research in *Daphnia* disease, as well as other systems where parasites infect through host feeding.

Tables and Figures

Table 4.1: Metrics used to quantify steps and mechanisms of the infection process. For each measure, I provide its description or equation, along with sample sizes (*N*) for laboratory-reared and field-collected hosts. Sample sizes varied due to the ability to accurately quantify a particular metric. For instance, I did not count 'lumen spores' in individuals where spores could not be reliably distinguished from other material in the gut. Additionally, 'haemocytes' could not be counted for individuals without penetration of 'haemocoel spores'. *Note*: 'Terminal infections' were not measured on laboratory-reared animals and 'gut thickness' was not measured on field-collected animals.

Metric	Description or Equation	Lab *N*	Field *N*
Lumen spores	Ingested spores free-floating in the gut lumen	58	2039
Barrier spores	Spores only partially embedded in the gut epithelial barrier	136	2263
Haemocoel spores	Spores in the body cavity that can develop to later stages	136	2266
Haemocytes	Immune cells aggregated on spores in the body cavity	108	2065
Gut thickness	The width of the gut epithelium where spores penetrate	79	-
Body size	Length from center of the eye to base of the tail spine	112	1786
Terminal infection	Terminal infection status at nine days post-inoculation	-	510
Exposure	Σ (lumen spores, barrier spores, haemocoel spores)	58	2039
Attack	Σ (barrier spores, haemocoel spores)	136	2263
Infection	= haemocoel spores	136	2266
Attack frequency	Attack / exposure	59	2023
Gut penetrability	Infection / attack	136	2262

Table 4.2. Generalized linear models assessing potential predictors of terminal infection outcomes. Numbers in parentheticals indicate the model set that each model belongs to: (1) – Exposure, (2) - Body size, (3)- Barriers, (4)- Immune responses, (5)- Pre-body cavity interactions, (6)- Within-host battle, (7)- Total defenses. Predictors include 'exposure' (cumulative number of all spores within the host's body), 'guts' (gut penetrability), 'haemocytes' (average number of haemocytes per spore), and 'size' (body size of the host). Additive effects of predictors are indicated with '+'. I use '*' to denote when a model combines both the additive and interactive effects of predictors. Provided for each model are: *K* (the number of estimated parameters), ΔAIC (indicating model performance relative the best-ranked model), and relative likelihood (w_i, the probability that the model fits best, given the suite of models considered). Additional output (AIC and estimates) is presented in Appendix D.4. Models from the 'Total defenses' set (7), which incorporated exposure, gut penetrability ('guts'), and average haemocytes per spore ('haemocytes'), were the highest ranked with a combined relative likelihood (w_i) of 0.93. The interaction between gut penetrability and the haemocyte response (guts*haemocytes) was consistently represented among the three top-ranked models, suggesting an important interaction effect between host barriers and immune responses.

Model Set	Predictors	K	ΔAIC	w_i
(7) Total defenses	**exposure*guts*haemocytes**	**8**	**0.00**	**0.84**
(7) Total defenses	**exposure + guts*haemocytes**	**5**	**4.41**	**0.09**
Global model	exposure*size*guts*haemocytes	16	4.91	0.07
(7) Total defenses	exposure*haemocytes + guts	5	14.21	0.00
(5) Pre- body cavity	exposure + size*guts	5	17.07	0.00
(3) Barriers	exposure + guts	3	17.38	0.00
(3) Barriers	exposure*guts	4	17.77	0.00
(5) Pre- body cavity	exposure + size + guts	4	19.23	0.00
(7) Total defenses	exposure + guts + haemocytes	4	19.37	0.00
(5) Pre- body cavity	exposure*guts + size	5	19.70	0.00
(7) Total defenses	exposure*guts + haemocytes	5	19.77	0.00
(5) Pre- body cavity	exposure*size*guts	8	20.26	0.00
(5) Pre- body cavity	exposure*size + guts	5	20.70	0.00
(6) Within-host battle	exposure*size*haemocytes	8	32.21	0.00
(6) Within-host battle	exposure + size*haemocytes	5	34.35	0.00
(6) Within-host battle	exposure*haemocytes + size	5	40.12	0.00
(2) Body size	exposure + size	3	42.31	0.00
(4) Immune responses	exposure*haemocytes	4	42.85	0.00
(2) Body size	exposure*size	4	43.86	0.00
(6) Within-host battle	exposure + size + haemocytes	4	44.25	0.00
(1) Exposure	exposure	2	44.94	0.00
(6) Within-host battle	exposure*size + haemocytes	5	45.80	0.00
(4) Immune responses	exposure + haemocytes	3	46.89	0.00
Null model	Intercept-only	1	48.31	0.00

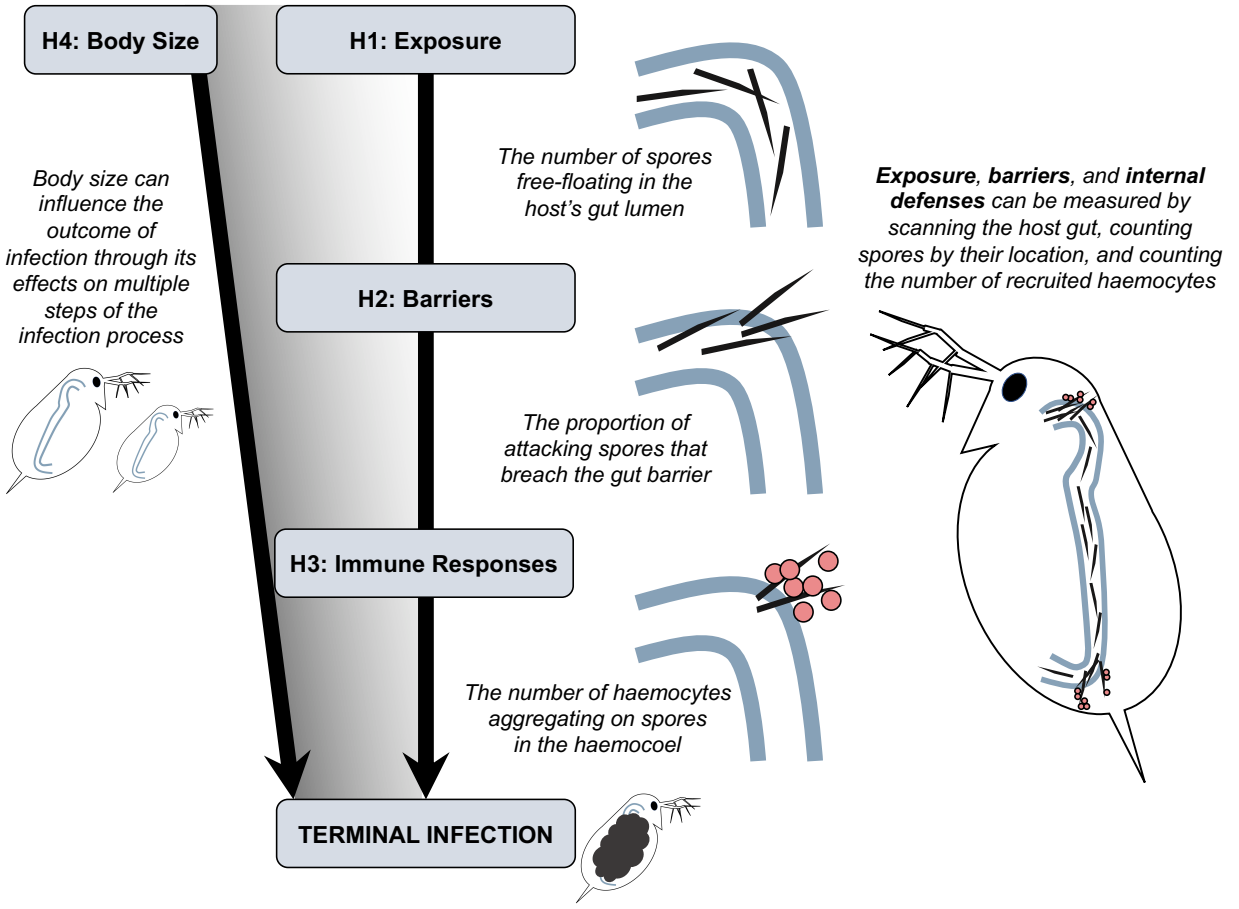

Figure 4.1. The four drivers of infection, as well as associated empirical measurements in *Daphnia dentifera*. Hypotheses one to three (H1:H3) focus on three sequential steps of the infection process, any of which may be the strongest driver of terminal infection. Hypothesis four (H4) proposes that body size influences the outcome of terminal infection through its potential effects (gray shading) on the full set of drivers. Terminal infection is reached when the host possesses late infection stages from which it cannot recover (described in Appendix D.1). To measure exposure (H1), barriers (H2), and immune responses (H3), I scanned the full length of the *Daphnia* gut and classified spores based on their location within the host's body (following a set of metrics and calculations [Table 4.1]). For example, the enlarged gut diagram depicted here has 4 lumen spores, 2 barrier spores, and 2 haemocoel spores, resulting in an exposure value of 8, attack of 4, and infection of 2. For gut thickness (barriers, H2), I measured height of epithelial cells at the anterior (top) and posterior (bottom) bends of the gut, where spores most commonly penetrate (see full body diagram, to right). For my measure of immune response (H3), I counted host haemocytes. Here, the enlarged gut diagram has seven haemocytes aggregating on the spores in its haemocoel, or 3.5 haemocytes per spore.

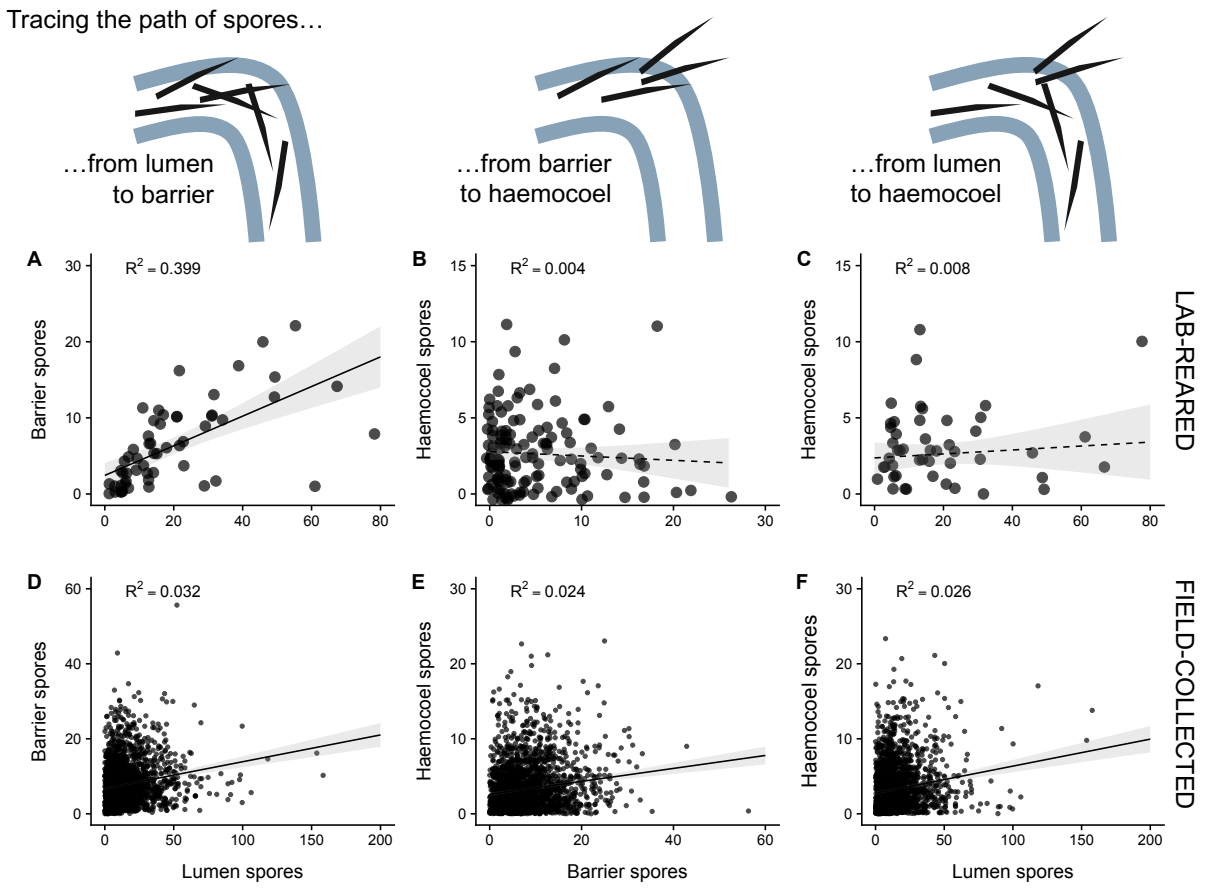

Figure 4.2. Testing H1 ("exposure drives infection") by tracing the path of fungal spores after they are ingested. Exposure-infection relationships become decoupled as spores move from the gut lumen, across the gut barrier, and into the host body cavity. Lumen spores are positively associated with barrier spores (left column: **A** and **D**). Weak or non-significant associations occur between barrier spores and successfully penetrated haemocoel spores (central column: **B** and **E**). Ultimately, number of lumen spores explains less than 3% of successfully penetrated haemocoel spores (right column: **C** and **F**). Top row plots (**A**-**C**) are laboratory-reared *Daphnia*, and bottom row (**D**-**F**) are field-collected *Daphnia*; each point represents a single individual. Solid regression lines indicate significant relationships, dashed lines indicate non-significant relationships, and gray shading around the regression lines represents the standard error of the fit regression. Further information on the path spores take and how they are classified is provided in Figure 4.1 and Table 4.1.

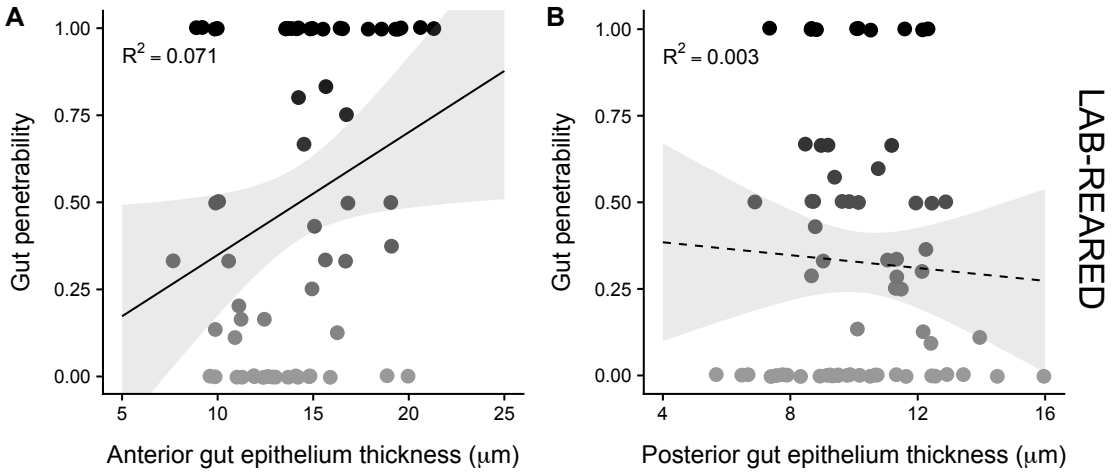

Figure 4.3. Testing H2 ("gut thickness creates a barrier to infection"), I assessed whether gut penetrability (i.e., proportion of attacking spores that successfully penetrate the body cavity: Table 4.1) was explained by the thickness of the gut epithelium. **A.** Thicker anterior epithelia are associated with higher gut penetrability. **B.** In the posterior region of the gut, there is no association between gut epithelium thickness and gut penetrability. In both panels, each point represents a unique laboratory-reared individual, and points shade from gray to black as gut penetrability increases (light gray: 0%; black: 100%). The solid line indicates a significant relationship, the dashed line indicates a non-significant relationship, and gray shading around the regression lines represents the standard error of the fit regression.

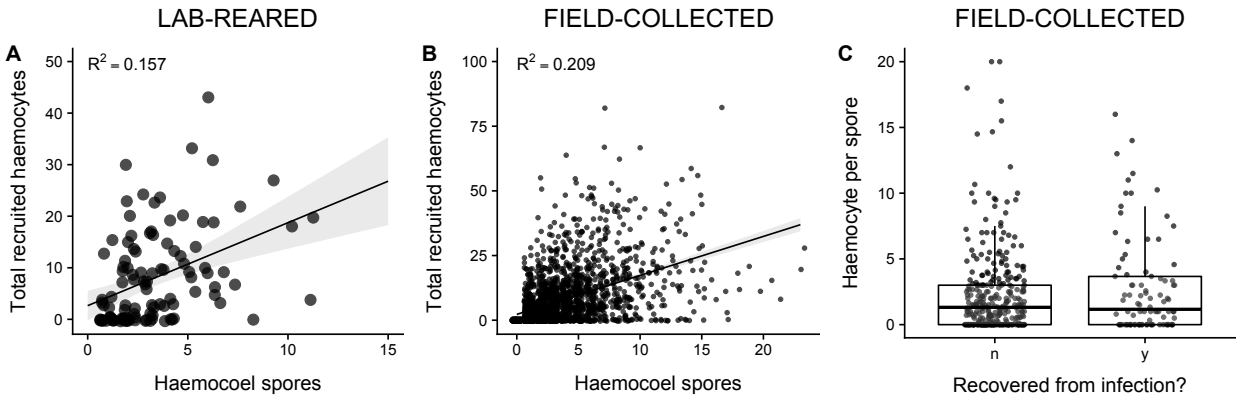

Figure 4.4. Testing H3 ("haemocytes mediate recovery"), I examined haemocytes as symptoms of infection and causes of recovery. For both laboratory-reared (**A**) and field-collected (**B**) *Daphnia*, recruited haemocytes increased as a function of spores infecting the body cavity, suggesting that infection intensity may be an important factor for interpreting haemocyte-recovery relationships. **C.** Field-collected individuals that achieved early infections were tracked until they recovered from infection or succumbed to terminal infection and the number of haemocytes per spore was not associated with recovery. Solid lines indicate significant relationships and shading around the line represents the standard error of the fit regression.

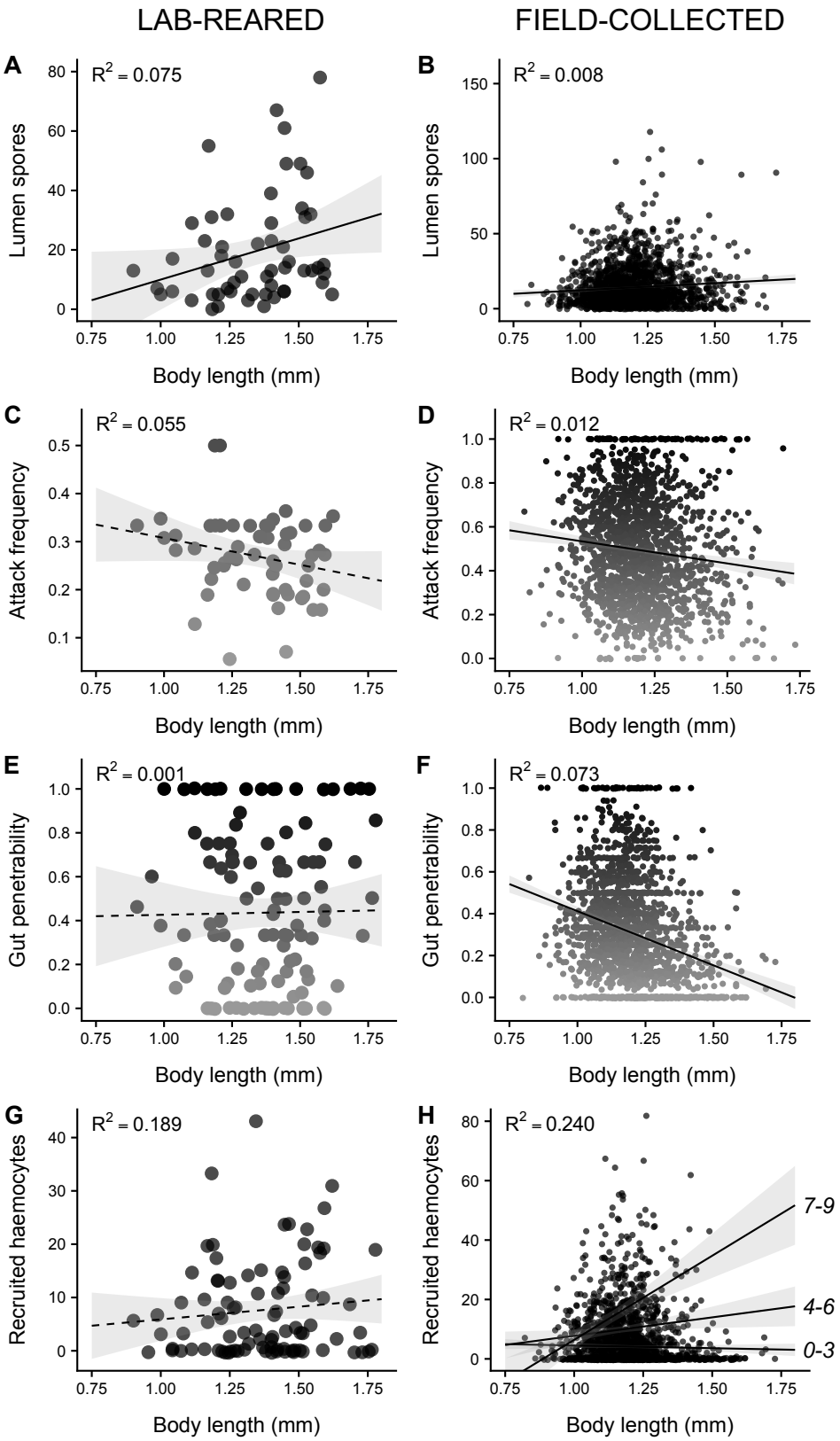
LAB-REARED
FIELD-COLLECTED
A
B
C
D
E
F
G
H
R^2 = 0.075
R^2 = 0.008
R^2 = 0.055
R^2 = 0.012
R^2 = 0.001
R^2 = 0.073
R^2 = 0.189
R^2 = 0.240
Lumen spores
Attack frequency
Gut penetrability
Recruited haemocytes
Body length (mm)
7-9
4-6
0-3

Figure 4.5.

Figure 4.5. – continued. Body size can have a complex relationship with host susceptibility due to its potentially opposing effects on multiple steps of infection. Testing H4 ("body size influences infection"), I examined the effects of body size on spore consumption, attack frequency, gut penetrability, and the haemocyte response, for laboratory-reared (left column) and field-collected (right column) hosts. Although body size (**A**/**B**) increased spore consumption, both the (**C**/**D**) attack (attack / exposure) and (**E**/**F**) gut penetrability (infection / attack) decreased with host body size. The dose-dependent haemocyte response (**G**/**H**) also increased with body size for field-collected *Daphnia*, where lines indicate the intensity of infection at 0-3, 4-6, and 7-9 haemocoel spores (93% of individuals had infections within the range of 0-9 haemocoel spores). Although the direction of relationships was fairly consistent among the two populations, not all relationships were significant for laboratory-reared *Daphnia* (given less power of tests). Across all panels, points represent unique individuals, and points shade from gray to black as attack frequency and gut penetrability increases (light gray: 0%; black: 100%). Solid lines indicate significant relationships, dashed lines indicate non-significant relationships, and shading around the line represents the standard error of the fit regression.

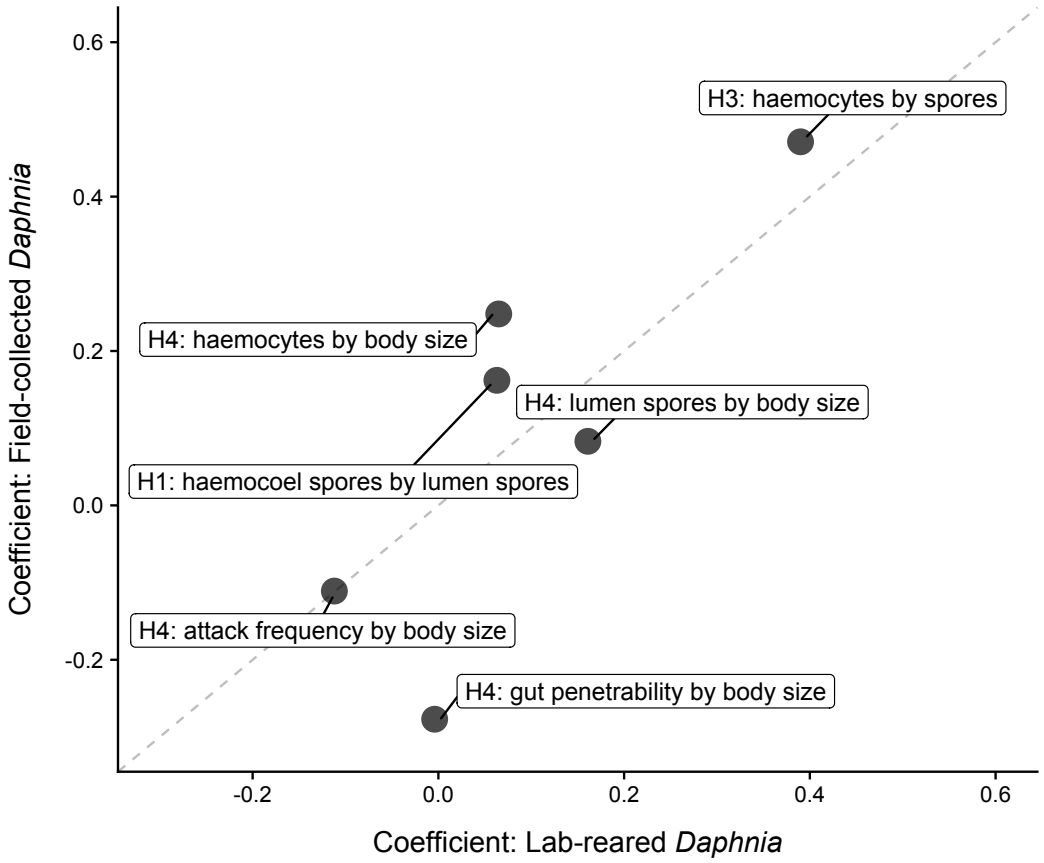

Figure 4.6. Comparing hypothetical drivers of infection among laboratory-reared and field-collected *Daphnia*. Each point represents the regression coefficient for a given y by x analysis from H1, H3 and H4. Coefficients were standardized to the same currency by performing analyses on z-transformed data. The gray dashed 1:1 line indicates perfect correspondence among coefficients. In H1 ("exposure drives infection"; Fig. 4.2) I tested whether ingested lumen spores predicted successfully penetrated haemocoel spores, here indicated by 'H1: haemocoel spores by lumen spores'. I could not compare the results of H2 ("gut thickness creates a barrier to infection") because I did not have gut thickness measurements for field-collected animals. In H3 ("haemocytes mediate recovery"; Fig. 4.4) I tested whether total haemocyte recruitment increased with the number of spores infecting the body cavity, here indicated by the label 'H3: haemocytes by spores'. I could not compare the effects of haemocytes on recovery because I did not have terminal infection status for laboratory-reared animals. In H4 ("body size influences infection"; Fig. 4.5) I assessed how body size affected multiple steps of the host-parasite interaction: spore ingestion ('H4: lumen spores by body size'), attack frequency ('H4: attack frequency by body size') and gut penetrability ('H4: gut penetrability by body size'). In H4 I also tested whether body size increased immune responses by evaluating the effects of body size, haemocoel spores, and their interaction on total recruited haemocytes – the coefficient for the interaction between body size and haemocoel spores is plotted here as 'H4: haemocytes by body size'. Relationships are highly consistent among laboratory-reared and field-collected *Daphnia dentifera,* with no difference in standardized regression coefficients among the two populations.

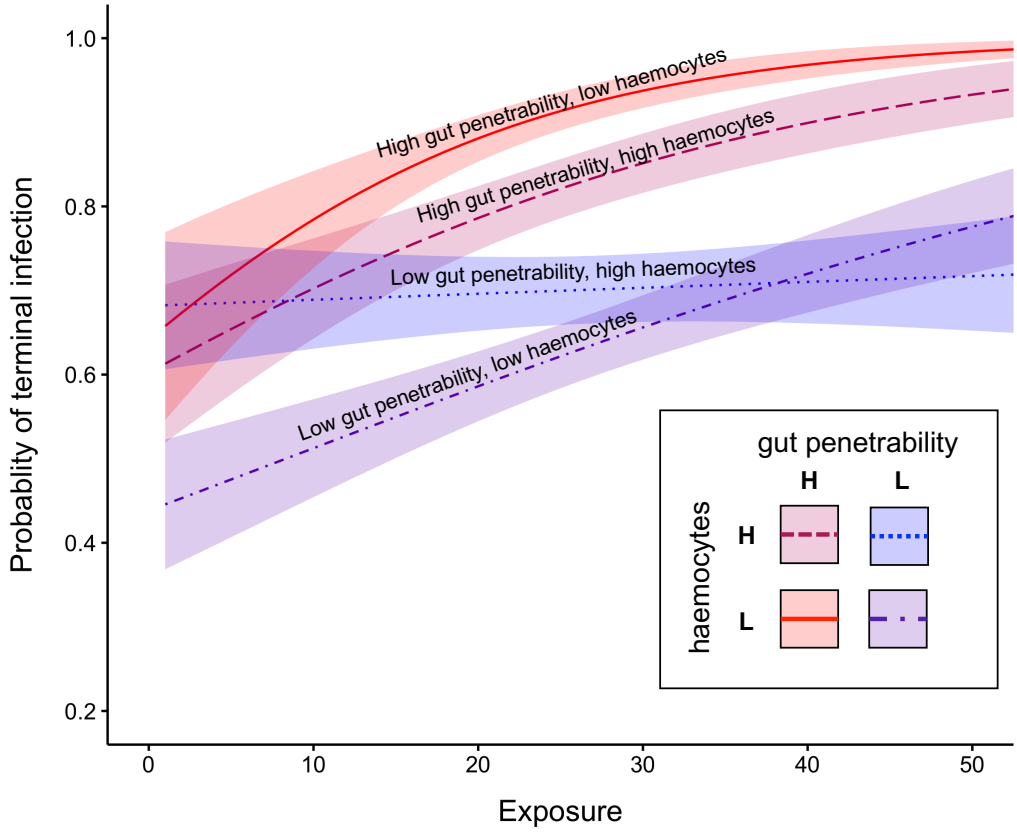

Figure 4.7. Predicted terminal infection probabilities from the top ranked "total defenses" model (Table 4.2) are plotted as a function of exposure (see Table 4.1). To illustrate the interaction between gut penetrability and haemocytes, I plot lines and standard error shading for four host classes, categorized by whether they fall above (H: high) or below (L: low) the median level of gut penetrability and the median haemocyte response (haemocytes per spore). Low gut penetrability generally decreases the risk of terminal infection: the probability of terminal infection is highest for *Daphnia* with high gut penetrability and lowest for *Daphnia* with low gut penetrability. Intermediate terminal infection risk emerges for *Daphnia* with high gut penetrability and high haemocyte responses: when *Daphnia* barriers are poor, haemocytes aid in recovery. While the three aforementioned classes share similar exposure-terminal infection curves, the fourth class (low gut penetrability, high haemocytes) shows consistently high susceptibility over the range of exposure. These *Daphnia* may be highly susceptible to terminal infection when their barriers fail, such that haemocytes are more a symptom of susceptibility than a cause of recovery.

REFERENCES

Acevedo-Whitehouse, K. & A.L. Duffus. 2009. Effects of environmental change on wildlife health. Philosophical Transactions of the Royal Society B: Biological Sciences 364:3429-3438.

Adema, C.M., C.J. Bayne, J.M. Bridger, M. Knight, E.S. Loker, T.P. Yoshino & S.M. Zhang. 2012. Will all scientists working on snails and the diseases they transmit please stand up? PLoS Neglected Tropical Diseases 6:e1835.

Adema, C.M. & E.S. Loker. 2015. Digenean-gastropod host associations inform on aspects of specific immunity in snails. Developmental & Comparative Immunology 48:275-283.

Anderson, R.M. & R.M. May. 1981. The population dynamics of microparasites and their invertebrate hosts. Philosophical Transactions of the Royal Society B: Biological Sciences 291:451-524.

Auld, S.K.J., J.A. Scholefield & T.J. Little. 2010. Genetic variation in the cellular response of *Daphnia magna* (Crustacea: Cladocera) to its bacterial parasite. Proceedings of the Royal Society B: Biological Sciences 277:3291-3297.

Auld, S.K.J.R., A.L. Graham, P.J. Wilson & T.J. Little. 2011. Elevated haemocyte number is associated with infection and low fitness in wild *Daphnia magna*. Functional Ecology 26:434-440.

Auld, S.K.J.R., K.H. Edel & T.J. Little. 2012. The cellular immune response of *Daphnia magna* under host-parasite genetic variation and variation in initial dose. Evolution 66:3287-3293.

Azambuja, P., E.S. Garcia, P.J. Waniek, C.S. Vieira, M.B. Figueiredo, M.S. Gonzales, C.B. Mello, D.P. Castro & N.A. Ratcliffe. 2017. *Rhodnius prolixus*: from physiology by Wigglesworth to recent studies of immune system modulation by *Trypanosoma cruzi* and *Trypanosoma rangeli*. Journal of Insect Physiology 97:45-65.

Bartholomay, L.C., G.F. Mayhew, J.F. Fuchs, T.A. Rocheleau, S.M. Erickson, M.T. Aliota & B.M. Christensen. 2007. Profiling infection responses in the haemocytes of the mosquito, *Aedes aegypti*. Insect Molecular Biology 16:761-776.

Bayne, C.J., U.K. Hahn & R.C. Bender. 2001. Mechanisms of molluscan host resistance and of parasite strategies for survival. Parasitology 123:S159-S167.

Becker, D.J., D.G. Streicker & S. Altizer. 2015. Linking anthropogenic resources to wildlife-pathogen dynamics: a review and meta-analysis. Ecology Letters 18:483-495.

Behringer, D.C., M.J. Butler & J.D. Shields. 2006. Avoidance of disease by social lobsters. Nature 441:421.

Bertram, C.R., M. Pinkowski, S.R. Hall, M.A. Duffy & C.E. Cáceres. 2013. Trait-mediated indirect effects, predators, and disease: test of a size-based model. Oecologia 173:1023-1032.

Beldomenico, P.M., S. Telfer, S. Gebert, L. Lukomski, M. Bennett & M. Begon. 2009. The vicious circle and infection intensity: the case of *Trypanosoma microti* in field vole populations. Epidemics 1:162-167.

Beldomenico, P.M. & M. Begon. 2010. Disease spread, susceptibility and infection intensity: vicious circles? Trends in Ecology and Evolution 25:21-27.

Boughton, R.K., G. Joop & S.A.O. Armitage. 2011. Outdoor immunology: methodological considerations for ecologists. Functional Ecology 25:81-100.

Bradley, J.E. & J.A. Jackson. 2008. Measuring immune system variation to help understand host-pathogen community dynamics. Parassitology 135:807-23.

Buck, J.C., R.F. Hechinger, A.C. Wood, T.E. Stewart, A.M. Kuris & K.D. Lafferty. 2017. Host density increases parasite recruitment but decreases host risk in a snail-trematode system. Ecology 98:2029-2038.

Buck, J.C., S.B. Weinstein & H.S. Young. 2018. Ecological and evolutionary consequences of parasite avoidance. Trends in Ecology & Evolution 33:619-632.

Burnham, K.P., and D.R. Anderson. 2002. Model selection and multimodel inference: a practical information-theoretic approach. Springer.

Bush, A.O., K.D. Lafferty, J.M. Lotz & A.W. Shostak. 1997. Parasitology meets ecology on its own terms: Margolis et al. Revisited. The Journal of Parasitology 83:575-583.

Byers J.E., A.H.M., Blakeslee, E. Linder, A.B. Cooper & T.J. Cooper. 2008. Controls of spatial variation in the prevalence of trematode parasites infecting a marine snail. Ecology 89:439-451.

Cáceres, C.E., S.R. Hall, M.A. Duffy, A.J. Tessier, C. Helmle & S. MacIntyre. 2006. Physical structure of lakes constrains epidemics in *Daphnia* populations. Ecology 87:1438-1444.

Cáceres, C.E., A.J. Tessier, M.A. Duffy & S.R. Hall. 2014. Disease in freshwater zooplankton: what have we learned and where are we going? Journal of Plankton Research 36:326-333.

Civitello, D.J., S. Pearsall, M.A. Duffy & S.R. hall. 2013. Parasite consumption and host interference can inhibit disease spread in dense populations. Ecology Letters 16:626-634.

Civitello, D.J., R.M. Penczykowski, A.N. Smith, M.S. Shocket, M.A. Duffy & S.R. Hall. 2015. Resources, key traits and the size of fungal epidemics in *Daphnia* populations. Journal of Animal Ecology 84:1010-1017.

Combes, C. 2001. Parasitism: the ecology and evolution of intimate interactions. The University of Chicago Press.

Coustau, C., B. Gourbal, D. Duval, T.P. Yoshino, C.M. Adema & G. Mitta. 2015. Advances in gastropod immunity from the study of the interaction between the snail *Biomphalaria glabrata* and its parasites: a review of research progress over the last decade. Fish and Shellfish Immunology 46:5-16.

Cressler, C.E., W.A. Nelson, T. Day & E. McCauley. 2014. Disentangling the interaction among host resources, the immune system and pathogens. Ecology Letters 17:284-93.

Davis, M.M. & Y. Engstrom. 2012. Immune response in the barrier epithelia: lessons from the fruit fly *Drosophila melanogaster*. Journal of Innate Immunity 4:273-283.

Des Roches, S., D.M. Post, N.E. Turley, J.K. Bailey, A.P. Hendry, M.T. Kinnison, J.A. Schweitzer & E.P. Palkovics. 2018. The ecological importance of intraspecific variation. Nature Ecology & Evolution 2:57-64.

Diamond, S.F. & J.G. Kingsolver. 2011. Host plant quality, selection history and trade-offs shape the immune responses of *Manduca sexta*. Proceedings of the Royal Society B: Biological Sciences 278:289-297.

Dittmer, J., A.V. Koehler, F-J. Richard, R. Poulin & M. Sicard. 2011. Variation of parasite load and immune parameters in two species of New Zealand shore crabs. Parasitology Research 109:759-767.

Downs, C.J., J.S. Adelman & G.E. Demas. 2014. Mechanisms and methods in ecoimmunology: integrating within-organism and between-organism processes. American Zoologist 54:340-352.

Downs C.J., L.A. Schoenle, B.A. Han, J.F. Harrison & L.B. Martin. 2019. Scaling of host competence. Trends in Parasitology 35:182-192.

Duffy, M.A., S.R. Hall, C.E. Cáceres & A.R. Ives. 2009. Rapid evolution, seasonality, and the termination of parasite epidemics. Ecology 90:1441-1448.

Dwyer, G., J.S. Elkinton & J.P. Buonaccorsi. 1997. Host heterogeneity in susceptibility and disease dynamics: tests of a mathematical model. The American Naturalist 150:685-707.

Ebert, D. 1995. Ecological interactions between a microsporidian parasite and its host. Journal of Animal Ecology 64:361-369.

Ebert, D. 2005. Ecology, Epidemiology, and Evolution of Parasitism in *Daphnia* [Internet] (National Library of Medicine (US), National Center for Biotechnology Information). Available at: http://www.ncbi.nlm.nih.gov/entrez/query.fcgi?db=Books. Accessed 17 January 2017.

Eisenberg, M.C., S.L. Robertson & J.H. Tien. 2013. Identifiability and estimation of multiple transmission pathways in cholera and waterborne disease. Journal of Theoretical Biology 324:84-102.

Elendt B.-P. & V. Storch. 1990. Starvation-induced alterations of the ultrastructure of the midgut of *Daphnia magna* Straus, 1820 (Cladocera). Journal of Crustacean Biology 10:79-86.

Ellner, S.P., L.E. Jones, L.D. Mydlarz and C.D. Harvell. 2007. Within-host disease ecology in the sea fan *Gorgonia ventalina*: modeling the spatial immunodynamics of a coral-pathogen interaction. The American Naturalist 170: E143-E161.

Esch, G.W. & J.C. Fernandez. 1994. Snail-trematode interactions and parasite community dynamics in aquatic systems: a review. The American Midland Naturalist 131:209-237.

Evans, H.C., S.L. Elliot & D.P. Hughes. 2011. Ophiocordyceps unilateralis: a keystone species for unraveling ecosystem functioning and biodiversity of fungi in tropical forests? Communicative and Integrative Biology 4:598-602.

Feng, Z., J. Velasco-Hernandez & B. Tapia-Santos. 2013. A mathematical model for coupling within-host and between-host dynamics in an environmentally-driven infectious disease. Mathematical Biosciences 241:49-55.

Fontes, I., H. Hartikainen, C. Williams & B. Okamura. 2017. Persistence, impacts and environmental drivers of covert infections in invertebrate hosts. Parasites and Vectors 10:542.

Franz, A.W.E, A.M. Kantor, A.L. Passarelli & R.J. Clem. 2015. Tissue barriers to arbovirus infection in mosquitoes. Viruses 7:3741-3767.

Fredensborg, B., K.M. Mouritsen & R. Poulin. 2006. Relating bird distributions and spatial heterogeneity in trematode infections in an intertidal snail- from small to large scale. Marine Biology 149:257-283.

Garcia-Garcia, E., J. Gallindo-Villegas, J. Mulero. 2013. Mucosal immunity in the gut: the non-vertebrate perspective. Developmental and Comparative Immunology 40:278-288.

Gibson, A.K., J. Jokela & C.M. Lively. 2016. Fine-scale spatial covariation between infection prevalence and susceptibility in a natural population. The American Naturalist 188:1-14.

Gilbert, G.S. & I.M. Parker. 2006. Invasions and the regulation of plant populations by pathogens. Pages 289-306 in: M.W. Cadotte, S.M. McMahon & T. Fukami (Eds.) Conceptual ecology and invasion biology: reciprocal approaches to nature. Springer.

Gillespie, D.T. 1977. Exact stochastic simulation of coupled chemical reactions. The Journal of Physical Chemistry 81:2340-2361.

Goatley, C.H.R. & D.R. Bellwood. 2016. Body size and mortality rates in coral reef fishes: a three-phase relationship. Proceedings of the Royal Society B: Biological Sciences 283: 20161858.

Graham, A.L., I.M. Cattadori, J.O. Lloyd-Smith, M.J. Ferrari & O.N. Bjornstad. 2007. Transmission consequences coinfection: cytokines writ large? Trends in Parasitology 23:284-291.

Graham, A.L., D.M. Shuker, L.C. Pollitt, S.K.J.R. Auld, A.J. Wilson & T.J. Little. 2011. Fitness consequences of immune responses: strengthening the empirical framework for ecoimmunology. Functional Ecology 25:5-17.

Grimstad, P.R. & E.D. Walker. 1991. *Aedes-triseriatus* (Diptera, Culicidae) and La-Crosse Virus. 4. Nutritional deprivation of larvae affects the adult barriers to infection and transmission. Journal of Medical Entomology 28:378-386.

Hall, M.D. & D. Ebert. 2012. Disentangling the influence of parasite genotype, host genotype and maternal environment on different stages of bacterial infection in *Daphnia magna*. Proceedings of the Royal Society B: Biological Sciences 279:3176-3183.

Hall, S.R., L. Sivars-Becker, C. Becker, M.A. Duffy, A.J. Tessier & C.E. Cáceres. 2007. Eating yourself sick: transmission of disease as a function of foraging ecology. Ecology Letters 10:207-218.

Hall, S.R., C.J. Knight, C.R. Becker, M.A. Duffy, A.J. Tessier & C.E. Cáceres. 2009. Quality matters: resource quality for hosts and the timing of epidemics. Ecology Letters 12:118-128.

Hall, S.R., R. Smyth, C.R. Becker, M.A. Duffy, C.J. Knight, S. MacIntyre, A.J. Tessier & C.E. Cáceres. 2010. Why are *Daphnia* in some lakes sicker? Disease ecology, habitat structure, and the plankton. BioScience 60:363-375.

Hall, S., C.R. Becker, M.A. Duffy & C.E. Cáceres. 2010. Variation in resource acquisition and use among host clones creates key epidemiological trade-offs. American Naturalist 176:557-565.

Hall, S.R., C.R. Becker, M.A. Duffy & C.E. Cáceres. 2011. Epidemic size determines population-level effects of fungal parasites on *Daphnia* hosts. Oecologia 166:833-842.

Hall, S.R., C.R. Becker, M.A. Duffy & C.E. Cáceres. 2012. A power-efficiency trade-off in resource use alters epidemiological relationships. Ecology 93:645-56.

Halliday, F.W., J. Umbanhowar & C.E. Mitchell. 2018. A host immune hormone modifies parasite species interactions and epidemics: insights from a field manipulation. Proceedings of the Royal Society B: Biological Sciences 285 doi: 10.1098/rspb.2018.2075.

Handel, A. & P. Rohani. 2015. Crossing the scale from within-host infection dynamics to between-host transmission fitness: a discussion of current assumptions and knowledge. Philosophical Transactions of the Royal Society B: Biological Sciences 370:20140302.

Harvell, C.D., C.E. Mitchell, J.R. Ward, S. Altizer, A.P. Dobson, R.S. Ostfeld & M.D. Samuel. 2002. Climate warming and disease risks for terrestrial and marine biota. Science 296:2158-2162.

Harvell, C.D., S. Altizer, I.M. Cattadori, L. Harrington & E. Weil. 2009. Climate change and wildlife diseases: when does the host matter the most? Ecology 90:912-920.

Hawley, D.M. & S.M. Altizer. 2011. Disease ecology meets ecological immunology: understanding the links between organismal immunity and infection dynamics in natural populations. Functional Ecology 25:48-60.

Hechinger, R.F. & K.D. Lafferty. 2005. Host diversity begets parasite diversity: bird final hosts and trematodes in snail intermediate hosts. Proceedings of the Royal Society B: Biological Sciences 272:1059-1066.

Hechinger, R.F., A.C. Wood & A.M. Kuris. 2011. Social organization in a flatworm: trematode parasites form soldier and reproductive castes. Proceedings of the Royal Society B: Biological Sciences 278:656:665.

Hing, S., E.J. Narayan, R.C.A. Thompson & S.S. Godfrey. 2016. The relationship between physiological stress and wildlife disease: consequences for health and conservation. Wildlife Research 43:51-60.

Hollingsworth, T.D., et al. 2015. Quantitative analyses and modeling to support achievement of the 2020 goals for nine neglected tropical diseases. Parasites & Vectors 8:630.

Izhar, R. & F. Ben-Ami. 2015. Host age modulates parasite infectivity, virulence and reproduction. Journal of Animal Ecology 84:1018-1028.

Izhar, R., J. Routtu & F. Ben-Ami. 2015. Host age modulates within-host parasite competition. Biology Letters 11: 20150131.

Johnson, P.T.J. & R.B. Hartson. 2009. All hosts are not equal: explaining differential patterns of malformations in an amphibian community. Journal of Animal Ecology 78:191-201.

Kalbfleisch, J.D., J.F. Lawless & W.M. Vollmer. 1983. Estimation in Markov models from aggregate data. Biometrics 39:907-919.

Kiesecker, J.M. 2011. Global stressors and the global decline of amphibians: tipping the stress immunocompetency axis. Ecological Research 26:897-908.

Koch, V., L.B. Brooks & W.J. Nichols. 2006. Population ecology of the green/black turtle (Chelonia mydas) in Bahía Magdalena, Mexico. Marine Biology 153:35-46.

Kuraishi, T., O. Binggeli, O. Opota, N. Buchon & B. Lemaitre. 2011. Genetic evidence for a protective role of the peritrophic matrix against intestinal bacterial infection in *Drosophila melanogaster*. Proceedings of the National Academy of the Sciences 108:15966-15971.

Kuris, A.M., et al. 2008. Ecosystem energetic implications of parasite and free-living biomass in three estuaries. Nature 454:515-518.

Lafferty, K.D. & A.K. Morris. 1996. Altered behavior of parasitized killifish increases susceptibility to predation by bird final hosts. Ecology 77:1390-1397.

Lafferty, K.D. & A.M. Kuris. 2002. Trophic strategies, animal diversity and body size. Trends in Ecology and Evolution 17:508-513.

Lafferty, K.D. et al., 2008. Parasites in food webs: the ultimate missing links. Ecology Letters 11:533-546.

Lafferty, K.D., G. DeLeo, C.J. Briggs, A.P. Dobson, T. Gross & A.M. Kuris. 2015. A general consumer-resource population model. Science 349:854-857.

Lemaitre, B. & J. Hoffmann. 2007. The host defense of *Drosophila melanogaster*. Annual Review of Immunology 25:697-743.

Lochmiller, R.L. & C. Deerenberg. 2000. Trade-offs in evolutionary immunology: just what is the cost of immunity? Oikos 88:87-98.

Loker, E.S., C.M. Adema, S.M. Zhang & T.B. Kepler. 2004. Invertebrate immune systems—not homogeneous, not simple, not well understood. Immunological Reviews 198:10-24.

Lloyd-Smith, J.O., S.J. Schreiber, P.E. Kopp & W.M. Getz. 2005. Superspreading and the effect of individual variation on disease emergence. *Nature* 438:355-9.

Low, M. & T. Part. 2009. Patterns of mortality for each life-history stage in a population of endangered New Zealand Stitchbird. Journal of Animal Ecology 78:761-771.

Lozano, G.A. 1991. Optimal foraging theory: a possible role for parasites? Oikos 60:391- 395.

Lynch, M. & B. Walsh. 1998. Genetics and analysis of quantitative traits. Sinauer Associates, Inc. Sunderland, Massachusetts, USA.

Marquet, P.A., A.P. Allen, J.H. Brown, J.A. Dunne, B.J. Enquist, J.F. Gillooly, P.A. Gowaty, J.L. Green, J. Harte, S.P. Hubbell, J. O'Dwyer, J.G. Okie, A. Ostling, M. Ritchie, D. Storch & G.B. West. 2014. On theory in ecology. BioScience 64:701-710.

Martin, L.B., W.A. Hopkins, L.D. Mydlarz & J.R. Rohr. 2010. The effects of anthropogenic global changes on immune functions and disease resistance. Annals of the New York Academy of Sciences 1195:129-148.

Martin, L.B., S.C. Burgan, J.S. Adelman and S.S. Gervasi. 2016. Host competence: an organismal trait to integrate immunology and epidemiology. Integrative and Comparative Biology 56:1225-1237.

Martin, L.B., B. Addison, A.G.D. Bean, K.L. Buchanan. O.L. Crino, J.R. Eastwood, A.S. Flies, R. Hamede, G.E. Hill, M. Klaassen, R.E. Koch, J.M. Martens, C. Napolitano, E.J. Narayan, L. Peacock, A.J. Peel, A. Peters, N. Raven, A. Risely, M.J. Roast, L.A. Rollins, M. Ruiz-Aravena, D. Selechnik, H.S. Stokes, B. Ujvari & L.F. Grogan. 2019. Extreme competence: keystone hosts of infections. Trends in Ecology and Evolution 34:303-314.

McCallum, H., A. Fenton, P.J. Hudson, B. Lee, B. Levick, R. Norman, S.E. Perkins, M. Viney, A.J. Wilson & J. Lello. 2017. Breaking beta: deconstructing the parasite transmission function. Philosophical Transactions of the Royal Society B: Biological Sciences 372:20160084.

Metschnikoff, E. 1884. A disease of *Daphnia* caused by a yeast. A contribution to the theory of phagocytes as agents for attack on disease-causing organisms. Milestones in Microbiology (ed. T. Brock), pp. 132-138. American Society for Microbiology, Washington DC.

Michalski, M.L., S.M. Erickson, L.C. Bartholomay & B.M. Christensen. 2010. Midgut barrier imparts selective resistance to filarial worm infection in *Culex pipiens pipiens*. PLoS Neglected Tropical Diseases 4:e875.

Mideo, N., S. Alizon & T. Day. 2008. Linking within- and between-host dynamics in the evolutionary epidemiology of infectious disease. Trends in Ecology and Evolution 23:511-517.

Miguel-Aliaga, I., H. Jasper & B. Lemaitre. 2018. Anatomy and physiology of the digestive tract of *Drosophila melanogaster*. Genetics 210:357-396.

Miller, M.W. & H.J. Phaff. 1998. *Metschnikowia kamienski*. The yeasts: a taxonomic study. (ed. C.P. Kurzman and J.W. Fell), pp. 256-267. Elsevier.

Moreno-Garcia, M., A. Cordoba-Aguilar, R. Conde & H. Lanz-Mendoza. 2013. Current immunity markers in insect ecological immunology: assumed trade-offs and methodological issues. Bulletin of Entomological Research 103:127-139.

Mydlarz, L.D., L.E. Jones & C.D. Harvell. 2006. Innate immunity, environmental drivers, and disease ecology of marine and freshwater invertebrates. Annual Review of Ecology, Evolution, and Systematics 37:251-288.

Mydlarz, L.D., E.S. McGinty & C.D. Harvell. 2010. What are the physiological and immunological responses of coral to climate warming and disease? Journal of Experimental Biology 213:934-945.

Nguyen, N.M., et al. 2013. Host and viral features of human dengue cases shape the population of infected and infectious *Aedes aegypti* mosquitoes. Proceedings of the National Academy of the Sciences 110:9072-9077.

Ostfeld, R.S. & F. Keesing. 2000. Biodiversity and disease risk: the case of Lyme disease. Conservation Biology 14:722-728.

Pedersen, A.B. & S.A. Babayan. 2011. Wild immunology. Molecular Ecology 20:872-880.

Penczykowski, R.M., S.R. Hall, D.J. Civitello & M.A. Duffy. 2014. Habitat structure and ecological drivers of disease. Limnology and Oceanography 59:340-348.

Pila, E.A., J.T. Sullivan, X.Z. Wu, J. Fang, S.P. Rudko, M.A. Gordy & P.C. Hanington. 2016. Hematopoiesis in molluscs: a review of haemocyte development and function in gastropods, cephalopods and bivalves. Developmental and Comparative Immunology 58:119-128.

Pinaud, S., et al. 2016. A shift from cellular to humoral responses contributes to innate immune memory in the vector snail *Biomphalaria glabrata*. PLoS Pathogens 12:e1005361.

Plowright, R.K., S.H. Sokolow, M.E. Gormann, P. Daszak & J.E. Foley. 2008. Causal inference in disease ecology: investigating ecological drivers of disease emergence. Frontiers in Ecology and the Environment 6:420-429.

Poulin, R. 2013. Explaining variability in parasite aggregation levels among host samples. Parasitology 140:541-546.

Quaglia, A., B. Sabelli, and L. Villani. 1976. Studies on the intestine of Daphnidae (Crustacea, Cladocera) Ultrastructure of the midgut of *Daphnia magna* and *Daphnia obtusa*. Journal of Morphology 150:711-726.

R Core Team (2013). R: A language and environment for statistical computing. R Foundation for Statistical Computing, Vienna, Austria.

Rantala, M.J. & D.A. Roff. 2005. An analysis of trade-offs in immune function, body size and development time in the Mediterranean Field Cricket, *Gryllus bimaculatus*. Functional Ecology 19:323-330.

Real, L. 1977. The kinetics of functional response. American Naturalist 111:289-300.

Rynkiewicz, E.C., A.B. Pederson and A. Fenton. 2015. An ecosystem approach to understanding and managing within-host parasite community dynamics. Trends in Parasitology 31:212-221.

Sadd, B.M. & P. Schmid-Hempel (2008) Principles of ecological immunology. Evolutionary Applications 2:113-21.

Sánchez, M.I., P.N. Nikolov, D.D. Georgieva, B.B. Georgiev, G.P. Vasileva, P. Pankov, M. Paracuellos, K.D. Lafferty & A.J. Green. 2013. High prevalence of cestodes in *Artemia* spp. throughout the annual cycle: relationship with abundance of avian final hosts. Parasitology Research 112:1913-1923.

Schneider, C.A., W.S. Rasband & K.W. Eliceiri. 2012. NIH Image to ImageJ: 25 years of image analysis. Nature Methods 9:671-675.

Schulenberg, H., J. Kurtz, Y. Moret & M.T. Siva-Jothy. 2009. Introduction. Ecological immunology. Philosophical Transactions of the Royal Society B: Biological Sciences 364:3-14.

Schultz, T.W., and J.R. Kennedy. 1976. The fine structure of the digestive system of *Daphnia pulex* (Crustacea: Cladocera). Tissue and Cell 8:479-490.

Sheldon, B.C. & S. Verhulst (1996) Ecological immunology: costly parasite defences and trade-offs in evolutionary ecology. Trends in Ecology & Evolution 11:317-21.

Shibata, T., K. Maki, J. Hadano, T. Fujikawa, K. Kitazaki et al. 2015. Crosslinking of a peritrophic matrix protein protects gut epithelia from bacterial exotoxins. Plos Pathology 11:e1005244.

Shocket, M.S., A.T. Strauss, J.L. Hite, M. Slijivar, D.J. Civitello, M.A. Duffy, C.E. Cáceres & S.R. Hall. 2018. Temperature drives epidemics in a zooplankton-fungus disease system: a trait-driven approach points to transmission via host foraging. American Naturalist 191:435-451.

Shocket, M.S., D. Vergara, A. Sickbert, J. Walsman, A.T. Strauss, J.L. Hite, M.A. Duffy, C.E. Cáceres & S.R. Hall. 2018. Parasite rearing and infection temperatures jointly influence disease transmission and shape seasonality of epidemics. Ecology 99:1975-1987.

Siva-Jothy, M.T. & J.J.W. Thompson. 2002. Short-term nutrient deprivation affects immune function. Physiological Entomology 27:206-212.

Skirnisson, K. & K.V. Galaktionov. 2002. Life cycles and transmission patterns of digeneans in SW Iceland. Sarsia: North Atlantic Marine Science 87:144-151.

Sloan, M.A. & P. Ligoxygakis. 2017. Immunology of insect vectors: midgut interactions of sandflies and tsetse with kinetoplastid parasites as a paradigm for establishing infection. In: Ligoxygakis P. (ed) Insect Immunity. Advances in Insect Physiology. Elsevier.

Soderhall, K. (Ed). 2011. Invertebrate immunity. In series: Advances in Experimental Medicine and Biology, Vol. 708. Springer.

Sparkman, A.M. & M.G. Palacios. 2009. A test of life-history theories of immune defense in two ecotypes of the garter snake, *Thamnophis elegans*. Journal of Animal Ecology 78:1242-1248.

Stewart, T.E., M.E. Torchin & C.E. Cáceres. 2018. Invisible parasites and their implications for coexisting water fleas. Journal of Parasitology 104:101-105.

Stewart Merrill, T.E. & C.E. Cáceres. 2018. Within-host complexity of a plankton-parasite interaction. Ecology doi: 10.1002/ecy.2483.

Stewart Merrill, T.E., S.R. Hall, L. Merrill & C.E. Cáceres. 2019. Variation in immune defense shapes disease outcomes in laboratory and wild *Daphnia*. Integrative and Comparative Biology doi: 10.1093/icb/icz079

Strauss, A.T., M.S. Shocket, D.J. Civitello, J.L. Hite, R.M. Penczykowski, M.A. Duffy, C.E. Cáceres & S.R. Hall. 2016. Habitat, predators, and hosts regulate disease in *Daphnia* through direct and indirect pathways. Ecological Monographs 86:393-411.

Strauss A.T., A.M. Bowling, M.A. Duffy, C.E. Cáceres & S.R. Hall. 2018. Linking host traits, interactions with competitors and disease: mechanistic foundations for disease dilution. Functional Ecology 32:1271-1279.

Theilacker, G.H. & Y. Watanabe. 1989. Midgut cell height defines nutritional status of laboratory raised larval northern anchovy, *Engraulis mordax*. Fishery Bulletin 87:457-469.

Thieltges D.W. & K. Reise. 2007. Spatial heterogeneity in parasite infections at different spatial scales in an intertidal bivalve. Oecologia 150:569-581.

Tompkins, D.M., A.M. Dunn, M.J. Smith & S. Telfer. 2011. Wildlife disease: from individuals to ecosystems. Journal of Animal Ecology 80:19-38.

Triggs, A. & R.J. Knell. 2012. Interactions between environmental variables determine immunity in the Indian meal moth *Plodia interpunctella*. Journal of Animal Ecology 81:386-394.

Valtonen, T.M., A. Kleino, M. Ramet & M.J. Rantala. 2010. Starvation reveals maintenance cost of humor immunity. Evolutionary Biology 37:49-57.

Voyles, J., D.C. Woodhams, V. Saenz, A.Q. Byrne, R. Perez, G. Rios-Sotelo, M.J. Ryan, M.C. Bletz, F.A. Sobell, S. McLetchie, L. Reinert, E.B. Rosenblum, L.A. Rollins-Smith, R. Ibáñez, J.M. Ray, E.J. Griffith, H. Ross & C.L. Richards-Zawacki. 2018. Shifts in disease dynamics in a tropical amphibian assemblage are not due to pathogen attenuation. Science 359:1517-1519.

Wang, Z., et al. 2011. A systematic study on hemocyte identification and plasma prophenoloxidase from *Culex pipens quinquefasciatus* at different developmental stages. Experimental Parasitology 127:135-141.

Weinstein, S.B., J.C. Buck & H.S. Young. 2018A. A landscape of disgust. Science. 359:1213-1214.

Weinstein, S.B., C.W. Moura, J.F. Menendez & K.D. Lafferty. 2018B. Fear of feces? Tradeoffs between disease risk and foraging drive animal activity around raccoon latrines. Oikos 127:927-934.

APPENDIX A: GLOSSARY OF TERMS FOR THE *METSCHNIKOWIA BICUSPIDATA* LIFE CYCLE

Ascospore	An infectious fungal spore contained within or produced inside of an ascus. The ingestion of *Metschnikowia* ascospores by a planktonic host initiates the within-host life cycle.
Hyphae	The infection stage at which fungal hyphae emerge from fully infected spores. Hyphae are a vegetative growth form and can be observed extending toward and attaching to various internal host structures as well as other spores.
Sporocyst	The infection stage characterized by the presence of sporocysts, which are small sac-like structures often tightly aggregated in a dense mass in the host body cavity. Each sporocyst contains developing conidia.
Conidia	The infection stage at which conidia emerge from the sporocysts. Released conidia reproduce by budding and disperse through the host body cavity. This process builds up high intensity infections.
Ascus	The infection stage at which asci develop from the conidia. The elongated asci contain the ascospores that are infectious to the next generation of susceptible hosts. Asci are released upon host death.

APPENDIX B: SUPPLEMENTARY MATERIALS FOR CHAPTER 2

Appendices:

B.1. MARKOV MODEL AND MAXIMUM LIKELIHOOD ESTIMATION

The Resistance Clearance Markov model (hereafter "RCM model") is a stochastic discrete-state continuous time Markov model with parameters estimated according to the maximum likelihood method adapted from Kalbfleisch et al. (1983). The model assumes a finite state space consisting of four epidemiological states, exposed (E), infected (I), uninfected (U) and dead (D), and is applied to longitudinal aggregate data in which the number of individuals occupying each state is observed through time, with separate cohorts of individuals being observed at each time point. The RCM model is time-homogeneous, such that observations are evenly spaced through time. Construction and implementation of the RCM model was accomplished in collaboration with Zoi Rapti and used the following steps:

Structuring of the Q Matrix

The transition rate matrix, or Q matrix, is a 4×4 matrix describing transition rates among states and is structured according to model assumptions (see Chapter 2, Methods). Transition rates q_{ij} from state i into state j are represented by parameters (λ), while the rates q_{ij} are such that each row of the transition matrix sums to zero. Our Q matrix takes the following form:

$$Q = \begin{bmatrix} -(\lambda_1 + \lambda_2 + \lambda_3) & \lambda_1 & \lambda_2 & \lambda_3 \\ 0 & -(\lambda_4 + \lambda_3) & \lambda_4 & \lambda_3 \\ 0 & 0 & -(\lambda_3) & \lambda_3 \\ 0 & 0 & 0 & 0 \end{bmatrix} \lambda$$

λ_1 = **Infection rate**. Transition from exposed to infected

λ_2 = **Resistance rate**. Transition from exposed to uninfected

λ_3 = **Mortality rate**. Transition from any state to dead.

λ_4 = **Clearance rate**. Transition from infected to uninfected

Modifying Q Matrix structure

State transitions were structured based on the biology of the *Daphnia-Metschnikowia* host-parasite interaction. An important deviation from other systems is that all *Daphnia* hosts began in the exposed class rather than beginning in the uninfected class and transitioning to exposed. We structured the Q matrix this way because our study design ensured exposure for all individuals.

States can be added to the model as necessary to reflect the biology of a particular host-parasite interaction. For instance, we condensed a complex within-host life cycle (Stewart Merrill & Cáceres 2018) into four translatable epidemiological states but could gain additional information about clearance by incorporating the full set of within-host stages. Importantly, the number of transition parameters increases non-linearly with the addition of host states, so when including additional states, care should be taken to ensure that model rates remain identifiable (Eisenberg et al. 2013).

Defining vectors

Vectors are defined from empirical data. Vector N_l' contains $N_j(t_l)$, the total number of individuals observed in state j at time t_l, for all states $1, \dots, k$, where $l = t_0 < t_1 < \cdots < t_m$. Vector M_l' contains the total number of individuals observed in states $1, \dots, k-1$ at time t_l.

$$N_l' = \{N_1(t_l), \dots, N_k(t_l)\}$$

$$M_l' = \{N_1(t_l), \dots, N_{k-1}(t_l)\}$$

Parameter estimation

Transition rates to populate the Q matrix were estimated via simulated annealing. First, a set of initial transition rates, or "initial guesses", was randomly selected from a range of values spanning 0 to 5. The distribution over states at time instances t_l were then evaluated and their square distance from the experimental data was calculated.

As the number of estimated parameters increases, arriving at a local minimum becomes more likely. We used simulated annealing to avoid this and to increase the probability of arriving

at the global minimum. Specifically, we used the MATLAB (The MathWorks Inc. 1994-2018) command "simulannealbnd" to find the minimum of the distance function.

Model quality assurance and quality control

The RCM model was run for 500 iterations per clone or combined pool. We counted the number of iterations that resulted in convergence and found that models converged for greater than 99% of iterations. We also assessed the sensitivity of the estimated transition rates to the initial guesses by plotting resulting rates against initial guesses. Visual inspection of these plots confirmed that the estimated transition rates were not influenced by the random initial guesses.

Resulting probability matrix

Exponentiation of the Q matrix produces the probability matrix, or P matrix, which describes the probability of transitions among states. In this matrix, each row sums to one and all elements are non-negative.

$$P = \begin{bmatrix} P_{E,E} & P_{E,I} & P_{E,U} & P_{E,D} \\ 0 & P_{I,I} & P_{I,U} & P_{I,D} \\ 0 & 0 & P_{U,U} & P_{U,D} \\ 0 & 0 & 0 & 1 \end{bmatrix}$$

E = **Exposed**. Hosts that have been exposed to parasites. In our system, hosts that have consumed fungal spores. All hosts are considered exposed during the 24 h inoculation period.

I = **Infected**. Hosts in which an infection has successfully established. In our system, hosts within which a fungal spore has crossed the gut epithelium any produced any of the within-host developmental stages of the parasite (e.g. spore, hyphae, sporocyst, conidia, ascus).

U = **Uninfected**. Uninfected hosts. In our system, hosts with no symptoms of infection or those whose infection has not advanced beyond the spore stage at day 8 post-infection.

D = **Dead**. Hosts that have succumbed to mortality.

B.2. ESTIMATING TRANSITION PROBABILITIES

Probability matrices were generated from each of 500 iterations of the RCM model. For each clone, we calculated the average probability for all state-to-state transitions. Because the RCM model is a continuous-time Markov process, a time period must be selected at which to estimate a particular probability.

We estimated resistance probabilities at $t = 2$ as this time period spans the time during which resistance is actively occurring. From $t = 0$ to $t = 1$ individuals are exposed to spores through inoculation. At $t = 1$, hosts are transferred to clean, spore-free water, but still retain a small number of infective spores in their gut lumen. By $t = 2$ hosts retain no spores in their gut lumen, precluding the possibility of further resistance.

We estimated clearance probabilities at $t = 8$ because infections are typically resolved by ten days post-exposure. At $t = 10$ hosts are either infected with late-stage infections or are uninfected. Hence, clearance is relegated to the time points prior to day 10.

We measured clearance and resistance over different time scales because our methods had a restricted exposure period. Experimental or observational studies in which hosts face continuous exposure may opt to estimate host defenses over more similar timescales. Selecting a time period for probability estimation is an important analytical step and should be conducted with careful consideration of the sampling protocol as well as the biology of the host-parasite interaction.

For direct comparison of probabilities among hosts, we standardized probabilities by scaling them to a mortality-free system, with the standardized probability, P_{s_i}, calculated as the original probability, P_i, divided by 1 minus the probability of mortality, P_m, for that state.

$$P_{s_i} = \frac{P_i}{1 - P_m}$$

B.3. ORDINARY DIFFERENTIAL EQUATIONS

ODE Structure

The ordinary differential equation (ODE) system describing the transitions from one epidemiological state to another reads as follows:

$$\frac{dE}{dt} = -(r + \beta + d)E$$

$$\frac{dI}{dt} = \beta E - (c + d)I$$

$$\frac{dU}{dt} = rE + cI - dU$$

$$\frac{dD}{dt} = dE + dI + dU$$

Classes E, I, U and D denote the exposed, infected, uninfected and dead classes, respectively, while r defines the resistance rate, β defines the infection rate, c defines the clearance rate and d defines the death rate. Since this is a linear system, it can be solved explicitly. The solution is:

$$E(t) = 10e^{-(r+\beta+d)t}$$

$$I(t) = \frac{10\beta}{\beta - c + r}\left(e^{-(c+d)t} - e^{-(r+\beta+d)t}\right)$$

$$U(t) = \frac{10}{\beta - c + r}\left((c - r)e^{-(r+\beta+d)t} - \beta e^{-(c+d)t} + (\beta - c + r)e^{-dt}\right)$$

$$D(t) = 10(1 - e^{-dt})$$

We used the initial conditions $E(0) = 10, I(0) = U(0) = D(0) = 0$ to evaluate the model through time.

Analytical Proofs

Using the above equations, we can define the following quantities which denote the fraction of infected and uninfected individuals over the total population (prevalence) in the absence of dead individuals:

$$PrevI(t) = \frac{I(t)}{E(t) + I(t) + U(t)} = \frac{\beta}{r + \beta - c}\left(e^{-ct} - e^{-(r+\beta)t}\right)$$

$$PrevU(t) = \frac{U(t)}{E(t) + I(t) + U(t)} = 1 - \frac{\beta}{r + \beta - c}e^{-ct} - \frac{r - c}{r + \beta - c}e^{-(r+\beta)t}$$

It is then straightforward to obtain the maximum value of $PrevI(t)$ and the time t^* where this value is attained as a function of the parameters:

$$t^* = \frac{1}{r+\beta-c} ln\left(\frac{r+\beta}{c}\right)$$

$$MaxPrevI = \frac{\beta}{r + \beta}\left(\frac{r + \beta}{c}\right)^{-\frac{c}{r+\beta-c}}$$

Similarly, one can define the slope of the line connecting the points $(t^*, PrevU(t^*))$ and $(10,\ PrevU(10))$:

$$Slope = \frac{\beta\left(e^{-10c} - \left(\frac{r + \beta}{c}\right)^{-\frac{c}{r+\beta-c}}\right) + (r - c)\left(e^{-10(r+\beta)} - \left(\frac{r + \beta}{c}\right)^{-\frac{r+\beta}{r+\beta-c}}\right)}{10(r + \beta - c) - ln\left(\frac{r + \beta}{c}\right)}$$

Parameter identifiability

Following Eisenberg et al. (2013), we assume that there might exist errors and uncertainty in the identification of individuals and their placement in the four epidemiological states. Hence, our working hypothesis is that we actually observe only a percentage of the actual populations:

$$y_1 = k_1 E$$

$$y_2 = k_2 I$$

$$y_3 = k_3 U$$

We omit the dead class because, since the population is conserved, it is redundant and so there is no need to monitor it. In what follows, the four rate parameters and the three proportionality parameters $k_j, j = 1 - 3$ are supposed to be unknown and need to be identified. The corresponding equations for y_i are:

$$y_1' = -(r + \beta + d)\, y_1$$

$$y_2' = \frac{k_2\, \beta}{k_1} y_1 - (c + d)\, y_2$$

$$y_3' = \frac{k_3\, r}{k_1} y_1 + \frac{k_3\, c}{k_2} y_2 - d\, y_3.$$

Now we suppose we have an alternative set of parameters $(x_1, x_2, x_3, x_4, x_5, x_6, x_7)$ instead of $(r, \beta, c, d, k_1, k_2, k_3)$. It then follows:

$$d = x_4$$

$$c + d = x_3 + x_4 \Longrightarrow c = x_3$$

$$r + \beta + d = x_1 + x_2 + x_4 \Longrightarrow r + \beta = x_1 + x_2$$

$$\frac{k_3\, c}{k_2} = \frac{x_7\, x_3}{x_6} \Rightarrow \frac{k_3}{k_2} = \frac{x_7}{x_6}$$

$$\frac{k_2\, \beta}{k_1} = \frac{x_6\, x_2}{x_5}$$

$$\frac{k_3\, r}{k_1} = \frac{x_7\, x_1}{x_5}$$

Dividing the last two equations and using the third and fourth from the bottom yields $r = x_1, \beta = x_2$. Hence, all four transition rates are identifiable.

B.4. WITHIN-HOST DYNAMICS

We used both deterministic and stochastic approaches to observe and describe the within-host dynamics of the system. First, we used Euler's method to solve the coupled ODEs parameterized with the rates estimated in section 1 of this appendix. We saved populations at all times from 0 to 10 days after exposure.

Using the instantaneous probabilities of transmission, resistance, clearance and mortality obtained in section 2 of this appendix, we ran a standard Gillespie algorithm (Gillespie, 1977) to generate 1,000 sample paths. In all runs, the initial conditions matched those of the experiment, namely all 10 individuals were placed in the Exposed state, with the Infected, Uninfected and Dead states having zero individuals each. We ran each simulation until the dead class was saturated with all individuals and/or before time reached 10 days. We saved all transition times and all populations at those times. We then averaged the populations in each epidemiological state and collected information on the aggregate dynamics.

As described in Chapter 2, figure 2.3, the Markov model-estimated resistance probabilities appear to constrain the maximum prevalence that can be achieved through time. This association can be observed in Fig. B.1 (below) where red points represent the Markov model-estimated resistance rates and the corresponding maximum prevalence values obtained through application of the Gillespie algorithm. In the right panel of Fig. B.1, the maximum prevalence estimated through application of the Gillespie algorithm corresponds well with empirical (observed) values for prevalence. Because prevalence is maximized on average at day 2 during the Gillespie algorithm, we plot the empirical prevalences for day 2. The estimates agree well with the data. The relationship between these variables is also described by the ODE model, and the blue line represents the analytical relationship between maximum prevalence and resistance rate. In summary, the association between resistance and maximum prevalence is causal and supported by the simple ODE model. The analytical proof for this relationship can be found in Appendix B.3.

A second potential relationship described in Chapter 2, figure 2.3 is that the growth of the uninfected class from day 2 (the time at which prevalence is maximized) to day 10 (the end of parasite development) is determined by clearance probabilities. That is, higher clearance rates and probabilities result in greater increases in the uninfected class through time. This relationship

is depicted in the left panel of Figure B.2 (below). On the x-axis is the Markov model-estimated clearance rate and on the y-axis is the growth of the uninfected class or "slope". This slope represents the change in the proportion of the live population that is uninfected from day 2 to day 10. The red points are those generated using the Gillespie algorithm. The blue points represent the analytical relationship between clearance and slope and confirm that the relationship is causal and supported by the ODE model. In the right panel, the slope values estimated through application of the Gillespie algorithm correspond well with empirical (observed) values. The analytical proof for this relationship can be found in Appendix B.3.

Figure B.1

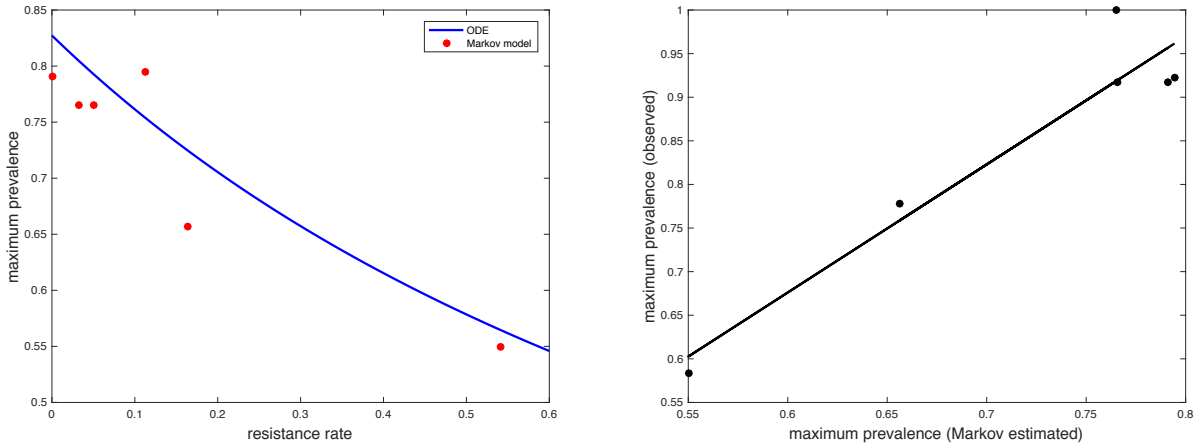

Figure B.2

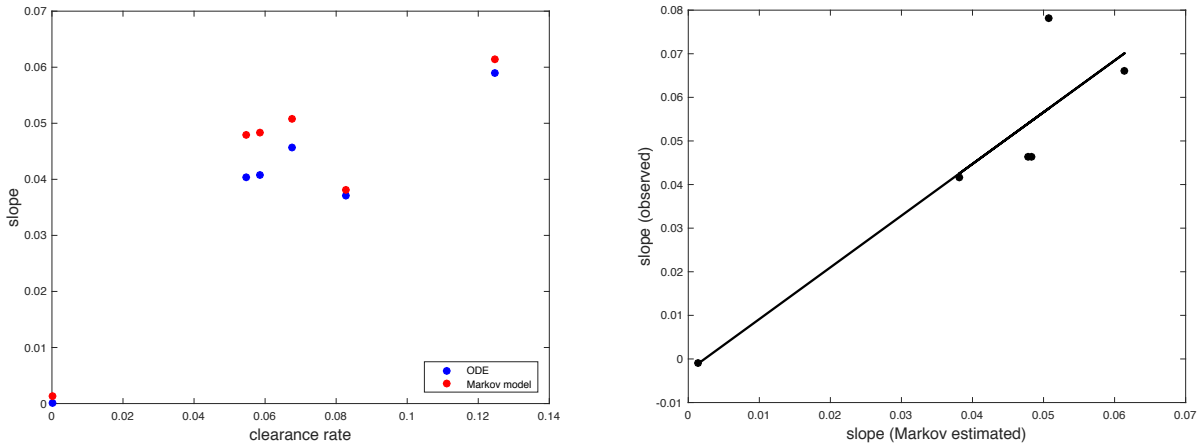

B.5. SAMPLE SIZES

Table B.1. Sample sizes for *Daphnia dentifera* clones. Each clone represents a unique multi-locus genotype. Sample sizes vary due to differential reproduction and mortality. Clones with sample sizes falling below 10 day^{-1} were combined into two pools, as indicated by superscripts, with combinations based on similarity of susceptibility.

Clone	Total N	N day^{-1}
CB 03-15	72	12
CB 22-63[2]	42	7
DW 14-27[1]	48	8
DW 22-58[1]	42	7
IL 16-48	66	11
ST	90	15
W2	72	12
W5[2]	48	8
Total	**480**	**80**

B.6. N VECTORS

N-vectors, or the number of individuals observed in each state at each time period (defined in appendix section B.1). As illustrated for clone W2, the order of states moving from top to bottom, is dead (d), infected (i), exposed (e) and uninfected (u) and vectors are presented for t_0 to t_{10}.

W2:

	t_0	t_2	t_4	t_6	t_8	t_{10}
d	0	0	1	0	1	0
i	0	7	9	10	4	3
e	12	0	0	0	0	0
u	0	5	2	2	7	9

CB 03-15

0	0	2	1	1	1
0	11	10	10	7	6
12	0	0	0	0	0
0	1	0	1	4	5

IL 16-48

0	5	0	6	5	3
0	6	9	5	1	3
11	0	0	0	0	0
0	0	2	0	5	5

ST

0	2	6	3	6	0
0	12	9	12	8	14
15	0	0	0	0	0
0	1	0	0	1	1

Pool 1 (DW 14-27 & DW 22-58)

0	3	3	6	3	4
0	11	9	7	8	6
15	0	0	0	0	0
0	1	3	2	4	5

Pool 2 (CB 22-63 & W5)

0	6	7	7	9	7
0	7	7	7	0	2
15	0	0	0	0	0
0	2	1	1	6	6

B.7. Q-MATRICES

Transition intensity matrices, or *Q*-matrices, for host clones. See appendices B.1 and B.2 for definitions and matrix structure.

CB 03-15

$$Q = \begin{bmatrix} -1.0000 & 1.0000 & 0.0000 & 0.0000 \\ 0 & -0.0547 & 0.0547 & 0.0000 \\ 0 & 0 & 0.0000 & 0.0000 \\ 0 & 0 & 0 & 0 \end{bmatrix}$$

IL 16-48

$$Q = \begin{bmatrix} -1.1512 & 1.0000 & 0.0320 & 0.1192 \\ 0 & -0.1869 & 0.0677 & 0.1192 \\ 0 & 0 & -0.1192 & 0.1192 \\ 0 & 0 & 0 & 0 \end{bmatrix}$$

ST

$$Q = \begin{bmatrix} -1.1247 & 1.0000 & 0.1129 & 0.0118 \\ 0 & -0.0118 & 0.0000 & 0.0118 \\ 0 & 0 & -0.0118 & 0.0118 \\ 0 & 0 & 0 & 0 \end{bmatrix}$$

W2

$$Q = \begin{bmatrix} -1.5494 & 1.0000 & 0.5406 & 0.0088 \\ 0 & -0.0917 & 0.0829 & 0.0088 \\ 0 & 0 & -0.0088 & 0.0088 \\ 0 & 0 & 0 & 0 \end{bmatrix}$$

B.7. Q-MATRICES – continued

Pool 1 (DW 14-27 & DW 22-58)

$$Q = \begin{bmatrix} -1.0806 & 1.0000 & 0.0503 & 0.0303 \\ 0 & -0.0890 & 0.0587 & 0.0303 \\ 0 & 0 & -0.0303 & 0.0303 \\ 0 & 0 & 0 & 0 \end{bmatrix}$$

Pool 2 (CB 22-63 & W5)

$$Q = \begin{bmatrix} -1.2769 & 1.0000 & 0.1634 & 0.1135 \\ 0 & -0.2383 & 0.1248 & 0.1135 \\ 0 & 0 & -0.1135 & 0.1135 \\ 0 & 0 & 0 & 0 \end{bmatrix}$$

B.8. P-MATRICES

P- (probability) matrices for host clones. Matrices are provided for time points $t = 2$ and $t = 8$ at which resistance and clearance were measured, respectively.

CB 03-15

$t = 2$

$$P = \begin{bmatrix} 0.1352 & 0.8049 & 0.0598 & 0.0000 \\ 0 & 0.8965 & 0.1035 & 0.0000 \\ 0 & 0 & 1.0000 & 0.0000 \\ 0 & 0 & 0 & 1.0000 \end{bmatrix}$$

$t = 8$

$$P = \begin{bmatrix} 0.0003 & 0.6827 & 0.3169 & 0.0000 \\ 0 & 0.6461 & 0.3539 & 0.0000 \\ 0 & 0 & 1.0000 & 0.0000 \\ 0 & 0 & 0 & 1.0000 \end{bmatrix}$$

IL 16-48

$t = 2$

$$P = \begin{bmatrix} 0.1006 & 0.6108 & 0.0769 & 0.2116 \\ 0 & 0.6876 & 0.1007 & 0.2116 \\ 0 & 0 & 0.7884 & 0.2116 \\ 0 & 0 & 0 & 1.0000 \end{bmatrix}$$

$t = 8$

$$P = \begin{bmatrix} 0.0001 & 0.2326 & 0.1536 & 0.6137 \\ 0 & 0.2236 & 0.1627 & 0.6137 \\ 0 & 0 & 0.3863 & 0.6137 \\ 0 & 0 & 0 & 1.0000 \end{bmatrix}$$

ST

$t = 2$

$$P = \begin{bmatrix} 0.1061 & 0.7843 & 0.0863 & 0.0233 \\ 0 & 0.9767 & 0.0000 & 0.0233 \\ 0 & 0 & 0.9767 & 0.0233 \\ 0 & 0 & 0 & 1.0000 \end{bmatrix}$$

$t = 8$

$$P = \begin{bmatrix} 0.0001 & 0.8196 & 0.0902 & 0.0900 \\ 0 & 0.9100 & 0.0000 & 0.0900 \\ 0 & 0 & 0.9100 & 0.0900 \\ 0 & 0 & 0 & 1.0000 \end{bmatrix}$$

W2

$t = 2$

$$P = \begin{bmatrix} 0.0457 & 0.5419 & 0.3950 & 0.0174 \\ 0 & 0.8319 & 0.1507 & 0.0174 \\ 0 & 0 & 0.9826 & 0.0174 \\ 0 & 0 & 0 & 1.0000 \end{bmatrix}$$

$t = 8$

$$P = \begin{bmatrix} 0.0000 & 0.3302 & 0.6022 & 0.0677 \\ 0 & 0.4790 & 0.4533 & 0.0677 \\ 0 & 0 & 0.9323 & 0.0677 \\ 0 & 0 & 0 & 1.0000 \end{bmatrix}$$

B.8. Q-MATRICES – continued

Pool 1 (DW 14-27 & DW 22-58)

$t = 2$

$$P = \begin{bmatrix} 0.1149 & 0.7274 & 0.0987 & 0.0589 \\ 0 & 0.8371 & 0.1040 & 0.0589 \\ 0 & 0 & 0.9411 & 0.0589 \\ 0 & 0 & 0 & 1.0000 \end{bmatrix}$$

$t = 8$

$$P = \begin{bmatrix} 0.0002 & 0.4944 & 0.2897 & 0.2157 \\ 0 & 0.4910 & 0.2933 & 0.2157 \\ 0 & 0 & 0.7843 & 0.2157 \\ 0 & 0 & 0 & 1.0000 \end{bmatrix}$$

Pool 2 (CB 22-63 & W5)

$t = 2$

$$P = \begin{bmatrix} 0.0780 & 0.5231 & 0.1963 & 0.2025 \\ 0 & 0.6204 & 0.1771 & 0.2025 \\ 0 & 0 & 0.7975 & 0.2025 \\ 0 & 0 & 0 & 1.0000 \end{bmatrix}$$

$t = 8$

$$P = \begin{bmatrix} 0.0000 & 0.1428 & 0.2616 & 0.5956 \\ 0 & 0.1481 & 0.2563 & 0.5956 \\ 0 & 0 & 0.4044 & 0.5956 \\ 0 & 0 & 0 & 1.0000 \end{bmatrix}$$

B.9. RESISTANCE AND CLEARANCE PROBABILITIES

Table B.2. Resistance and clearance probabilities for host clones standardized to control for variation in host mortality. Resistance estimated at $t = 2$ and clearance estimated at $t = 8$ per model assumptions.

Host	Resistance	Clearance
CB 03-15	0.0598	0.3539
IL 16-48	0.0975	0.4212
ST	0.0884	0.0000
W2	0.4020	0.4862
Pool 1	0.1049	0.3740
Pool 2	0.2461	0.6338

B.10. EXPERIMENTAL CONFIRMATION

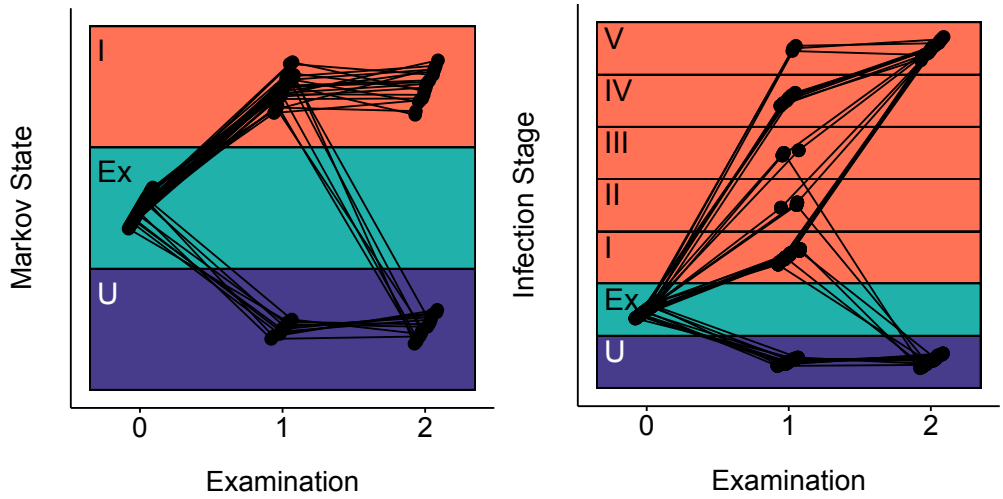

Figure B.3. Experimental evidence demonstrating hosts resisting and clearing infections. Here points represent individual hosts and lines connect the same hosts through time. Examination 0 represents exposure to the pathogen, examination 1 occurred at a varying time-point between days 2 and 8 post-exposure, and examination 2 occurred at ten days post-exposure. The right panel shows each individual's infection stage from the set of progressing infection stages (I-V, see Stewart Merrill & Cáceres 2018) and demonstrates that early infections are more susceptible to clearance than later stage infections. The left panel shows the same data, but represented with the states in the RCM model, and illustrates that 27% of exposed individuals (9 of 33) resisted infection, and 25% of infections were cleared (6 of 24), values falling within the range of probabilities predicted by the RCM model.

B.11. LITERATURE SURVEY FLOW CHART

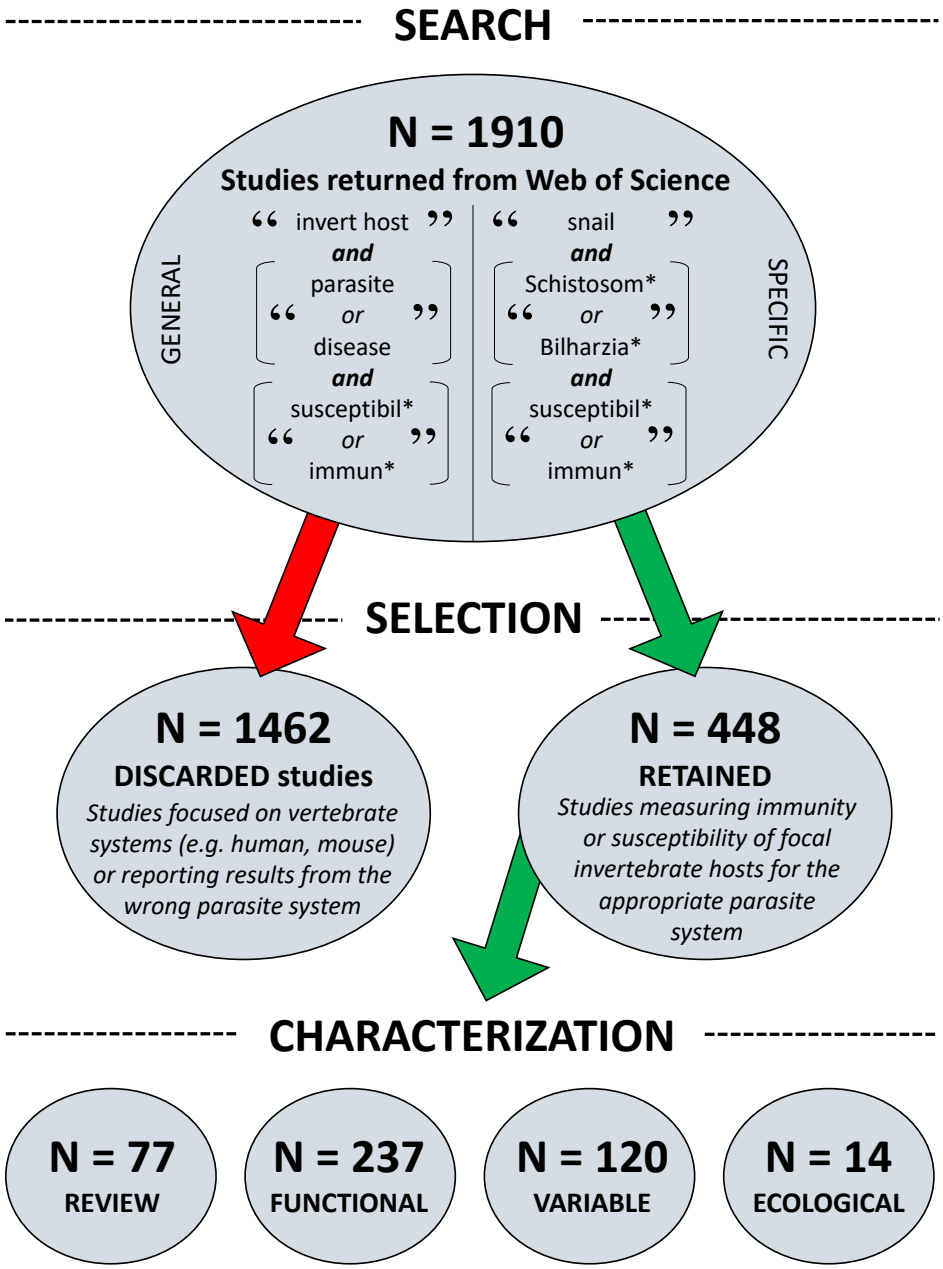

Figure B.4. Flowchart demonstrating the process by which papers were selected for use in the literature survey. Further information is described in the methods. Figure adapted from Des Roches et al. (2017) *Nature Ecol Evol*.

APPENDIX C: SUPPLEMENTARY MATERIALS FOR CHAPTER 3

Appendices:

C.1. SAMPLE SIZES, LAKE COORDINATES, AND SAMPLING REGIME

Table C.1. Sample sizes for *Daphnia dentifera* collected from six lakes in Central Indiana between 5-Jun and 4-Dec 2017. Latitude and longitude coordinates are provided for each lake. *Daphnia* hosts observed in the "Exposure" dataset appear in blue (Sample: Observed). *Daphnia* used in infection assays for the "Susceptibility" dataset appear in pale red (Sample: Inoculated), with pale orange indicating the subset of inoculated hosts that were held to determine infection statuses nine days post-inoculation (Sample: Held). In total, 6,781 *Daphnia* were processed, with 3,289 hosts observed for parasite exposure and 3,492 assayed for host susceptibility. Data are missing from some lakes and sampling events (indicated with "-") due to logistical issues that prohibited collection (e.g. lightning storms).

Lake	Sample	5-Jun	19-Jun	3-Jul	17-Jul	31-Jul	14-Aug	28-Aug	12-Sep	26-Sep	10-Oct	24-Oct	7-Nov	4-Dec
Beaverdam (*N* = 1215) 39.098201 N 87.146061 W	Observed	50	50	50	50	50	50	50	50	50	-	50	50	50
	Inoculated	59	56	58	50	48	50	47	50	50		50	49	48
	Held	-	-	14	-	20	-	18	-	25	-	25	-	25
Benefiel (*N* = 1213) 38.971357 N 87.255635 W	Observed	50	50	50	50	50	50	50	50	50	30	13	50	50
	Inoculated	64	59	55	43	50	50	50	50	50	50	9	47	43
	Held	-	-	14	-	18	-	25	-	25	-	4	-	25
Downing (*N* = 1258) 39.040029 N 87.244289 W	Observed	50	50	50	50	50	50	40	30	50	50	50	50	50
	Inoculated	54	57	58	50	47	50	50	26	50	50	48	49	49
	Held	-	-	19	-	17	-	13	-	21	-	25	-	25
Hale (*N* = 898) 38.972174 N 87.246607 W	Observed	7	27	11	40	20	33	26	11	50	50	40	37	46
	Inoculated	6	43	14	50	49	50	50	18	50	50	45	48	27
	Held	-	-	2	-	24	-	22	-	25	-	13	-	18
Midland (*N* = 1199) 39.124567 N 87.176551 W	Observed	26	50	49	50	40	50	50	13	50	50	50	50	50
	Inoculated	64	59	57	50	49	50	44	15	50	50	50	39	44
	Held	-	-	15	-	22	-	10	-	20	-	18	-	25
Star (*N* = 998) 39.001412 N 87.218320 W	Observed	-	-	-	50	50	50	50	50	50	50	50	50	50
	Inoculated	-	-	-	50	49	50	50	50	50	50	49	50	50
	Held	-	-	-	-	20	-	21	-	24	-	18	-	25

C.2. EXPOSURE, SUSCEPTIBILITY, AND PARASITE STAGE DATA

Table C.2. *Metschnikowia* exposure and *Daphnia* susceptibility data for the six study lakes from 5-Jun to 4-Dec-2017. Empty cells represent no associated data due to project design or too low of sample size to quantify susceptibility. *Metschnikowia* exposure (the number of attacking spores found within *Daphnia* hosts) was quantified as: abundance (Ab., average number of spores in all examined hosts), intensity (Int., average number of spores in exposed hosts), and maximum (Max, highest value of spores counted in all examined hosts). *Daphnia* susceptibility was quantified using monthly data (ST_m), where individuals were held nine days following inoculation to determine whether they succumbed to late infections, and using bimonthly data (ST_{bi}), where the presence of hyphae during initial observation was used as an indicator of future late infection. Spore thresholds (ST) were quantified from dose-response relationships to characterize susceptibility, where the spore threshold represents the number of attacking spores required to produce a 50% probability of late infection. Further information on dose-response relationships is provided in Appendix C.3. Finally, I include the parasite infection stages of hosts in the exposure dataset, where each stage (columns) has the number of individuals occupying that stage. U=uninfected, Att=attacked, Sp=spore, H=hyphae, SC=sporocyst, C=conidia, A=ascus. Stages follow those defined in Chapter 1 and Stewart Merrill & Cáceres 2018. Values in the table appear in red at the point of epidemic emergence, and gray shading represents the epidemic period.

Table C.2. – continued.

		Metschnikowia Exposure			*Daphnia* Susceptibility		*Metschnikowia* infection stages						
	Date	Ab.	Int.	Max	ST_m	ST_{bi}	Un	Att	Sp	H	SC	C	A
BEAVERDAM	5-Jun	0.00	0.00	0		3.8	50	0	0	0	0	0	0
	19-Jun	0.00	0.00	0		3.3	50	0	0	0	0	0	0
	3-Jul	0.00	0.00	0	0.0	0.6	50	0	0	0	0	0	0
	17-Jul	0.02	1.00	1		0.0	49	1	0	0	0	0	0
	31-Jul	0.00	0.00	0	2.7	1.3	50	0	0	0	0	0	0
	14-Aug	0.04	2.00	2		2.2	49	1	0	0	0	0	0
	28-Aug	0.00	0.00	0	3.7	1.2	50	0	0	0	0	0	0
	12-Sep	0.04	1.00	1		0.0	48	2	0	0	0	0	0
	26-Sep	0.00	0.00	0	0.0	0.0	50	0	0	0	0	0	0
	10-Oct												
	24-Oct	0.22	1.10	2	3.7	0.0	40	7	2	1	0	0	0
	7-Nov	0.18	4.50	8		0.0	48	0	1	1	0	0	0
	4-Dec	0.00	0.00	0	4.6	0.0	50	0	0	0	0	0	0
BENEFIEL	5-Jun	0.00	0.00	0		7.4	50	0	0	0	0	0	0
	19-Jun	0.02	1.00	1		6.3	49	0	0	0	1	0	0
	3-Jul	0.02	1.00	1	4.3	0.0	49	1	0	0	0	0	0
	17-Jul	0.00	0.00	0		1.7	50	0	0	0	0	0	0
	31-Jul	0.04	1.00	1	6.4	0.0	48	0	1	0	0	0	1
	14-Aug	0.04	1.00	1		3.4	48	2	0	0	0	0	0
	28-Aug	0.52	1.73	4	0.0	0.0	35	7	6	1	0	0	1
	12-Sep	0.94	1.74	5		2.3	23	8	5	2	1	3	8
	26-Sep	4.32	4.50	18	0.0	6.9	2	5	13	17	0	3	10
	10-Oct	1.70	2.13	8		0.0	6	6	1	1	1	4	11
	24-Oct	2.00	2.17	5		0.0	1	1	3	4	0	2	2
	7-Nov	1.96	2.18	7		3.9	5	3	10	12	1	10	9
	4-Dec	1.24	1.82	5	0.0	3.7	16	6	10	14	1	3	0
DOWNING	5-Jun	0.00	0.00	0		6.7	50	0	0	0	0	0	0
	19-Jun	0.04	1.00	1		6.1	48	1	1	0	0	0	0
	3-Jul	0.12	1.00	1	0.0	0.0	44	0	4	2	0	0	0
	17-Jul	0.60	1.15	2		8.9	24	9	2	2	2	6	5
	31-Jul	1.98	2.36	19	12.0	27.6	8	8	3	9	1	8	13
	14-Aug	1.78	2.41	7		0.0	13	9	4	9	1	7	7
	28-Aug	2.08	2.86	10	0.0	3.9	11	8	4	7	0	0	10
	12-Sep	1.60	2.09	6		6.2	7	5	2	7	0	4	5
	26-Sep	3.10	4.08	11	0.0	14.5	12	8	6	14	2	3	5
	10-Oct	2.86	3.11	10		0.0	4	3	6	15	10	3	9
	24-Oct	4.60	4.89	15	5.9	9.1	3	5	1	20	3	4	14
	7-Nov	3.02	3.21	11		45.4	3	6	10	17	1	8	5
	4-Dec	2.30	3.29	18	1.6	4.6	15	9	8	14	3	1	0

Table C.2. – continued.

		Metschnikowia Exposure			*Daphnia* Susceptibility		*Metschnikowia* infection stages						
	Date	Ab.	Int.	Max	ST_m	ST_{bi}	U	Att	Sp	H	SC	C	A
HALE	5-Jun	0.00	0.00	0		6.0	7	0	0	0	0	0	0
	19-Jun	0.07	1.00	1		6.0	25	1	0	1	0	0	0
	3-Jul	1.27	2.00	4		1.0	4	2	1	3	0	1	0
	17-Jul	0.43	1.31	3		4.4	27	3	5	2	0	1	2
	31-Jul	0.10	1.00	1	2.0	2.4	18	0	0	0	0	1	1
	14-Aug	0.03	1.00	1		0.7	32	0	0	1	0	0	0
	28-Aug	0.15	1.33	2	10.8	5.0	23	0	3	0	0	0	0
	12-Sep	0.73	2.00	5			7	1	1	1	0	0	1
	26-Sep	0.26	1.86	7	0.0	0.0	43	0	2	1	0	2	2
	10-Oct	1.24	1.88	6		0.0	17	11	3	10	0	5	4
	24-Oct	3.73	3.82	11		2.5	1	1	3	6	5	9	15
	7-Nov	14.08	14.08	32			0	0	0	2	3	25	7
	4-Dec	1.22	2.55	15	0.0	3.1	24	4	2	5	0	7	4
MIDLAND	5-Jun	0.00	0.00	0		0.0	26	0	0	0	0	0	0
	19-Jun	0.02	1.00	1		3.7	49	0	0	0	1	0	0
	3-Jul	0.02	1.00	1	19.0	21.0	48	1	0	0	0	0	0
	17-Jul	0.04	1.00	1		13.1	48	2	0	0	0	0	0
	31-Jul	0.03	1.00	1	27.0	11.7	39	0	1	0	0	0	0
	14-Aug	0.02	1.00	1		2.8	49	1	0	0	0	0	0
	28-Aug	0.18	1.29	2	7.9	12.5	43	5	1	1	0	0	0
	12-Sep	0.15	1.00	1		5.9	11	0	0	1	1	0	0
	26-Sep	0.06	1.00	1	0.0	4.5	47	2	1	0	0	0	0
	10-Oct	0.58	1.53	3		0.0	31	10	2	5	0	0	2
	24-Oct	2.96	3.02	9	0.0	12.7	1	13	8	9	4	3	12
	7-Nov	5.04	5.25	12		1.1	2	10	11	18	3	2	4
	4-Dec	1.04	2.60	8	1.8	5.8	30	2	1	2	1	11	3
STAR	5-Jun												
	19-Jun												
	3-Jul												
	17-Jul	1.18	1.74	7		3.8	16	8	12	12	0	0	2
	31-Jul	0.38	1.36	3	11.5	0.0	36	1	6	4	0	1	2
	14-Aug	0.16	1.14	2		0.0	43	1	2	1	1	0	2
	28-Aug	0.16	1.14	2	9.5	4.9	43	6	0	1	0	0	0
	12-Sep	0.26	1.18	2	4.4*	0.0	39	3	4	3	0	1	0
	26-Sep	1.46	1.92	6	4.4	0.0	12	7	10	5	1	7	8
	10-Oct	6.34	6.34	21		0.0	0	3	2	20	2	8	15
	24-Oct	12.00	12.00	28	0.0	0.0	0	0	1	19	0	6	24
	7-Nov	4.20	4.38	12		0.0	2	3	9	24	1	6	5
	4-Dec	0.62	1.48	5	0.0	2.7	29	4	6	8	0	1	2

C.3. DOSE-RESPONSE RELATIONSHIPS

Monthly data

Each month, a subset of inoculated *Daphnia* were held until 9 days post-inoculation to determine their infection fate (see Table C.1 "Held" for sample sizes). Using those infection fates, I generated dose response curves for each lake and time point. Generalized linear models (binomial distribution, logit link) were constructed that assessed the relationship between the number of attacking spores (spores that attempted to penetrate or successfully penetrated the host gut barrier; Chapter 4; Stewart Merrill et al. 2019) and infection status at nine-days post-inoculation. The half-saturation constant from each curve provides a standard metric for susceptibility that is simple to compare across lakes and time points. Typically called the ID50 (infection dose 50), I describe the half-saturation constant here as the "Spore Threshold", or the number of attacking spores required to produce at least a 50% probability of infection. As an example, the three plots below represent raw data (points) and associated dose-response curves for high (left, ST = 11.5), intermediate (center, ST = 4.6) and low spore thresholds (right, ST = 0). An infection probability of 50% is indicated with dashed lines, such that the intersection of the black dose-response curve and the 50% line indicates the Spore Threshold.

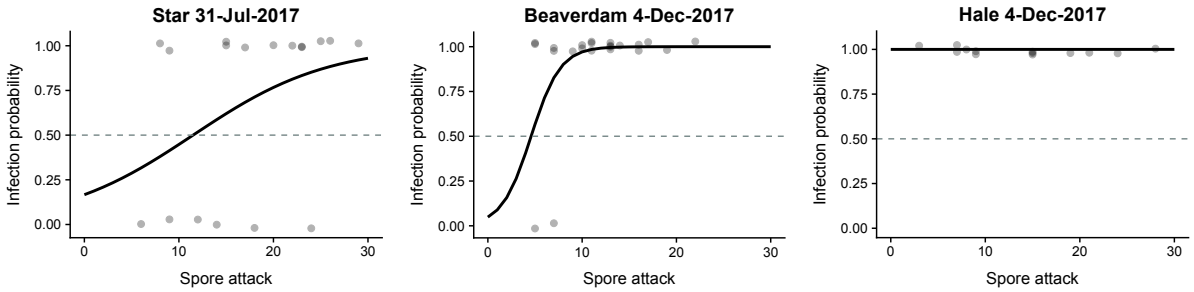

Theoretically, dose-response curves should be non-linear and saturating, and the majority of curves assumed this form. However, some curves deviated from the classic sigmoidal shape. For example, in the left plot below, 10/11 individuals became infected across all levels of attack with one uninfected individual pulling the curve (gray line) into a negative slope. In such cases, I evaluated the model's intercept (black line), where an intercept above 50% indicates that all spore attack values share a 50% probability of infection. Hence, in the left plot below the spore

threshold is zero ($ST_m = 0$). An additional example of a negative slope occurs in the right plot below, where the majority of individuals did not succumb to infection (only 2/14 became infected), but two infected individuals pulled the curve (gray line) into a negative slope. Again, in these cases I evaluated the model's intercept (black line), where an intercept below 50% indicates that hosts were able to recover from all spore attack values more than 50% of the time. Here, the spore threshold is the max value of attack ($ST_m = 19$).

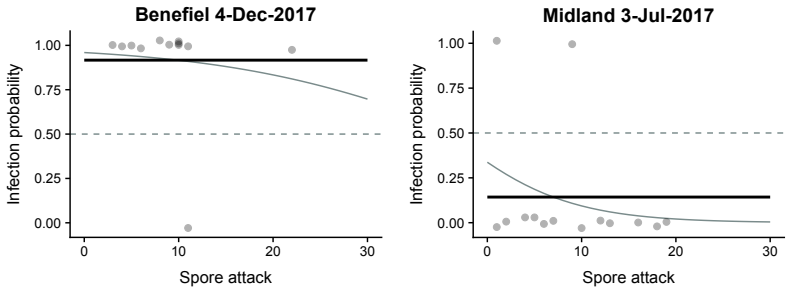

Why do these dose-response curves lose their classic shape? The answer to this question probably constitutes its own manuscript, but in brief, host variation over the course of infection can cause these curves to flatten out and/or lose their sigmoidal shape. For a *Metschnikowia* spore to achieve a late infection, it must cross the host's gut barrier and survive inside the host's body cavity. A spore's infection success then relies on: 1) success at the gut barrier and 2) success within the body cavity. While the probability of late infection *does* increase as a function of spores infecting the body cavity (in the classic dose-response curve shape), the probability that a spore will successfully enter the body cavity *does not* necessarily increase as a function of spores attacking the gut barrier (Chapter 4; Stewart Merrill et al. 2019). Differences in the penetrability of *Daphnia* gut barriers decouple this relationship: there are some individuals/genotypes for which only one attacking spore is needed to enter the body cavity, and others that can withstand dozens of attacking spores without any entering the body cavity. Broad variation in gut penetrability within a sample of hosts can the lead to an atypical dose-response curve shape. We evaluated dose-response curve shapes (typical and atypical) and variance in gut penetrability and found this to be the case. Variance in gut penetrability when samples had atypical curves was higher than samples with typical dose-response curve shapes (ANOVA, $F_{1,30} = 4.043$, $p = 0.053$)

Bimonthly data

Because the monthly dose-response curves had low sample sizes and were collected over a coarser timescale than the sampling regime, I also quantified spore thresholds using the full complement of inoculated hosts. With all inoculated hosts, I had higher sample sizes and a bimonthly sampling regime that matched that of *Metschnikowia* exposure. However, the majority of inoculated hosts were not held until day nine to examine their infection fate, so I needed an early indicator that signaled a high probability of future late infection. I looked back to the held individuals to find such an indicator and found that the presence of fungal hyphae (the stage of infection following spores infecting the body cavity) was a good indicator of future infection: among lakes and timepoints, one hypha consistently resulted in a >50% probability of late infection. So, I could estimate spore thresholds for the full complement of inoculated hosts by determining the number of attacking spores necessary to produce one hypha. As an example, the three plots below represent raw data (points) and associated attack-hyphae relationships for high (left, $ST_{bi} = 5.8$), intermediate (center, $ST_{bi} = 3.9$), and low spore thresholds (right, $ST_{m} = 1.3$). The black line indicates the dose-response relationship between attacking spores and number of hyphae, and the dashed line indicates one hypha (≈50% probability of late infection), such that the intersection of these two lines represents the spore threshold.

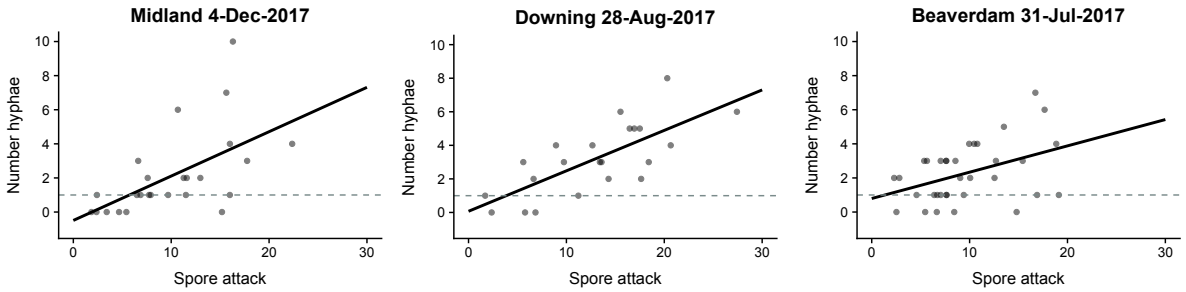

APPENDIX D: SUPPLEMENTARY MATERIALS FOR CHAPTER 4

Appendices:

D.1. WITHIN-HOST BIOLOGY AND EXTENDED DEFINITIONS

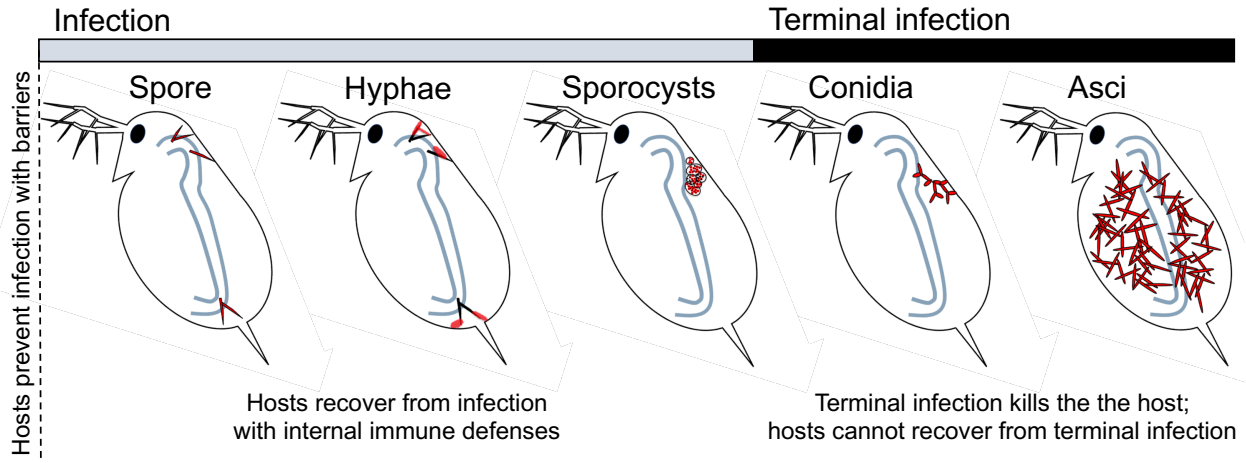

Figure D.1. Following infection of the *Daphnia* body cavity (haemocoel), *Metschnikowia bicuspidata* progresses through five morphologically distinct stages of development. These stages (spore, hyphae, sporocyst, conidia and asci) are described in part in Metschnikoff (1884), and in detail in Chapter 1 and Stewart Merrill & Cáceres (2018). All five within-host developmental stages represent forms of infection. Only the conidia and ascus stages represent terminal infection. *Daphnia* can resist (prevent) infection with barriers (e.g. the gut burrier). *Daphnia* can clear (recover from) infection with immune responses (e.g. haemocytes). Terminal infections consist of conidia and asci rapidly filling the body cavity and recovery does not occur. The ascus stage will kill the host so that infectious spores can be released back into the environment. The ascus stage typically results in the production of thousands to tens of thousands of new infectious spores. In the first part of the Chapter 4 ("Identifying mechanisms of infection"), I mechanistically test four drivers of infection during the early stages of this host-parasite interaction. That is, I assess: H1) how exposure drives the number of spores infecting the body cavity; H2) how gut penetrability blocks spores from infecting the body cavity; H3) how many haemocytes recruit to spores infecting the body cavity, and H4) how these processes are affected by body size. In the second part of the manuscript ("Integrating infection steps to understand susceptibility"), I use the traits measured in H1 to H4 to predict terminal infections. Because terminal infections represent host susceptibility, I can determine which host traits strongly influence host susceptibility.

Extended definitions of spore categories described in Table 4.1

Lumen spores: Spores that have been ingested by the host and are free-floating in the gut lumen (the hollow portion of the gut). This metric tells me how many spores a *Daphnia* generally eats at a given time so is a proxy for spore ingestion. Importantly, the gut is a high flow-through system, so lumen spores represent a snapshot of spore ingestion. A spore observed in the lumen still has infection potential. A lumen spore's possible trajectories include: being defecated with waste, being blocked by the gut barrier, or successfully entering the host body cavity.

Barrier spores: Spores that have attempted to infect the body cavity but have been blocked by the gut barrier. Their physical attempts to infect the host count them among the attacking spores, while their failure to infect the host allows me to calculate the host's gut penetrability. Spores embedded in the gut barrier lose their infection potential. Barrier spores remain stuck in the gut epithelium with their tail ends usually dangling into the gut lumen. I suspect that barrier spores may slowly disintegrate due to digestive enzymes in the gut lumen, or that they are removed when the *Daphnia* molts and sheds its gut lining.

Haemocoel spores: Spores that have successfully passed the gut barrier and infected the host's haemocoel, or body cavity. These spores directly indicate a host's level of infection. Their successful passage across the gut barrier allows me to calculate the host's gut penetrability. Additionally, spores infecting the haemocoel are attacked by host haemocytes (immune) which I can count to quantify the immune response. A haemocoel spore's possible trajectories include being killed by the host (via haemocytes or other immune response) or releasing fungal hyphae. While it is possible that haemocoel spores could die naturally (due to poor quality or lack of within-host resources), this is not something I can visually observe and quantify.

Exposure: Exposure sums all of the spores observed inside of the *Daphnia*: lumen spores, barrier spores, and haemocoel spores. Hence, this measure combines spores that still have the potential to infect the host with spores that have attacked the host and either failed (barrier) or succeeded (haemocoel). I used exposure to develop exposure-terminal infection curves. These curves allowed me to ask how gut barriers, haemocytes, and body size explain variation in the

exposure-terminal infection relationship. Importantly, exposure is *not* a proxy for spore ingestion because of how attacking spores and infecting spores integrate over time. For example, a single *Daphnia* could have a low spore ingestion rate, but if has a high attack frequency, the barrier and/or haemocoel spores will accumulate and artificially inflate its exposure. Likewise, a single *Daphnia* could have a high spore ingestion rate, but if it has a low attack frequency, barrier/haemocoel spores will not accumulate and it will have artificially low exposure. Lumen spores are a more robust metric for spore ingestion.

Attack: This metric sums barrier spores and haemocoel spores. Attack refers to the direct physical interaction between the host and parasite, and tells us how many spores attempted to cross the gut barrier and infect the host (although we note that these spores are passive, not active propagules). The spores that comprise attack (barrier and infection) integrate over time. Hence, the level of attack is a cumulative tally from inoculation to observation.

Infection: This metric refers directly to the number of spores infecting the body cavity (haemocoel spores). The haemocoel spores that indicate infection integrate over time. Hence, the level of infection is a cumulative tally of how many spores infected the body cavity from inoculation to observation.

D.2. LABORATORY CONDITIONS

Laboratory-reared hosts

In the lab, I reared ten unique multi-locus *Daphnia* genotypes originally collected from lakes in Central Indiana and Michigan. In the rearing protocol, I sought to eliminate maternal effects using standardized laboratory conditions for three generations (Lynch & Walsh 1998). During standardization, *Daphnia* were maintained individually in 50 ml falcon tubes containing 45 ml filtered lake water. They were fed three times per week with the high-quality algae, *Ankistrodesmus falcatus*, at 1 mg C/L. Tubes were kept in temperature-controlled chambers at 21°C on a 16:8 hour light:dark cycle and had water changes three times per week. Experimental individuals were collected from standardized mothers as neonates and were reared individually in 50 ml falcon tubes with daily feedings of 1 mg C/L *A. falcatus*. I experimentally inoculated eight-day-old *Daphnia*.

Field-collected hosts

Field-collected *Daphnia* were sampled from six lakes in Central Indiana between 4-Jun and 4-Dec 2017. After collection, adult *Daphnia* were isolated individually into 15 ml falcon tubes containing 10 ml filtered lake water. *Daphnia* were then fed 1 mg C/L *A. falcatus* and moved to temperature-controlled chambers at 21°C on a 16:8 hour light:dark cycle. Experimental inoculations occurred 24 hours after collection.

D.3. GENERAL LINEAR MODEL OUTPUT

Table D.1: Full statistical output for the eighteen general linear models constructed to evaluate hypothesis 1 (exposure drives infection), 2 (gut thickness creates a barrier to infection), 3 (haemocytes mediate recovery) and 4 (body size influences infection). For each model predictor, I include the hypothesis (H), associated figure (Fig.), sample size (*N*), response variable, coefficient (Est.), standard error (Std Err), *p* value and R^2. Gray highlighted cells indicate laboratory-reared *Daphnia*, and white cells indicate field-collected *Daphnia*.

H	Fig.	*N*	Response	Predictor	Est.	Std Err	*p*	R^2
1	4.2A	58	barrier sp.	lumen sp.	0.195	0.032	<0.001	0.399
	4.2D	2039	barrier sp.	lumen sp.	0.071	0.009	<0.001	0.032
	4.2B	136	haemocoel sp.	barrier sp.	-0.028	0.038	0.455	0.004
	4.2E	2262	haemocoel sp.	barrier sp.	0.086	0.012	<0.001	0.024
	4.2C	58	haemocoel sp.	lumen sp.	0.013	0.020	0.510	0.008
	4.2F	2038	haemocoel sp.	lumen sp.	0.036	0.005	<0.001	0.026
2	4.3A	63	gut pen.	anterior gut thickness	0.035	0.016	0.035	0.071
	4.3B	68	infection	posterior gut thickness	-0.009	0.022	0.672	0.003
3	4.4A	108	haemocytes	haemocoel sp.	1.609	0.362	<0.001	0.157
	4.4B	1933	haemocytes	haemocoel sp.	1.508	0.067	<0.001	0.209
4	4.5A	56	lumen sp.	body length	27.730	13.23	0.041	0.075
	4.5B	1624	lumen sp.	body length	9.434	2.629	<0.001	0.008
	4.5C	57	attack freq.	body length	-0.112	0.063	0.080	0.055
	4.5D	1611	attack freq.	body length	-0.201	0.046	<0.001	0.012
	4.5E	112	gut pen.	body length	0.026	0.178	0.886	0.001
	4.5F	1730	gut pen.	body length	-0.518	0.045	<0.001	0.073
	4.5G	90	haemocytes	haemocoel sp.	-1.912	3.083	0.537	0.189
				body size	-5.150	8.729	0.557	
				haemocoel sp*body size	2.475	2.140	0.251	
	4.5H	1441	haemocytes	haemocoel sp.	-5.571	0.782	<0.001	0.240
				body size	-10.829	2.653	<0.001	
				haemocoel sp*body size	5.975	0.668	<0.001	

D.4. COMPLETE AIC MODEL SET AND RESULTS

Table D.2: Full model structure for models competed under an information-theoretic framework. Each model belongs to a 'set', indicated by parentheticals and described in the methods. To denote model structure, I abbreviate exposure as 'E', gut penetrability as 'G', haemocytes per spore as 'H', and host body size as 'S'. Additive effects are represented by '+', and ':' represents the interaction between two factors. For instance, 'E + S + E:S' ('exposure*size' in the main text) denotes that the model includes exposure, body size, and the interaction between exposure and body size. I provide estimates for each single predictor within a model, as well as each model's AIC value and weight (w_i). The global model, that contains all possible additive and interactive effects, is abbreviated as 'glbl'.

		Single predictor estimates:					
Set	**Full model structure**	**E**	**G**	**H**	**S**	**AIC**	w_i
(1)	E	0.018				446.56	0.00
(2)	E + S	0.019			-1.926	443.93	0.00
(2)	E + S + E:S	0.056			-1.117	445.48	0.00
(3)	E + G	0.019	2.982			419.00	0.00
(3)	E + G + E:G	0.005	1.782			419.40	0.00
(4)	E + H	0.018		0.008		448.51	0.00
(4)	E + H + E:H	0.033		0.123		444.48	0.00
(5)	E + G + S	0.020	2.902		-0.362	420.85	0.00
(5)	E + G + S + E:G	0.006	1.754		-0.262	421.32	0.00
(5)	E + G + S + E:S	0.061	2.913		0.530	422.32	0.00
(5)	E + G + S + G:S	0.020	-9.668		-2.662	418.70	0.00
(5)	E + G + S + E:G + E:S + S:G + E:S:G	-0.081	-22.274		-4.245	421.89	0.00
(6)	E + H + S	0.019		0.009	-1.925	445.87	0.00
(6)	E + H + S + E:H	0.034		0.123	-1.970	441.75	0.00
(6)	E + H + S + E:S	0.056		0.008	-1.120	447.42	0.00
(6)	E + H + S + H:S	0.020		-1.647	-3.841	435.97	0.00
(6)	E + H + S + E:H + E:S + H:S + E:H:S	0.072		-2.246	-3.255	433.84	0.00
(7)	E + G + H	0.019	2.983	-0.001		421.00	0.00
(7)	E + G + H + E:G	0.005	1.784	-0.002		421.40	0.00
(7)	E + G + H + E:H	0.036	3.068	0.124		415.84	0.00
(7)	E + G + H + G:H	0.021	4.654	0.296		406.04	0.09
(7)	E + G + H + E:G + E:H + G:H + E:G:H	0.011	2.360	0.129		401.63	0.84
glbl	E + G + H + S + E:G + E:H + E:S + G:H + G:S + H:S + E:G:H + E:G:S + E:H:S + G:H:S + E:G:H:S	0.108	-16.474	1.216	-3.289	406.54	0.07